MAGNETOTELLURIC
3D INVERSION WORKSHOP IV
31 July - 2 August, 2026

MT3DINV4 Programme and Abstracts

Memorial University of Newfoundland
St. John’s, Newfoundland
31 July – 02 August 2026

Sponsors

Gold: Dias, Raglan Mine (Glencore), Viridien

Silver: Barrick, Enthalpion/IoMT, Fleet, MTGS, Moombarriga, Phoenix, Quantec, Zonge

Bronze: Campbell & Walker, KEGS Foundation, Novaminex

Logistical Support: Memorial University

MT3DINV3: Residual Sponsorship Funds

MAGNETOTELLURIC
3D INVERSION WORKSHOP IV
31 July - 2 August, 2026

MT3DINV4 Programme

8:30 – 9:00: Breakfast; 10:30 – 11:00 Morning tea break;
12:30 – 13:30: Lunch; 15:00 – 15:30: Afternoon tea break

Friday 31st July – MT3DINV4F – Forward Model	
Morning	**Afternoon**
9:00: Intro to workshop	13:30: Randall Mackie
9:15: Intro to MT3DINV4F	13:45: Flavio Manara
9:30: Seyed Masoud Ansari	14:00: Nico Skibbe
9:45: Wouter Deleersnyder	14:15: Rylan Stutters
10:00: Brady Fry	14:30: Deniz Varilsuha
10:15: Mitra Kangazian Kangazi	14:45: Shunguo Wang
10:30: Tea break	*15:00: Tea break*
11:00: Mikhail Kruglyakov	15:30: Andrew Williamson
11:15: Yinchu Li	15:45: Posters
11:30: Jason Liu	
11:45: Jianbo Long	
12:00: Posters	16:30: Open discussion
12:30: Lunch	*17:00: Nominal end*

Saturday 1st August – MT3DINV4S – Secret Model	
Morning	**Afternoon**
9:00: Intro to MT3DINV4S	13:30: Nico Skibbe
9:15: Seyed Masoud Ansari	13:45: Han Song
9:30: Hao Dong	14:00: Deniz Varilsuha
9:45: Mitra Kangazian Kangazi	14:15: Andrew Williamson
10:00: Yinchu Li	14:30: Alan Jones – The reveal
10:15: Jason Liu	14:45: Discussion
10:30: Tea break	*15:00: Tea break*
11:00: Hossam Marzouk	15:30: Posters
11:15: Martin Musila	
11:30: Posters	16:30: Open discussion
12:30: Lunch	*17:00: Nominal end*

<table>
<tr><th colspan="2">Sunday 2nd August – MT3DINV4R – Real Data Model</th></tr>
<tr><th>Morning</th><th>Afternoon</th></tr>
<tr><td>9:00: Intro to MT3DINV4R</td><td rowspan="11">13:30: Geotools demo</td></tr>
<tr><td>9:15: Alan Jones</td></tr>
<tr><td>9:30: Jianbo Long</td></tr>
<tr><td>9:45: Xushan Lu</td></tr>
<tr><td>10:00: Pankaj Mishra</td></tr>
<tr><td>10:15: Aideliz Montiel Alvarez</td></tr>
<tr><td>10:30: Tea break</td></tr>
<tr><td>11:00: Maxim Smirnov</td></tr>
<tr><td>11:15: Posters</td></tr>
<tr><td>12:00: Open discussion</td></tr>
<tr><td>12:15: Closing</td></tr>
<tr><td>12:30: Lunch</td><td>17:00: Nominal end</td></tr>
</table>

MT3DINV4F – Forward Model

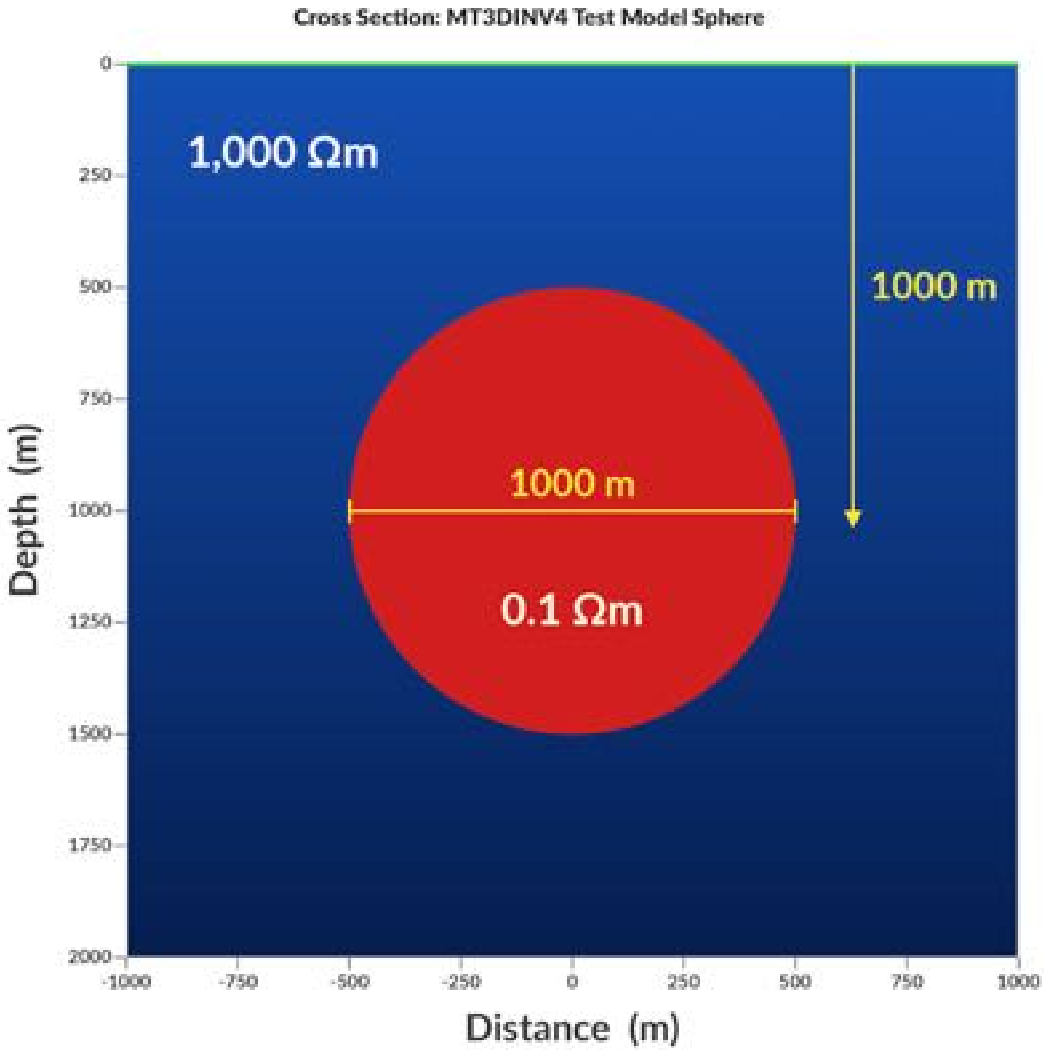

Three-dimensional MT forward modelling for MT3Dinv4 Workshop: Test Model simulations

Seyed Masoud Ansari
Geological Survey of Canada, Natural Resources Canada, Ottawa, Canada
seyedmasoud.ansari@nrcan-rncan.gc.ca

Summary of forward modelling – sphere in half-space

Forward modelling was carried out for a conductive spherical anomaly with a resistivity of 0.1 Ω.m and a radius of 500 m. The sphere was centered at a depth of 1000 m within a 1000 Ω.m half-space. Figure 1 shows a vertical section through the central part of the computational domain, illustrating the mesh structure and the local refinement at MT stations. The forward response was computed using the finite element code of Ansari et al. (2020), which solves the vector–scalar potential formulation of the Helmholtz equations on unstructured meshes. The mesh used here consisted of approximately 3 million cells. The computation time was approximately 600 s per frequency on an Amazon EC2 R6a instance equipped with an AMD EPYC 7R13 processor. The maximum memory required for each forward solution was approximately 180 GB. In total, responses were calculated for 70 frequencies. Figure 2 presents the apparent resistivity, phase and tipper responses for six selected frequencies along the central profile defined by -5000 m $< x < 5000$ m and $y = 0$ m. The apparent resistivity responses show sensitivity to the conductive sphere, spanning from the lowest frequency to a relatively high frequency. In contrast, the phase responses progressively lose sensitivity as the frequency decreases. The tipper responses exhibit a characteristic crossover behaviour. The sounding curves at a site located at (-750,-70) are shown in Figure 3. These results indicate that the influence of the conductive sphere on the apparent resistivity becomes evident at approximately 1000 Hz ($\log_{10} T = -3$). At approximately the same frequency, the x component of Tipper (T_x) becomes dominant over the y component (T_y).

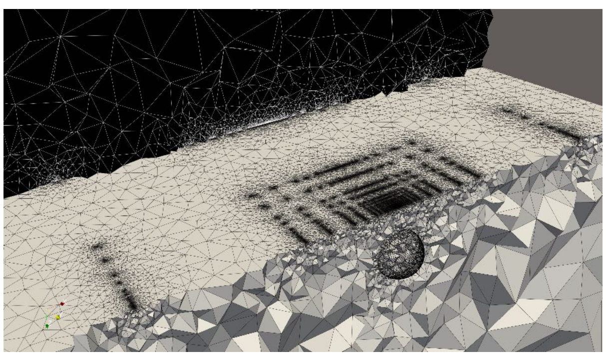

Figure 1: View of the unstructured tetrahedral mesh used for the forward modelling. The mesh is locally refined around the MT sites at the Earth's surface and within the conductive sphere. A vertical section through the air layer at $y = 5000$ m is also shown in black.

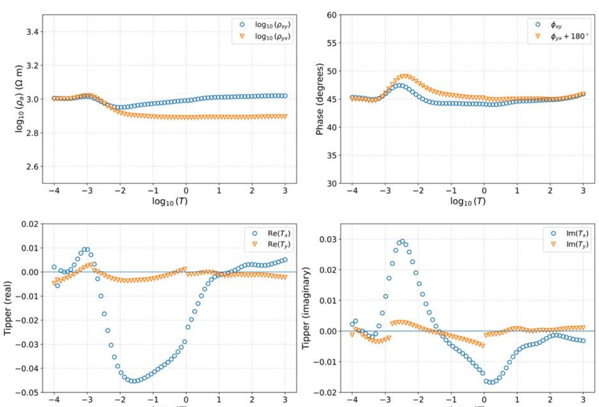

Figure 3: Sounding curves of apparent resistivity, phase, and tipper responses at site MT680 with coordinates $x = -750$ m and $y = -70$ m.

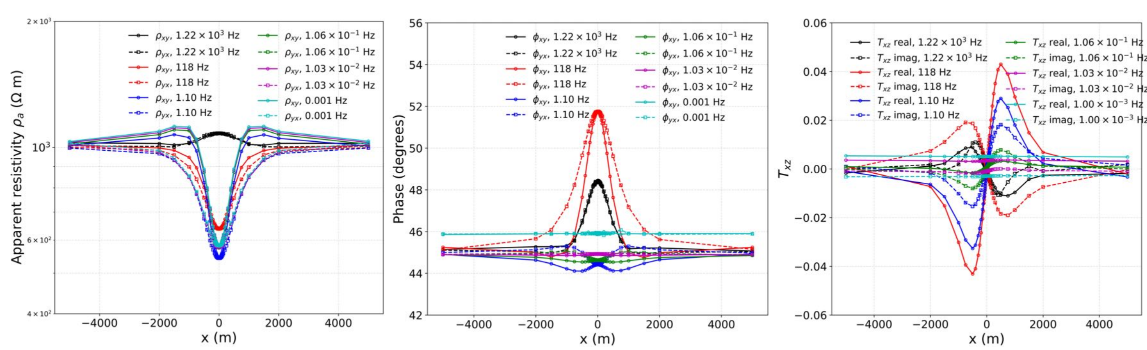

Figure 2: Apparent resistivity, phase, and tipper responses calculated for six representative frequencies along the central profile, defined by -5000 m $< x < 5000$ m and $y = 0$ m.

Reference: Ansari, S. M., Schetselaar, E., Craven, J., and Farquharson, C., 2020, Three-dimensional magnetotelluric numerical simulation of realistic geologic models. Geophysics, 85 (5): E171–E190.

3D MT modelling using custEM - case for a conductive sphere in a resistive half-space model

Chengdong Chen[1], Timothy A. Minshull[2], Gaye Bayrakci[3], Sebastian Hölz[4], and Joonsang Park[5]

[1]School of Ocean and Earth Science, University of Southampton, Southampton, UK, Chengdong.Chen@soton.ac.uk

[2]School of Ocean and Earth Science, University of Southampton, Southampton, UK

[3]Department of Science and Technology, National Oceanography Centre, Southampton, UK

[4]GEOMAR, Helmholtz Centre for Ocean Research, Kiel, Germany

[5]Norwegian Geotechnical Institute (NGI), Oslo, Norway

This study presents a three-dimensional magnetotelluric (MT) forward modelling example for a conductive sphere (0.1 Ω·m with a radius of 500 m and the centre is 1000 m below the surface) embedded in a resistive half-space (1000 Ω·m) using custEM, an open-source program developed with the finite element method (FEM). The computational domain extends from -10000 km to 10000 km in all three spatial directions to minimise boundary effects. Electromagnetic responses were calculated over a range of 71 frequencies (10 kHz – 0.001 Hz, with 10 points per decade) to simulate the MT response of the subsurface model. The forward simulations were performed using 8 parallel threads, requiring a total computation time of ~20 mins with a maximum memory usage of 12 GB. The resulting synthetic responses along an E-W profile from (-5000,0) to (5000,0) demonstrate the capability of custEM to accurately model three-dimensional MT response using an unstructured finite element mesh with satisfactory accuracy, providing a benchmark for further investigating 3D MT modelling and inversions.

The coarse mesh that punches above its weight: a trick for 3D MT

W. Deleersnyder[1]* and L.J. Heagy[1]

[1] *University of British Columbia, Geophysical Inversion Facility, * wdls@eoas.ubc.ca*

The wide range in frequencies, the large spatial extent, and high conductivity contrast make the conductive sphere in a resistive background a hard MT forward problem. In earlier work, we approximated time-domain electromagnetic data with coarse meshes, joined with the accuracy of simplified physics analytical models [1]. Here, we explore to what extent we can model the response of the conductive sphere on the coarse mesh, with only the homogeneous background analytical model to calibrate the result. We approximate the full response $\mathscr{F}_{3D}(\mathbf{m})$ with

$$\widetilde{\mathscr{F}}_{3D}(\mathbf{m}) = \frac{\mathscr{F}_{ana}(\mathbf{m}_{bg})}{\mathscr{F}_{3D,C}(\mathbf{m}_{bg})}\mathscr{F}_{3D,C}(\mathbf{m}), \tag{1}$$

where $\mathscr{F}_{ana}(\mathbf{m}_{bg})$ is the evaluation of the homogeneous background $\mathbf{m}_{bg}$ with the analytical model, and $F_{3D,C}$ is the evaluation on a coarse mesh, which does not necessarily generate accurate results in absolute terms. The approximation is exact in two limits: (1) when you evaluate the homogeneous background in $\mathbf{m}$, and (2) when you refine $F_{3D,C}$ in such a way it becomes exact.

We use SimPEG's TreeMesh to construct the coarse mesh. We used 7 088 cells ranging from 125 m cells up to 2 000 m cells, and used the spatial dimensions as in Figure 1A. It takes 106 seconds to run two coarse mesh evaluations (background and sphere models) and compute the analytic at all 71 frequencies on Apple's M1 chip MacBook Pro (2021). To tackle the discretization problem and to represent a sphere on rectangular cells, we used harmonic averaging [2]. In Figure 1B, we show the modeling error in terms of total RMS error, summed for all data, for 3% noise and a noise floor of 10^{-5} mV/(km·nT). The calibrated result (1) follows the coarse mesh result for low frequencies, switches to a more accurate combination of the two individually in the mid-range, and approximates the analytical, homogeneous result for high frequencies (at which the sphere lies deeper than the skin depth). When comparing the modeling error (in % this time) for different frequencies and receiver locations (see Fig 1C), we observe a consistent error (between 2-3.25%) right above the sphere and for most frequency ranges, except for the highest frequencies because this is where the solution approaches the homogeneous halfspace.

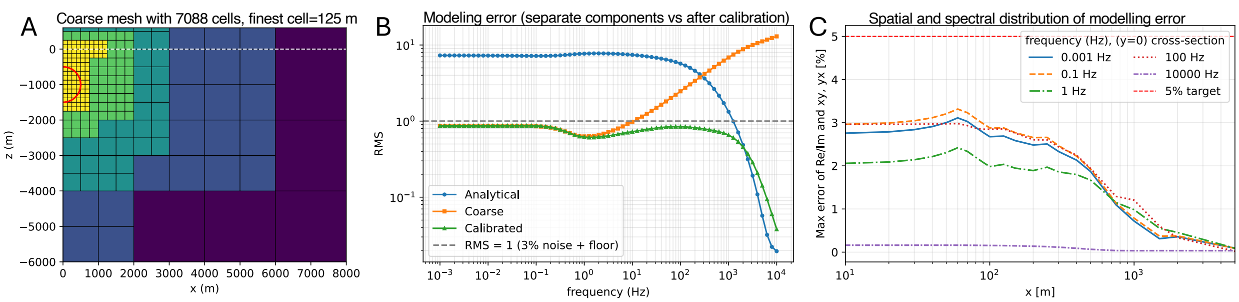

The modeling error for the calibrated result, however, depends on the mesh used. We expect a reduction in the modeling error if finer meshes are being used. In Figure 2, we observe a convergence, as expected, in the low frequency range. In the mid-frequency range (the induction range) all meshes overshoot the response, because all discretizations fail to model the eddy currents that only occur in the thin shell of the sphere ($\delta = 503\sqrt{0.1\Omega\cdot\text{m}/500\text{Hz}} \approx 7.11$ m). The smallest cell size needed is around 2δ, yielding a minimum OcTree mesh of 3+ million cells, which we do not attempt on the aforementioned machine. We hypothesize that the 125 m cell size mesh does slightly better in that induction range due to cancellation of modeling error biases. The calibration cancels the modeling error each coarse mesh suffers from in the high frequency range.

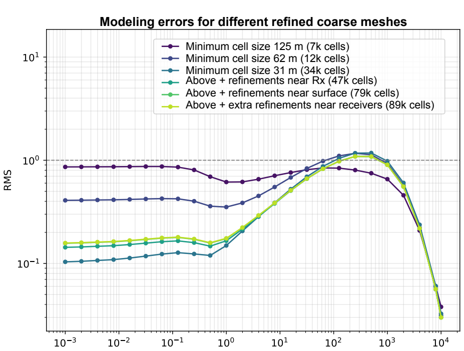

[1] Deleersnyder, W., & Slob, E. (2026). Fast approximate physics method for 3D time-domain electromagnetic modeling. *Geophysics*, 91(2), A7-A11. `https://doi.org/10.1190/GEO-2025-0566`

[2] Stutters, R., Deleersnyder, W., Soler, S. & Heagy, L.J. (2026). Techniques for Improving MT Forward Simulations with Octree Meshes. *In 4th MT 3D inversion workshop (MT3DINV4)* 2026.

MTDinv4 Magnetotelluric Forward Model using SimPEG

Author: Robert Eso — rob.eso@novaminex.com, Nova Mining Exploration Solutions Inc.

A forward modelling exercise to simulate the response of a conductive sphere in a resistive half space was performed using SimPEG (Cockett, 2015), this being the author's first time using the open-source geophysical package. An octree adaptive discretization was used. Mesh design was driven by the electromagnetic skin depth $\delta = 503 \cdot \sqrt{(\rho/f)}$ m. The skin depth of the 0.1 Ohm-m conductive sphere at 10kHz is 1.6 meters, however with the depth to the top of the sphere being located 500m below the surface, means that the sphere effectively only sees frequencies of 1000Hz and below, and at 1000Hz the skin depth of the 0.1 Ohm-m sphere is 5m, thus 6.25m was chosen as the smallest cell size as that value evenly divides 100m by 16, and thus will subdivide nicely with the octree discretization. The mesh extents were determined iteratively, by forward modelling the lowest frequency and expanding the mesh until the response at this frequency was unchanged by further expansion. The resulting mesh contained 572,566 cells. Frequencies were solved sequentially, using an LU direct matrix factorization, with an average time per frequency of 46.1 seconds, with each factorization taking 2.5GB of memory. The run was completed on a high-end personal desktop computer, with a total run time of 54.7 minutes.

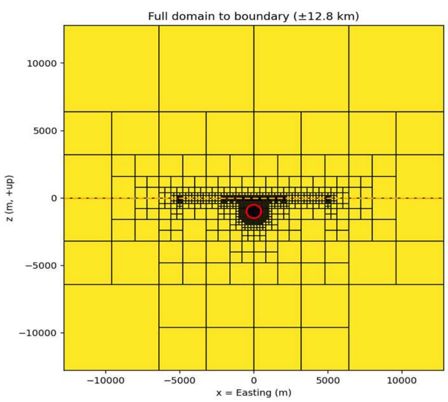

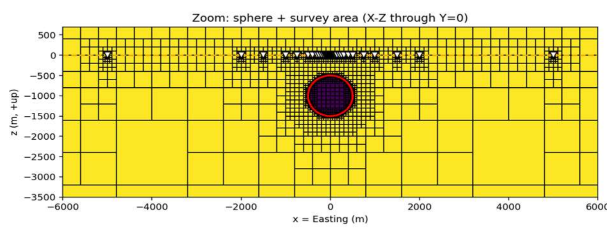

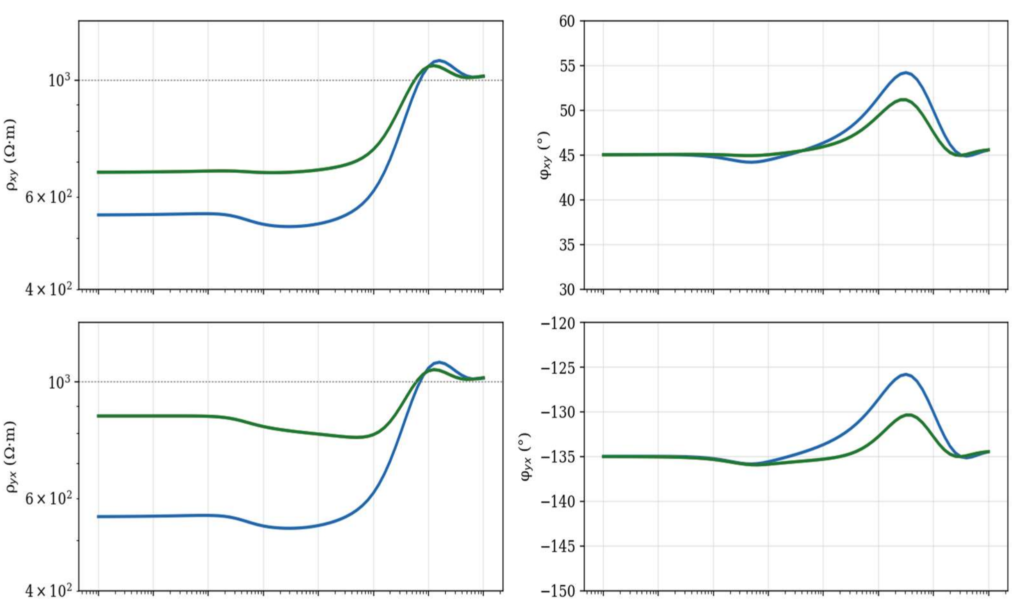

3D Magnetotelluric Forward Model using COMSOL Multiphysics

Samuel Butler, Cesar Fernandez, University of Saskatchewan

Abstract

In this poster, we present a three-dimensional (3D) magnetotelluric forward model to evaluate the response of a conductive sphere embedded in a layered Earth, using the commercial finite-element package Comsol Multiphysics. The AC/DC module in Comsol can be used to solve Maxwell's equations in the quasi-static limit for modeling the magnetotelluric response. Comsol Multiphysics (Comsol, 2014) is a finite element software that solves partial differential equations. One of the main advantages of COMSOL is its graphical user interface (GUI), which facilitates the solution of complex single-physics and multiphysics problems in discretized domains. In addition, the platform reduces the need for extensive programming when solving partial differential equations such as Maxwell's equations (Li \& Butler, 2021). Another advantage of COMSOL is its flexibility in modeling complex geometries and coupling different physical effects within the same model.

Although the finite element method has become widely used in the application of MT modeling using different computer programs and software, Comsol Multiphysics has not been widely used in MT studies (Li and Butler, 2021). Our model imposes magnetic fields on the outer boundaries that are determined from analytical solutions for fields in a layered Earth and these act as the forcing in the model. The excitation of the model is achieved by enforcing a tangential magnetic field $\mathbf{H_0}$ on all of the outer domain boundaries. In this 3D simulation, the computational domain is defined as a cube. The cube includes regions that represent air of very low conductivity (z<0 km) and ground (z >0 km). Each ground layer is assumed to be isotropic and homogeneous. A conductive sphere with a resistivity of 0.1 Ω·m is embedded in the model, with its center located at a depth of 1000 m. The electrical permittivity and the magnetic permeability within the layers are assumed to be those of free space, 8.85×10^{-12} F/m and $4\pi\times10^{-7}$ H/m respectively.

Comsol solves complex single or multi- physics problems in a meshed domain. To satisfy the resolution in frequency domain studies, the mesh is defined that there are at least a few element edges over one skin depth unit. It is important that the domain size is sufficiently large that the outer boundary conditions are not significantly affecting the solution (Butler and Zhang, 2016). Therefore, the domain outer boundaries need to be at least 2 skin depths away from the point of interest to minimize the boundary effects (Li and Butler, 2021). For high frequency simulations, the effects of the conducting sphere were represented by an impedance boundary condition so that very high mesh resolution within the sphere was not necessary.

Another important aspect considered during the mesh generation was the inclusion of refinement surfaces for both the high- and low-frequency groups. In both cases, the surface at $z = 0$ and the first subsurface layer were considered for mesh refinement. Additionally, at the $z = 0$ surface, the 2025 receiver locations were included as local mesh refinement points. However, this refinement strategy was applied only down to a frequency of 0.7943 Hz. For frequencies below this value, including the lowest frequencies in the model, the meshing process generated an error indicating that an adequate mesh resolution could not be guaranteed. Therefore, for frequencies lower than 0.7943 Hz, the receiver locations were not included as mesh refinement points. The forward model was computed for each of the 71 frequencies using two propagation angles, $\alpha = 0°$and $\alpha = 90°$, where α is defined as the counterclockwise angle between the horizontal component of the wave propagation direction and the x-axis. The simulated electric and magnetic field components obtained for these two orientations were then used to calculate the impedance tensor and tipper values using the corresponding field relationship equations.

Title: AI Multiphysics Inversion (AIMI) – a framework for accelerated 3-D inverse modeling
Authors: Brady Fry(1,2,3) and Adam Schultz(1,2,3)
Institutions: [1]IoMT LLC, [2]Enthalpion Energy LLC, [3]Oregon State University

Motivation. Compact hybrid CPU–GPU machines with unified memory now make it realistic to run preliminary 3-D magnetotelluric inversions in the field, fast enough to steer acquisition while a survey is still underway, with new-generation multiphysics inversion frameworks. **AIMI – A**rtificial **I**ntelligence accelerated **M**ultiphysics **I**nversion, currently in active development, implements a GPU accelerated 3-D MT forward solver which is an essential element of both main branches of AIMI – an AI prefilter stage, the development of which requires accurate and fast forward solutions, and a classical inversion stage, which also benefits from the fast forward solver, as well as other algorithmic features optimized for GPU computing. Followed by the intention to add single and joint inversion of MT, CSEM and gravity data next, with other data types to follow.

The forward solution in native CUDA C++. AIMI retains ModEM's[1] staggered Yee discretization, boundary fields, and divergence correction, so results are directly comparable. Iterative refinement pairs a double-precision flexible-GMRES outer loop — the accuracy guarantee, halting only on the true residual b−Ax — with work-dominant single-precision inner solves on the GPU. The same D-ILU preconditioner is re-ordered into diagonal-plane "wavefronts" the GPU can parallelize, and unified memory holds a single copy of the model.

Trust, but verify. We benchmark against ModEM's own GPU solver matching output grades by RMS misfit against a semi-analytic sphere[2] and by cross-code agreement on a real survey.

Table 1. Forward solve on one DGX Spark, at matched output grade — the two GPU solvers (AIMI, ModEM BiCG) against ModEM's CPU QMR reference. Sphere: ~4.5M unknowns; Newberry: ~6.5M unknowns

Imped. Data set	Solver	RMS Deviation	Speed vs QMR	Memory vs QMR	Compute
Sphere — 132×132×72, 71 freq, 2,025 sites	QMR	6.5 (analytic sol'n)	---	---	13 CPU cores
	BiCG	4.5 (analytic sol'n)	+62%	-84%	1 GPU + 1 core
	AIMI	**3.4** (analytic sol'n)	**+65%**	**-88%**	1 GPU + 1 core
Newberry — 177×166×114, 27 freq, 250 sites	QMR	---	---	---	7 CPU cores
	BiCG	0.1 (QMR sol'n)	+90%	-64%	1 GPU + 1 core
	AIMI	**1.0 (QMR sol'n)**	**+89%**	**-74%**	1 GPU + 1 core

Beyond parity. At this early stage of this work, we show large speedups over ModEM's CPU solver; AIMI has now reached parity with ModEM's best GPU solver — at lower memory, with a provably-safe stop, and no tolerance tuning. The near-term path beyond parity is architectural: adaptive octree meshes, for both the forward and inverse solutions, which shrink cost precisely where a rectilinear grid is most wasteful — accommodating topography and refining near sharp structure. Large reductions in memory footprint frees up resources to implement joint multiphysics solutions.

---

[1] Kelbert, A., Meqbel, N., Egbert, G. D., & Tandon, K. (2014). ModEM: A modular system for inversion of electromagnetic geophysical data. Computers and Geosciences, 66, 40–53, Elsevier. https://doi.org/10.1016/j.cageo.2014.01.010
[2] Cockett, R., Kang, S., Heagy, L. J., Pidlisecky, A., & Oldenburg, D. W. (2015). SimPEG: An open source framework for simulation and gradient based parameter estimation in geophysical applications. Computers & Geosciences.

Forward response of a sphere in a half-space using a high order hybrid mesh

Erik Gallardo-Romero[1]*

GGI Gallardo Geophysical Imaging[1]*

Email: egallardo@ggi-geophysics.com

1. METHOD

The magnetotelluric (MT) response of the MT3DINV4 forward model was calculated using a newly developed high-order finite-element (FE) algorithm for hybrid meshes. This novel hybrid FE method allows the combined use of unstructured tetrahedral elements and triangular prisms to divide the simulation domain. MT responses are evaluated on a 5000 km × 5000 km × 5000 km simulation domain divided into 138,996 triangular prisms and 233,652 tetrahedra. The first 400 m of the subsurface are represented by 10 layers of perfectly sealed triangular prisms with an initial thickness of 4 m in the top layer and a thickness increment in depth by a factor of 1.4. The prismatic elements just above the embedded sphere have a lateral edge length ranging between 30 to 100 m and about 200 m in the rest of the 10 km x 10 km evaluation area. The deep subsurface (>400 m depth) of the simulation domain, the spherical body and the air layer are discretized into tetrahedral elements. These tetrahedral elements are refined close to the sphere´s surface up to a minimum edge length of 40 m and then increased to a maximum edge length of 800 km in the boundaries of the simulation domain. To ensure accurate forward responses, second-order vector shape functions are used to interpolate electric and magnetic fields within each element. Forward responses are computed at the full 2025 receiver locations for the complete 0.001 Hz – 10,000 Hz frequency range. The computation was performed on a 10-node cluster of 20 cores and 128 GB RAM capacity per node. 70 GB memory was used on each node to compute the forward responses. The required computing time for all 71 frequencies was 83 minutes.

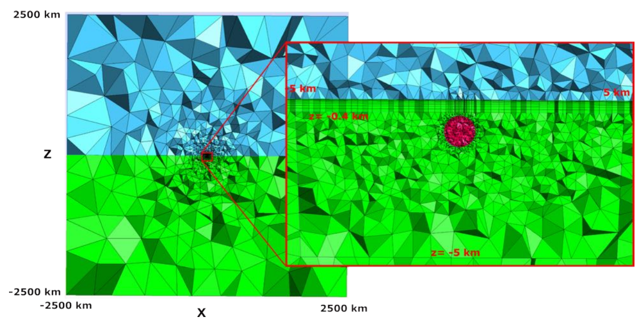

Figure 1. Forward modeling hybrid mesh used by the high-order FE approach.

2. RESULTS

Computed forward responses were compared with the analytical solution along a (-5000,0) to (5000,0) profile and at sounding position (500,0), where H_z maximizes (Figure 2). In periods longer than 0.1 s, obtained error values are lower than 2% in apparent resistivity and phase in all the evaluated points along the profile. The calculated tipper responses coincide very well with the analytical values at long periods in both real and imaginary components. Within the 0.001 to 0.01 s period range, greater error values are obtained with a peak maximum error value of 5% in apparent resistivity and 2.5% in phase.

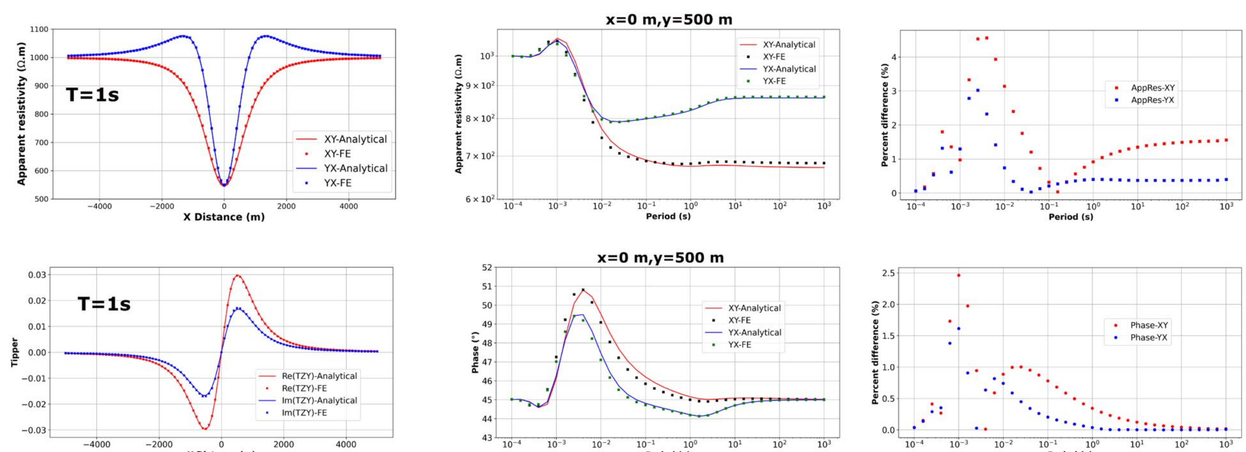

Figure 2. Left: Analytical and computed apparent resistivity and tipper values for T=1s along the profile (-5000,0) to (5000,0). Middle: Analytical and computed apparent resistivity and phase values at x=0 m, y=500 m. Right: Percent difference between the calculated and analytical values at the x=0 m, y=500 m

Forward modelling of a sphere in a half-space

Mitra Kangazian[1], Mehrdad Darijani[2], Meghdad Darijani[2], Colin Farquharson[1]

[1]Department of Earth Sciences, Memorial University of Newfoundland
St. John's, Newfoundland and Labrador, Canada

[2]Geotexera Inc., St. John's, Newfoundland and Labrador, Canada

Abstract

We compute the impedances tensor and tipper values of the sphere model shown in Fig. 1 for a range of frequencies from 0.001 Hz to 10kHz (5 points per decade) using the edge-based finite-element (FE) approach with a time-dependence of $e^{i\omega t}$ (Jahandari and Farquharson, 2017) . The dimension of the computational domain is 30 km $\times$ 30 km $\times$ 30 km; x positive East, y positive North, and z positive up

The open source program TetGen (Si, 2015) is used to discretize the model. We also used ZAMINEX software (Geotexera Inc.) to generate another tetrahedral mesh for this model (see Table 1). One of the capabilities of ZAMINEX software is generating meshes with less number of cells compared to TetGen.

The computations were performed on the Siku cluster (Digital Research Alliance of Canada) using a compute node equipped with two Intel Xeon Gold 6248 processors (40 CPU cores in total) running at 2.50 GHz and 188 GiB of RAM.

Table 1: Comparison of the computational performance of the TetGen and ZAMINEX meshes.

Mesh	**Number of Cells**	**Computation Time per Frequency**	**Maximum Memory per Frequency**
TetGen	2,073,728	50 min	16.6 GiB
ZAMINEX	1,328,447	22 min	9.8 GiB

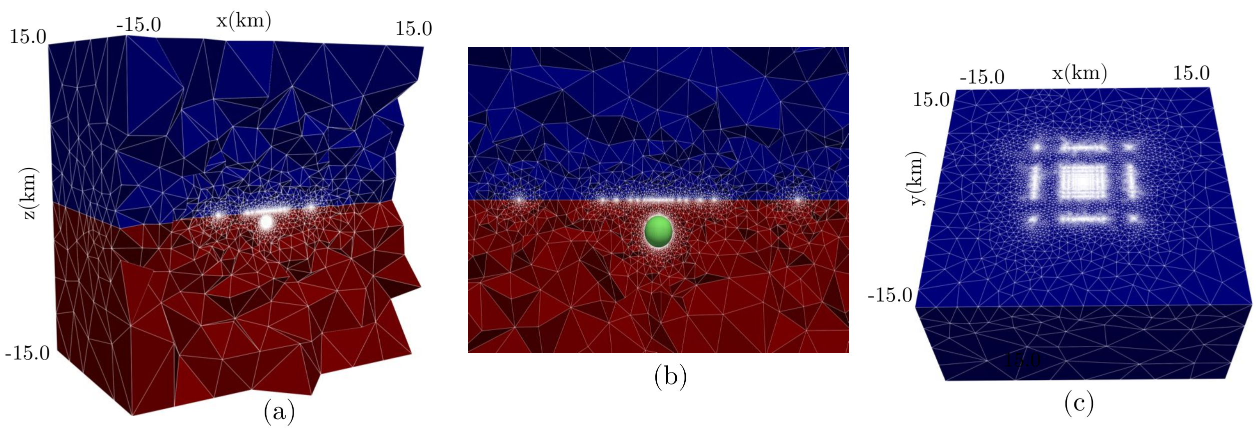

Figure 1: (a) The computational domain used to compute the forward response of a sphere with a conductivity of 10.0 S/m embedded in a homogeneous half-space with a conductivity of 10^{-3} S/m. The sphere has a radius of 500 m, and its center is located at a depth of 1000 m. (b) A close view of the computational domain. (c) The refinement of the mesh around the observation points.

References

Jahandari, H., and C. G. Farquharson, 2017, 3-D minimum-structure inversion of magnetotelluric data using the finite-element method and tetrahedral grids: Geophysical Journal International, **211**, 1189–1205.

Si, H., 2015, Tetgen, a delaunay-based quality tetrahedral mesh generator: ACM Trans. Math. Softw, **41**, 11.

Three-Dimensional Magnetotelluric Forward Modelling Using High-Order Integral Equation Method

Mikhail Kruglyakov[*,1] Alexey Kuvshinov[2,3]

[1]Universitiy of Otago, New Zealand
[2]School of Geosciences and Info-Physics, Central South University, Changsha, China
[3]Institute of Geophysics, ETH Zürich, Zürich, Switzerland

The application of the integral equation (IE) approach to three-dimensional electromagnetic modelling dates back to the pioneering works of Raiche (1974) and Hohmann (1975). Over more than five decades, the development of IE-based forward modelling codes has largely focused on addressing the computational challenges faced by both code developers and end users and on overcoming the IE approach limitations.

Following this long-standing research direction, we present at this workshop one of the major advances achieved during the last decade: a solver based on the so-called high-order polynomial (HOP) integral equation method. The term high-order refers to the use of a piece-wise polynomial (PWP) representation of the electric field (up to fifth-order polynomials) in contrast to conventional IE solvers that employ a piece-wise constant (PWC) approximation.

The system of linear equations is constructed using the Galerkin method, which not only guarantees the convergence of the iterative solution but also ensures that the resulting system matrix remains well conditioned regardless of the polynomial order. Replacing the PWC approximation with the PWP representation significantly improves the accuracy of the numerical solution, particularly for models with large conductivity contrasts. Such contrasts produce sharp spatial variations in the electric field, which can be captured accurately either by using extremely fine PWC meshes (often at prohibitive computational cost) or by employing the HOP approach.

The HOP method has been implemented in the parallel code GEMMIE. Its hybrid parallelization strategy (MPI + OpenMP) enables efficient utilization of thousands of computational cores, allowing users to balance solution accuracy, computational speed, and resource consumption according to the requirements of a given problem.

These capabilities were fully exploited in the solution of Task 1.

MT3DINV4 Task 1: forward and inverse tests of a conductive sphere in a half-space with finite-difference (ModEM) and finite-element (FEMTIC) codes

Yinchu Li

School of Earth and Atmospheric Sciences, Georgia Institute of Technology, Atlanta, GA, USA

In Task 1 of MT3DINV4, I forward-model the full magnetotelluric response of a 0.1 Ω m sphere of radius 500 m centred 1000 m deep in a 1000 Ω m half-space: impedance and tipper at 2,025 receivers and 71 frequencies from 10 kHz to 0.001 Hz ($e^{+i\omega t}$; X=North, Y=East). The responses are computed with the finite-difference (FD) code ModEM (Egbert & Kelbert, 2012), cross-checked with the unstructured tetrahedral finite-element (FE) code FEMTIC (Usui, 2015), and benchmarked against the MTSphere semi-analytical solution (Vallée & Moussaoui, 2023), and both codes are then used to invert the computed responses.

The ModEM mesh (106×106×67 earth cells, 7.5×10^5 total) has a uniform 50 m core measuring 2.5 km horizontally and 2 km deep (50×50×40 cells, centred on the sphere axis and containing the sphere at 500–1500 m depth), surrounded by ×1.5 geometric padding that reaches well beyond the ±5 km station footprint. Two refinements matter most in my ModEM mesh: the 1,568 cells the sphere surface cuts through carry a volume-fraction-weighted harmonic-mean conductivity, which keeps the sphere's volume right to 0.01%; and the top 250 m is re-gridded into nine layers ramping from 12.5 to 44.5 m to resolve the 160–500 m host skin depths above 1 kHz. FEMTIC instead uses three band-optimized sphere-conforming tetrahedral meshes (0.12, 0.63 and 2.6 million elements for <0.1 Hz, 1 kHz–0.1 Hz and 10–1 kHz), with local refinement around every station. The full survey costs about 16.5 core-hours with ModEM (impedance plus tipper, one 24-core node) and about 20 core-hours with FEMTIC across the three meshes.

Accuracy is assessed at three surface stations ($z = 0$): the sphere centre $(0, 0)$, the sphere edge $(500, 0)$, and an off-symmetry site $(500, -250)$. The response matches the analytic off-diagonal apparent resistivities ρ_{xy} and ρ_{yx} to 5.3% RMS over all 71 frequencies (3.7, 8.0 and 4.4% in the >40 Hz, 1–40 Hz and <1 Hz bands; worst single point 14.6%) and the phase to 0.61° RMS. FEMTIC reaches about 2.9% in the 1 kHz–0.1 Hz band and 6.0% at 10–1 kHz. A baseline mesh that assigns each boundary cell entirely to sphere or host, with no near-surface layering, misfits by 10.3% and 1.49°, so the factor-of-two gain comes from the interface and near-surface treatment. The mid-band error looks like a staircasing artifact of the curved interface: refining the FD mesh alone did not remove it, while the sphere-conforming FE mesh shows no such deficit.

As a credibility check, both codes re-invert the submitted responses on independent, re-parameterized meshes from a uniform 1000 Ω m start. Both recover the conductor in the right place and at ∼1 km depth: FEMTIC (Gauss–Newton) reaches normalized RMS ≈0.12 and ModEM (NLCG) ≈0.22, both below 1.0 because the 5% error floor might be too conservative for noise-free data; FEMTIC already images the sphere clearly on its first iteration (nRMS 0.89).

References

Egbert, G. D. & Kelbert, A. (2012). *Geophysical Journal International*, 189(1), 251–267.

Usui, Y. (2015). *Geophysical Journal International*, 202(2), 828–849.

Vallée, M. A. & Moussaoui, M. (2023). *Exploration Geophysics*, 54(4), 362–375.

GPU-Accelerated 3D MT Forward Modelling: What Would You Try if Forwards Were Fast?

Jason Liu*, Junseo Shin, Paul Köttering
Vorticity Inc.
*Presenting author

Three-dimensional magnetotelluric forward modelling is often constrained by the computational time and memory required to solve large problems repeatedly. We present a new GPU-accelerated 3D MT forward-modelling code designed to reduce these computational constraints and make large-scale modelling studies more practical.

The implementation uses GPU-based sparse direct solving, with a particular focus on reducing forward-modelling time for repeated calculations. We apply the code to the MT3DINV4 Task 1 sphere-in-a-half-space model. The computed responses are compared with the analytical solution to assess the accuracy of the implementation. We also present the performance of the code and visualize the full spatial sensitivity of the measurements across multiple frequencies.

As an extension to the prescribed task, we repeat the forward calculation for 100 different sphere conductivities. The scientific formulation itself is conventional; the primary contribution is computational. By applying GPU sparse direct solving to 3D MT modelling, we aim to make larger meshes, broader parameter sweeps, full-sensitivity calculations, and repeated modelling experiments accessible within practical timeframes. This raises a broader question: what new MT experiments become possible when forward modelling is no longer the dominant computational constraint?

Task 1: MT3D Forward Modelling with ModEM

Xiaojun (Jon) Liu
Natural Resources Canada, Geological Survey of Canada-Calgary

For conducting this forward modelling task, the ModEM and MTpy are used to generate the input data of geo-electrical model and geometry of receiver coordinators and conduct the forward computation. The synthetic MT datasets include four impedance components, $Z_{xx}, Z_{xy}, Z_{yx}, Z_{yy}$, which is output from forward module of ModEM (Kelbert et al., 2014).

Background resistivity is 1000 Ωm and anomalous body is 0.1 Ωm. The base-10 logarithm of resistivity is saved in the input file. Because of the Python coding reason, the anomalous body is not exactly same as the sphere shape on the MTNet website.

The grid is [nx, ny, nz] = [112, 112, 45]. The cell size in north and east directions: [3000.0, 2000.0, 1000.0, 500.0, 100.0, 50.0] + [20.0]*100 + [50.0, 100.0, 500.0, 1000.0, 2000.0, 3000.0]. The cell size in vertical direction: [10.0, 20.0, 20.0, [50.0]*30, 100.0, 200.0, 400.0, 600.0, 800.0, 1000.0, 2000.0, [3000.0]*5]]. MTPy is used to create the input files (Krieger et al., 2014). Station coordinates are same as the website, showing in Figure 1.

The total number of frequencies is 71 with range from 1.0e+04 to 1.0e-03 Hz. The computation time of ModEM modelling is 2.0 hours and 2.52 minutes with the computer hardware: CPU Intel i9-10885Hx8 cores, 128G RAM Dell Precision 7750 laptop.

Figure 2-5 are figures of the forward response at different periods and receivers for comparison.

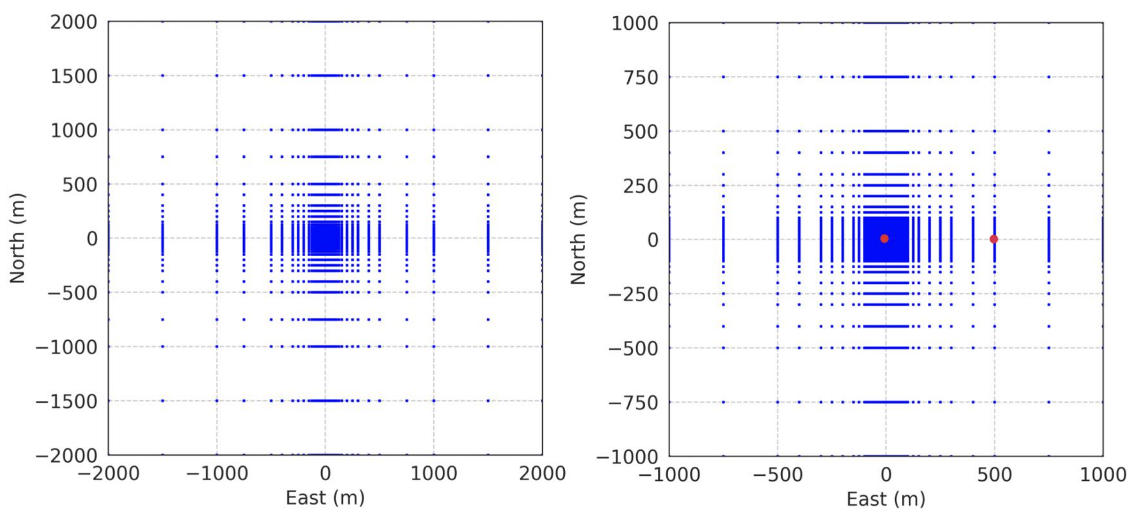

Figure 1. Receiver station distribution.

MT 3D Modelling and Inversions using a finite element method with unstructured tetrahedral meshes

Jianbo Long [1*] and Peter Lelievre [2]
1. Department of Earth Sciences, Memorial University of Newfoundland
2. Department of Computer Science and Mathematics, Mount Allison University

Task1 – Forward Modelling

The E-field Helmholtz equation was used for the 3D forward modelling of the sphere conductor model, which was solved using a first-order vector finite element (FE) method and using an unstructured tetrahedral mesh generated by Tetgen. The mesh has 391,546 cells in total. The sphere's surface was first triangulated with 448 triangular facets before generating the 3D tetrahedral mesh. Local refinements of the mesh around the observations and inside the sphere are added to ensure numerical accuracy. The MT responses were computed at a total of 11 locations at the surface from x=-5000 m to x=5000 m, y=0 (i.e., the E-W profile) over the center of the sphere, and at 22 frequencies logarithmically sampled from 10k Hz to 0.001 Hz. The matrix equation was solved using the MUMPS direct solver. The total computing running time is about 2 hours on a 32-core desktop computer.

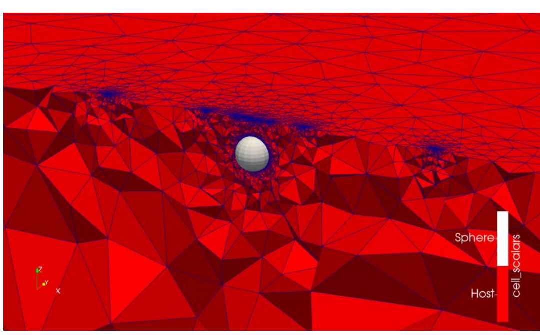

Fig.1. View of 3D tetrahedral mesh.

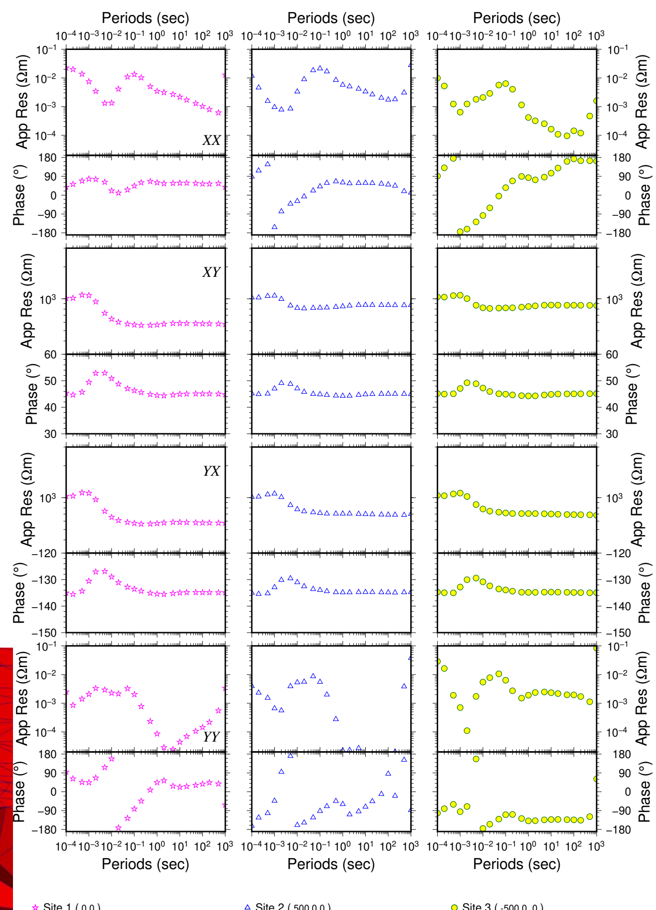

Fig.2. Calculated MT impedances.

3D MT Modeling of a Sphere Using Finite Differences

Randall Mackie, Viridien

I have carried out 3D forward MT modeling using RLM-3D of a conductive sphere (0.1 ohm-m) in a resistive background (1000 ohm-m) for the purpose of benchmarking against a recently developed analytical program developed by Vallée and Moussaoui (2023). The sphere was projected onto a finite difference mesh with a spacing of 10m horizontally and vertically in the area encompassing the sphere. A simple volume-averaged resistivity was used where the sphere boundary intersected the finite difference cells. At distances beyond 100m away from the sphere boundary, the mesh cells increased by a factor of 1.2 up to a distance of 10km horizontally and 20km vertically, resulting in a mesh with dimensions of 178x178x192, not including added air layers. Forward responses were computed at 71 frequencies from 10,000 – 0.001 Hz.

While this is a conceptually simple model, it's quite challenging from a numerical perspective, given the sharp boundary with a large conductivity contrast. The combination of low frequencies and low conductivity of the background result in a very stiff system of equations to solve. Even though RLM-3D explicitly includes a gradient-divergence augmentation (Mackie and Watts, 2012) to improve convergence, these types of models still tend to be challenging to converge at the lowest frequencies. RLM-3D uses the PETSc library and typical solution settings include use of biconjugate gradients stabilized and incomplete LU on the sub-blocks, but in this case, we used direct LU solves on the sub-blocks with Mumps as the direct solver, resulting in good convergence in a reasonable amount of time.

Mackie and Watts, 2012, DOI: https://doi.org/10.1190/segam2012-1248.1

Vallée and Moussaoui, 2023, DOI: https://doi.org/10.1080/08123985.2022.2162382

Geometry and Discretisation Errors in Magnetotelluric Modelling of a Conductive Sphere

Flavio Manara[1*], Alexander Grayver[2], Matthew J. Comeau[1]
[1]Department of Geosciences and Engineering, Delft University of Technology, Delft, The Netherlands
[2]Institute of Geophysics and Meteorology, University of Cologne, Köln, Germany

Numerical electromagnetic modelling requires conductivity structures and electromagnetic fields to be discretized on a finite mesh. On meshes composed of axis-aligned cells, curved interfaces are approximated by a series of steps. This can alter the volume, shape, and effective position of a conductive body. Refinement (i.e. a reduction of mesh cell dimensions) reduces this geometric error but increases computational cost. This is particularly true for conventional rectilinear meshes, which are typically used in finite-difference modelling schemes. In such cases, further refining the mesh near a local feature also requires refining the entire core model region, thereby introducing substantial unnecessary computational costs. In contrast, finite-element methods offer greater flexibility through local refinement and meshes that conform to material boundaries.

In this study, we investigate how mesh refinement and curved-interface representation affect the magnetotelluric response of a conductive sphere in a resistive half-space. The numerical experiments are performed using GoFEM [1, 2], a finite-element framework based on the deal.II library [3]. The frequency-domain problem is solved using a scattered-field formulation on locally refined hexahedral meshes. Three representations of the sphere are compared (see figure 1): a cell-centred staircase approximation on an octree mesh; the same mesh with volume-fraction homogenisation of cells intersected by the interface; and a boundary-conforming mesh obtained by projecting interface vertices onto the analytical sphere.

The three representations are evaluated over several refinement levels by examining the represented geometry, the convergence of the impedance and tipper responses, and the computational cost. Preliminary results indicate that all three approaches converge, but at different rates. The boundary-conforming results stabilise most smoothly, whereas the staircase solutions remain more sensitive to refinement as the represented volume and shape of the sphere change. Overall, the numerical results from all three representations agree closely with the semi-analytical solution used as reference [4] across the investigated wide period range and at all receiver locations. At periods longer than 10 seconds, however, a small relative error up to a few per cent in apparent resistivity (or $\approx 13\Omega m$) was observed, with the maximum above the center of the sphere. This leads us to look for another reference to gauge the accuracy of our solution. At these periods, the electromagnetic fields vary over distances much larger than the sphere and the response of the sphere is therefore expected to approach the electrostatic limit. When we compare our numerical results with an analytical electrostatic solution [5], we find a very close agreement of 0.2 % in apparent resistivity. Remarkably, such excellent agreement can be achieved with only a very moderate number of cells, leading to short computing times of a few minutes and small RAM per frequency.

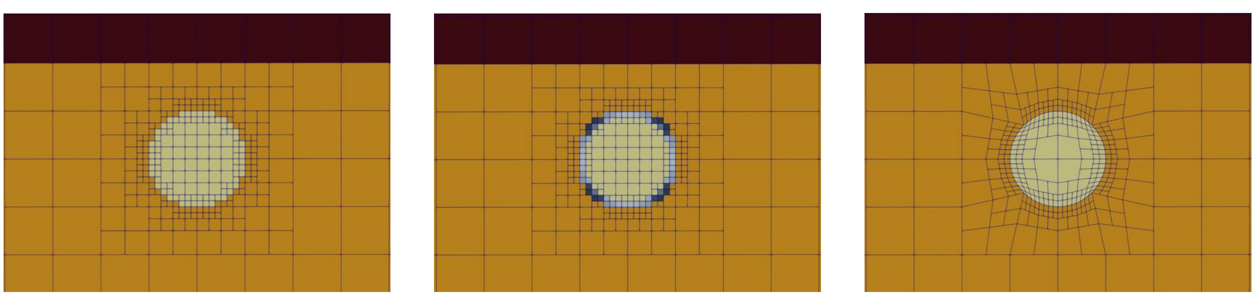

(a) Staircase   **(b)** Staircase + Homogenisation   **(c)** Boundary-Conforming

Figure 1: Representations of the conductive sphere at a nominal interface resolution of approximately 62.5 m. *(a) cell-centred staircase, (b) volume-fraction homogenisation, and (c) boundary-conforming mesh. Colours indicate conductivity values. Intermediate values in (b) represent cells intersected by the interface, which are assigned effective conductivities according to their material volume fractions.*

[1] Alexander V Grayver and Markus Bürg. Robust and scalable 3-d geo-electromagnetic modelling approach using the finite element method. *Geophysical Journal International*, 198(1):110–125, 2014.
[2] Alexander V Grayver and Tzanio V Kolev. Large-scale 3d geoelectromagnetic modeling using parallel adaptive high-order finite element method. *Geophysics*, 80(6):E277–E291, 2015.
[3] Daniel Arndt, Wolfgang Bangerth, Maximilian Bergbauer, Bruno Blais, Marc Fehling, Rene Gassmöller, Timo Heister, Luca Heltai, Martin Kronbichler, Matthias Maier, et al. The deal. ii library, version 9.7. *Journal of Numerical Mathematics*, 33(4):403–415, 2025.
[4] Marc A Vallée and Mouhamed Moussaoui. Modelling the electromagnetic response of a sphere located in a layered earth. *Exploration Geophysics*, 54(4): 362–375, 2023.
[5] DF Aldridge and DW Oldenburg. Direct current electric potential field associated with two spherical conductors in a whole-space 1. *Geophysical prospecting*, 37(3):311–330, 1989.

Three-Dimensional Magnetotelluric Forward Modeling of a Conductive Sphere in a Resistive Half-Space: Analytical and Numerical Benchmarking

Leonardo A. Martins[1*]

[1]Instituto de Astronomia, Geofísica e Ciências Atmosféricas, Universidade de São Paulo, Brazil, *martinsla@usp.br

Benchmarking three-dimensional magnetotelluric (MT) forward modeling codes against analytical solutions is essential for validating numerical implementations before their application to real geological problems. This work presents the forward modeling setup for the MT3DINV4 workshop benchmark, which consists of a conductive sphere (0.1 Ω·m, radius 500 m, center depth 1000 m) embedded in a resistive half-space (1000 Ω·m), a geometry for which a rigorous analytical solution exists for any source-receiver configuration (Vallée and Moussaoui, 2023, Expl. Geophys., 54, 362–375).

Two independent forward models were computed for this benchmark. The analytical solution was evaluated using the algorithm of Vallée and Moussaoui (2023). The numerical solution was computed using the ModEM finite-difference code (Egbert and Kelbert, 2012, GJI, 190, 140–162; Kelbert et al., 2014, CG, 66, 40–53). Both solutions were evaluated at 2025 receivers on an irregular 45×45 grid centered on the sphere axis (10 m spacing near the axis to 5000 m at the grid edges) and at 71 log-spaced frequencies from 0.001 to 10,000 Hz.

The finite-difference grid was designed to satisfy two accuracy criteria simultaneously. First, cells within and around the sphere must resolve the skin depth inside the sphere material, $h \le \frac{\delta_s}{5}$, where δ_s reaches ~700 m near the sphere's inductive resonance and decreases to ~50 m at 10 Hz; a minimum cell size of h = 25 m was adopted, giving $\delta_s/h \ge 2$ across the frequency band of interest. Second, the staircase approximation of the spherical boundary, assigned per-cell (xc, yc, zc) as

$$\rho_{cell} = \begin{cases} \rho_s & if \quad (x_c - x_s)^2 + (y_c - y_s)^2 + (z_c - z_s)^2 \le a^2 \\ \rho_0 & otherwise \end{cases}$$

where (xs, ys, zs) and a are the sphere centre and radius. It introduces a geometric impedance error of $\frac{\Delta Z}{Z} \approx \frac{3h}{2a} \approx 7.5\%$, which represents an upper bound on the expected accuracy at this resolution. The resulting grid contains 86×86×134 cells, of which 33,552 represent the sphere interior, with 500 km horizontal and 300 km vertical padding to avoid edge effects at the lowest modeled frequency.

Two orthogonal profiles were extracted at T = 1 s (1 Hz): one running along the X axis directly over the sphere center, and one along the Y axis offset 25 m from the center.

Agreement between the two solutions is excellent along both profiles. Phase differences remain below 0.2° everywhere, including directly over the sphere. Apparent resistivity differences peak at approximately 3.5–3.7% at the profile center, directly over the sphere axis, where the ModEM staircase discretization error is expected to be largest, and decrease smoothly and monotonically with distance to about 1% at the profile edges (|d| ≥ 2000 m). This peak value is well within, and roughly half of, the 7.5% upper bound predicted by the staircase estimate, indicating that the h = 25 m grid resolution comfortably satisfies the design criteria for this benchmark. Tipper differences follow the same spatial pattern, peaking near the sphere (ΔT_Y up to ~3 percentage points at the profile center for both profiles) and decaying toward zero at the profile edges. Repeating the comparison at additional periods within the sphere's inductive response window (0.1–20 s) shows the same behavior with progressively smaller peak differences than at T = 1 s, indicating that the 1 s period represents a conservative (upper-bound) case for the reported misfit rather than an anomalous one.

These results confirm that the ModEM finite-difference solution reproduces the Vallée and Moussaoui (2023) semi-analytical benchmark to within a few percent across the full range of tested periods, with the residual misfit concentrated directly over the sphere and consistent in magnitude with the staircase discretization error anticipated from the grid design criteria. This benchmark configuration and comparison methodology provide a validated reference dataset for the MT3DINV4 workshop and a quantitative baseline for evaluating future finite-difference and finite-element implementations against the semi-analytical sphere solution.

GPU-Accelerated High-Order Finite-Element Modelling of the MT3DINV4 Sphere Benchmark

Ce Qin* — Henan Polytechnic University, Jiaozuo 454000, China, ce.qin@hpu.edu.cn

We used the MT3DINV4 conductive-sphere benchmark to assess an accelerated three-dimensional magnetotelluric (MT) forward solver. The full impedance tensor and vertical magnetic transfer functions were computed at 71 logarithmically spaced frequencies from 10 kHz to 0.001 Hz. Responses were evaluated at 90 locations along the recommended east–west profiles at $Y = 0$ and $Y = -250$ m. The calculations used a GPU-accelerated implementation of the matrix-free, high-order edge finite-element method of Qin and Grayver (2026). The electric field was discretized with second-order Nédélec basis functions on a locally refined octree mesh, and the linear systems were accelerated by a low-order-refined preconditioner. Matrix-free operator evaluation avoids explicitly assembling the high-order matrix and exposes the element-local arithmetic needed for efficient execution on modern accelerators.

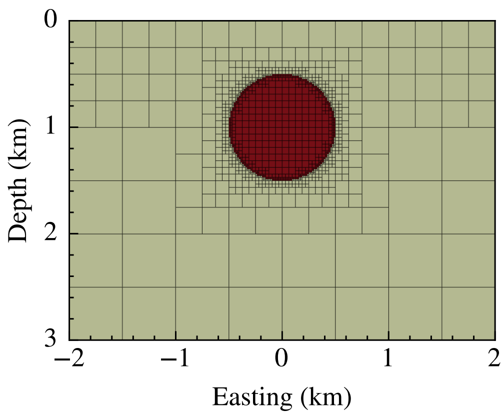

Figure 1: Cross-section of the locally refined octree mesh around the conductive sphere.

The octree mesh was refined locally in several stages within the central region, inside the conductive sphere, along the sphere boundary and around receivers (Fig. 1). The property mesh contains 66,820 hexahedral cells; with second-order basis functions, the receiver-refined state mesh has 69,970 cells and 1,513,274 degrees of freedom.

Across the complete frequency range, the numerical responses closely follow the analytical solution. Fig. 2 shows the responses at $(0, 0)$ and $(500, 0)$ m, corresponding to the grid centre and the sphere edge where the fields have characteristic extrema. On a single NVIDIA A100 GPU, the wall-clock time is less than 30 s per frequency. These results demonstrate that local octree refinement, second-order basis functions, and GPU acceleration can deliver accurate broadband 3-D MT responses with a compact mesh and short time-to-solution.

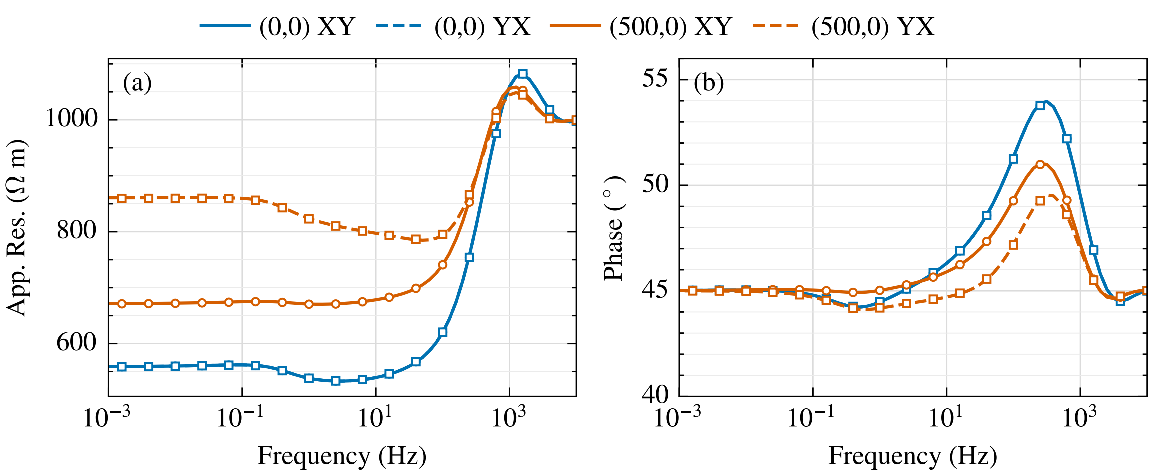

Figure 2: Apparent resistivities and phases at $(0, 0)$ and $(500, 0)$ m. Curves show the analytical solution; symbols show the numerical solution. YX phases are shifted by 180°.

References.

Qin, C. & Grayver, A., 2026, *Geophys. J. Int.*, 244, ggaf471, doi: 10.1093/gji/ggaf471.

Vallée, M. & Moussaoui, R., 2023, doi: 10.1080/08123985.2022.2162382.

Forward modeling results for the MT3DINV4 forward model

Changkai Qiu[1*], Yunhe Liu[2], Zhejian Hui[3]

[1]Key Laboratory of Deep Petroleum Intelligent Exploration and Development, Institute of Geology and Geophysics, Chinese Academy of Sciences, Beijing 100029, China

[2]College of Geo-exploration Science and Technology, Jilin University, Changchun, Jilin 130026, China

[3]College of Geophysics, Chengdu University of Technology, Chengdu, Sichuan 610059, China

E-mail: qiuchangkai@hotmail.com;

For the forward problem, we solve the curl-curl equation for the total electric field with non-homogeneous Dirichlet boundary conditions using Nédélec finite elements (FEs) on tetrahedral meshes. We solve the 2D MT problem on the two vertical planes twice using vector FEs on triangular meshes for each polarization direction to obtain these boundary conditions. The time dependence is $\mathrm{e}^{\mathrm{i}\omega t}$. The complex-valued FE system is transformed into an equivalent real-valued form and solved using the flexible generalized minimal residual (Flexible GMRES, FGMRES) method with an optimal block-diagonal preconditioner. This preconditioning is executed by the auxiliary-space Maxwell solver (AMS) based on the Hiptmair–Xu decomposition. We have applied similar solution techniques to controlled-source electromagnetic (CSEM) modeling (Qiu et al., 2021), and are currently preparing a follow-up study on MT simulations that integrates second-order FEs and a novel explicit divergence projection technique.

To accommodate the broad frequency band, we implemented a nested meshing strategy for the forward model. The outermost mesh (LF-Mesh), spanning $[1000\ \mathrm{km}]^3$, is designated to resolve the low-frequency band. From this domain, a $[600\ \mathrm{km}]^3$ sub-mesh (MF-Mesh) is extracted for the mid-frequency band, within which a localized $[40\ \mathrm{km}]^3$ sub-mesh (HF-Mesh) is further embedded for the high-frequency band. This effectively addresses the challenge that high-frequency calculations require not only volumetric refinement within the modeling domain but also finer discretization on the outer boundaries to accurately solve the 2D boundary conditions. Furthermore, we locally refined the mesh within the top 500 meters below the Earth's surface for the high-frequency simulations.

Numerical computations were conducted on a dedicated cluster node equipped with an AMD EPYC 9754 128-Core Processor and 2 TB of RAM. Specifically, we allocated 64 cores for the forward modeling. For a given frequency and a specific polarization mode (E_x or E_y), the forward modeling was performed using multi-core parallelization, whereas the execution of both

Vector Finite-Element Modeling of Three-Dimensional Magnetotelluric Responses on Unstructured Tetrahedral Meshes

Shikai Shen[1,2,3*], Xushan Lu[1,2,3], Minghong Liu[1,2,3], and Huaifeng Sun[1,2,3]
1. State Key Laboratory for Tunnel Engineering, Shandong University
2. Institute of Geotechnical and Underground Engineering, Shandong University
3. Laboratory of Earth Electromagnetic Exploration, Shandong University

For Task 1, forward responses were computed with the em3d-MT code (Liu et al., 2025), which is implemented in MATLAB. Using the $e^{i\omega t}$ time convention, the code solves the full-current electric-field equation, and Dirichlet boundary conditions were imposed on the outer boundary. This formulation retains both conduction and displacement currents and therefore avoids the quasi-static approximation, allowing em3d-MT to represent both diffusion- and wave-dominated behavior. The equation is discretized using the vector finite-element method on unstructured tetrahedral meshes. A two-level parallel scheme distributes frequency tasks among MPI processes and uses OpenMP within each process.

For the Task 1 sphere-in-half-space benchmark, the computational domain measures 150 km $\times$ 150 km $\times$ 160 km. The mesh contains 1,004,095 tetrahedra. Responses were calculated at 2,025 surface receivers on a 45 $\times$ 45 nonuniform grid spanning −5 to 5 km in both x and y and at 71 logarithmically spaced frequencies from 0.001 to 10,000 Hz. On a Linux workstation with 18 2.4-GHz CPU cores, a representative 1-Hz solve using nine MPI processes and two OpenMP threads per process required 12.39 GB of peak memory and 348.85 s; the complete 71-frequency simulation required 3,196.29 s. Figure 1 compares em3d-MT and MTSphere ρ_{xy} and ϕ_{xy} responses at 0.01 and 1,000 Hz. The first two columns show ρ_{xy} from MTSphere and em3d-MT, respectively; the third shows the relative error. The last two columns compare ϕ_{xy}. The codes agree well at 0.01 Hz, whereas discrepancies increase at 1,000 Hz, where shorter skin depths make the solution more sensitive to local mesh resolution.

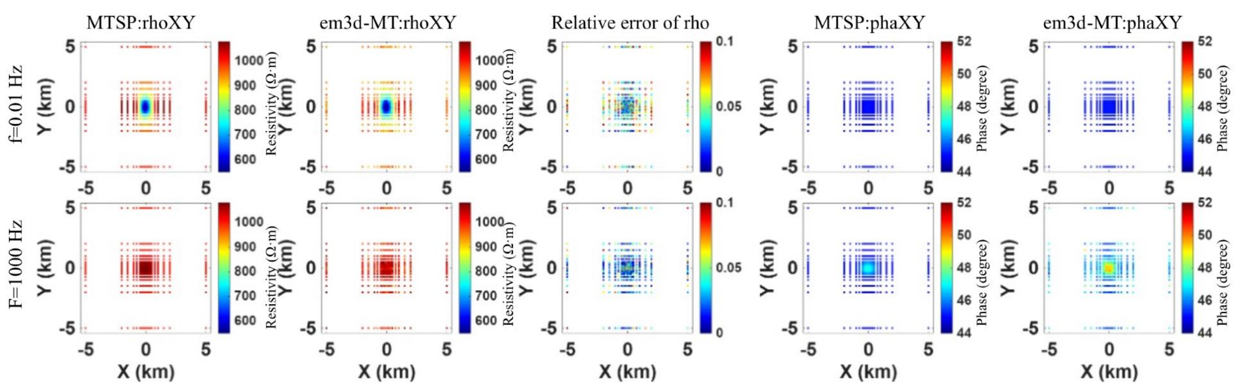

Figure 1. MTSphere and em3d-MT ρ_{xy} and ϕ_{xy} responses at 0.01 and 1,000 Hz. The top and bottom rows correspond to 0.01 and 1,000 Hz, respectively. The first and second columns show ρ_{xy} from MTSphere and em3d-MT; the third shows the relative error. The last three columns show the corresponding ϕ_{xy} responses.

References

Liu, M., X. Lu, H. Sun, Z. Zheng, J. Xie, S. Zhang, and S. Liu, 2025, em3d-MT: Three-dimensional forward modeling of radio-magnetotelluric data considering displacement currents in anisotropic media: Geophysics, 90, no. 5, F101–F113, doi: 10.1190/geo2025-0041.1.

MagnetotelluricsHD.jl : A scalable Julia package for Magnetotelluric modeling

Abhinav Pratap Singh[1]
[1] Georgia Institute of Technology

We present MagnetotelluricsHD.jl, a distributed, GPU-accelerated 3-D magnetotelluric (MT) forward solver written in Julia language. We discretize the complex valued electric-field formulation using a staggered grid based finite-volume method. By formulating the problem in terms of edge-integrated fields, we obtain a symmetric non-Hermitian linear system, which we solve using FGMRES with Auxiliary Maxwell Space (AMS) preconditioner. Our AMS formulation consists of L1-Jacobi smoothing, Nédélec-interpolation vector corrections decomposed into three smaller systems, and divergence correction. All the four systems are symmetric positive definite, and being much smaller than the curl-curl system, we solve them using sparse direct factorizations. Although the direct solvers are more memory- and compute-intensive than the iterative solvers, the cost is amortized through factorization reuse. What is more, the number of FGMRES iterations is also cut down significantly, leading to much shorter solve times.

The package supports inter-node parallelism across frequencies. Per frequency, we leverage intra-node parallelism to solve the AMS subsystems using Pardiso. This allows us to scale the forward computation across multiple nodes. We additionally extend the codes to leverage CUDA GPUs to further accelerate the solve times, and show scalability across multiple GPUs. In this work, we validate the solver against the analytical solution for a conductive sphere embedded in a resistive half-space and demonstrate its scalability across different parallel regimes. Future works involve developing adjoint solvers for integration with automatic differentiation libraries in Julia.

MT3DINV4 Task 1 modeling: custEMx

N. Skibbe[1], R. Rochlitz[1]
[1]LIAG Institute for Applied Geophysics

In the scope of the MT3DINV4 workshop we used the newly developed custEMx library to prepare modelling task 1.

CustEMx is based on the original custEM library from Rochlitz et al. (2019) and implements multiple forward and inversion routines for electromagnetic modelling and inversion. CustEMx is using a finite element library FEniCSx (Baratta et al., 2023), which we use for calculation of electric fields on unstructured tetrahedral meshes. We use Nédélec elements (edge elements) first kind of first or second polynomial order to solve the curl-curl equation of the electric fields for both CSEM or in this case MT. As tangential components for these function spaces are continuous implicitly, they are a common choice for curl-curl problems throughout many disciplines. For the MT case the boundary conditions are derived from analytic 1D solutions at the edge of the mesh. Two polarizations are used as common for these natural source cases. The resulting electric fields are curled into magnetic fields and then specific MT responses at predefined coordinates are calculated as requested in task 1. This engine will also be the core forward operator of the second task on the workshop.

We will show briefly the results but focus on the implementation of the MT part of custEMx to then have a good basis for subsequent discussion and exchange.

Baratta, I. A., Dean, J. P., Dokken, J. S., Habera, M., Hale, J. S., Richardson, C. N., Rognes, M.E., Scroggs, M. W., Sime, N., & Wells, G. N. (2023). DOLFINx: The next generation FEniCS problem solving environment

Rochlitz, R., N. Skibbe, and T. Günther 2019. custEM: Customizable finite-element simulation of complex controlled source electromagnetic data. Geophysics, 84(2): F17–F33.

Forward problem Task 1

M.Yu.Smirnov[1] and O.Rydman[1]
[1]Luleå University of Technology, Sweden

The forward model is a sphere in a half-space. Impedance transfer functions were computed at **2,025 locations** defined by a 45 × 45 grid. All positions are in metres relative to the geographic reference point defined in the task description. Impedances are submitted in EDI format.

Type of code used: FD MR3DMod
Mesh dimensions: 140x140x40
Computing time: approx. 5 min per period to relative accuracy of 1E-10
Hardware details: Desktop Intel Core Ultra 128 GB.

Model and discretization are depicted in Fig.1. The results as phase and apparent resistivity of the determinant of the impedance tensor are shown in Fig.2.

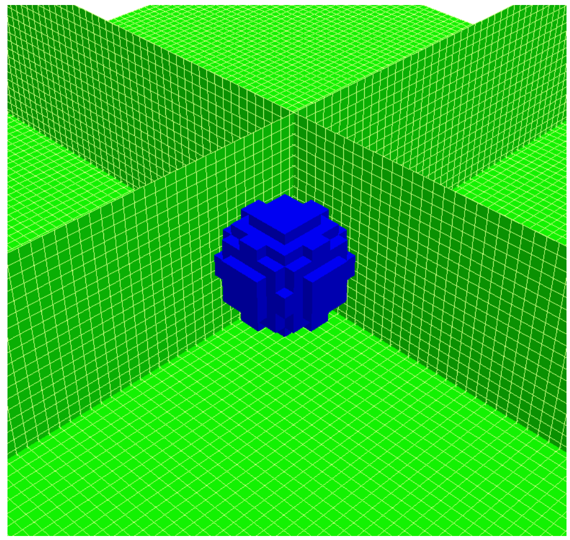

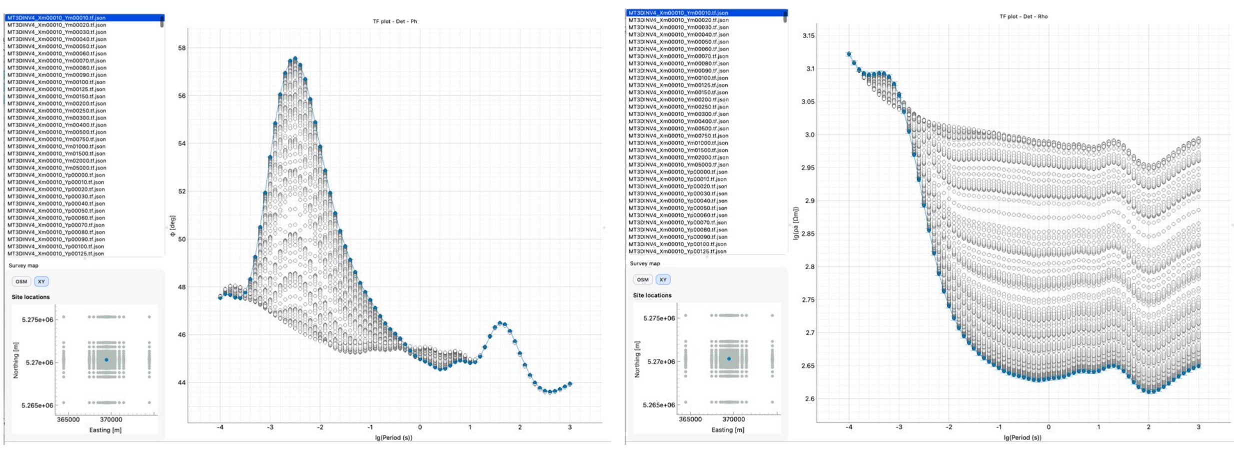

Figure 2 Phase and apparent resistivity of the determinant of the impedance tensor

Tailoring Meshes per Frequency with OcTree Meshes in SimPEG for 3D MT

Santiago Soler[1], Rylan Stutters[1], Lindsey J. Heagy[1]
[1] *Geophysical Inversion Facility, University of British Columbia*

Multi-frequency 3D MT simulations are conventionally run on a single mesh, which must resolve the shortest skin depth in the survey while also extending well beyond the longest. Since MT surveys commonly span many decades in frequency, this makes the mesh large, every forward simulation expensive, and that expense is multiplied hundreds of times over in an inversion. With SimPEG's meta-simulation framework, we instead give each frequency its own skin-depth-scaled octree mesh: a single fine mesh holds the conductivity model, and volume-averaging mappings carry it onto each simulation mesh (Figure 1). We benchmark against the analytic solution for a conductive sphere in a halfspace (Vallée & Moussaoui, 2023), with meshes of a few thousand cells reproducing the analytic impedances within 5% at all stations and frequencies . For this example (8 frequencies spanning 0.001 to 10,000 Hz, 22 stations), the forward simulation takes about 2 s serially, and under 1 s across 8 processes (the runtime is limited by the slowest frequency), in under 2 GB of memory; the equivalent single-mesh simulation takes several minutes and tens of GB.

Because the composite simulation exposes SimPEG's standard simulation methods like `dpred`, `Jvec`, and `Jtvec`, it fits directly into the inversion framework. Sensitivities are propagated through SimPEG's "mapping" objects, which define a transformation of the model and their associated derivatives (Kang et al., 2015), so the volume-averaging maps are transparent to the inversion machinery. The operations that dominate inversion run time inherit the same savings.

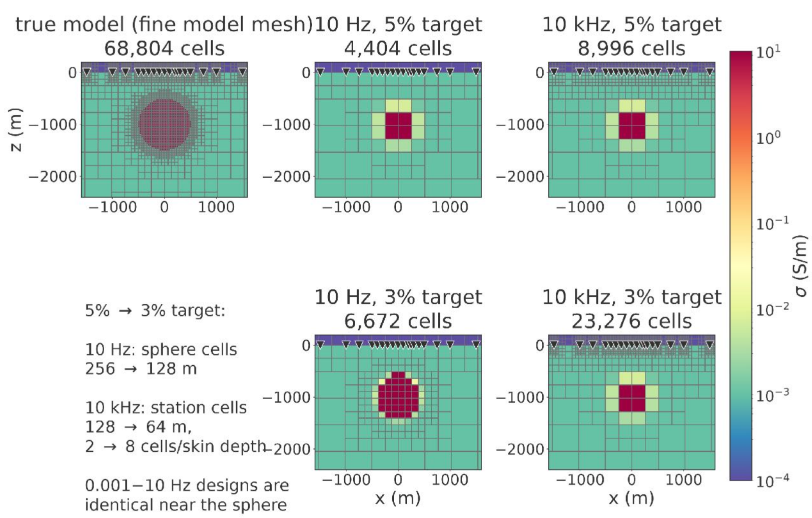

Figure 1. True model on the fine mesh (top left), and its volume-averaged conductivity on the 10 Hz and 10 kHz meshes for the 5% (top) and 3% (bottom) accuracy targets.

References

Cockett, R., Kang, S., Heagy, L.J., Pidlisecky, A. & Oldenburg, D.W. (2015) SimPEG: An open source framework for simulation and gradient based parameter estimation in geophysical applications. doi:10.1016/j.cageo.2015.09.015

Heagy, L.J., Cockett, R., Kang, S., Rosenkjaer, G.K. & Oldenburg, D.W. (2017) A framework for simulation and inversion in electromagnetics. doi:10.1016/j.cageo.2017.06.018

Kang, S., Cockett, R., Heagy, L.J. & Oldenburg, D.W. (2015) Moving between dimensions in electromagnetic inversions. doi:10.1190/segam2015-5930379.1

Stutters, R., Deleersnyder, W., Soler, S. & Heagy, L.J. (2026) Techniques for Improving MT Forward Simulations with Octree Meshes. 4th MT 3D inversion workshop (MT3DINV4).

Vallée, M.A. & Moussaoui, M. (2023) Modelling the electromagnetic response of a sphere located in a layered earth. doi:10.1080/08123985.2022.2162382

Techniques for Improving MT Forward Simulations with Octree Meshes

R. Stutters*, W. Deleersnyder, S. Soler, and L.J. Heagy
University of British Columbia, Geophysical Inversion Facility
* Presenting Author

Mesh refinement drives a tradeoff between accuracy and computational costs for Magnetotelluric forward modelling. We conduct simulations in the SimPEG framework to investigate this tradeoff and evaluate various Octree mesh refinement schemes against the analytic solution for a conductive sphere in a resistive halfspace. We also present volume averaging techniques to reduce inaccuracies associated with representing the sphere using discretized cells.

Two refinement scheme parameters are studied: refinement around the sphere and refinement around the receivers. Comparison to the analytic solution and computation time are used as figures of merit as these parameters are independently varied. The percent residuals of the simulated impedances follow a linear relationship as refinement is varied (Figure 1).

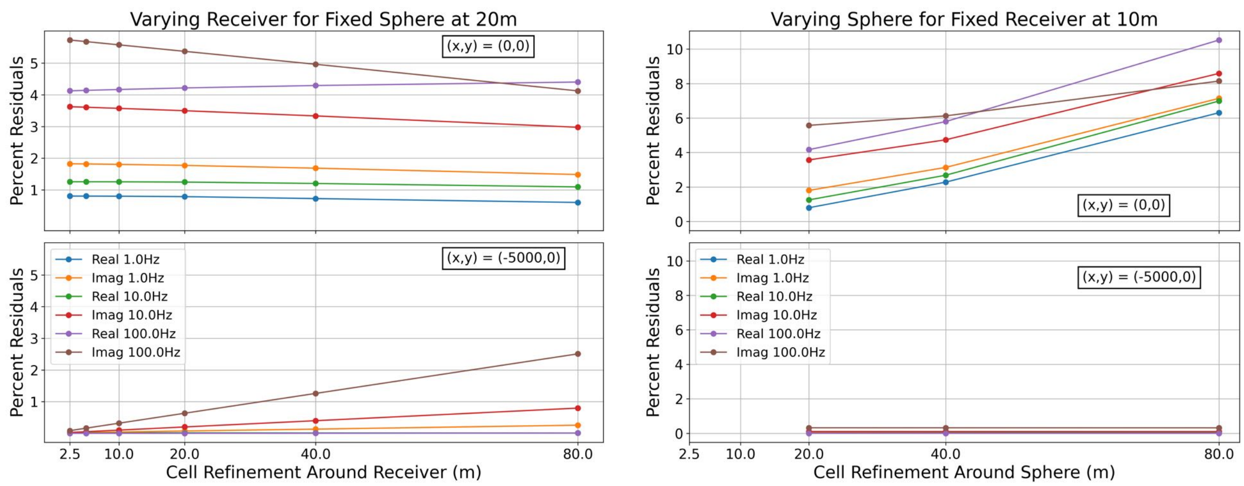

Figure 1: Impedance residuals for varying refinement schemes.
The same mesh is used to simulate all frequencies.

Volume averaging techniques are applied to the model by assigning conductivities based on the fraction of a cell which is enclosed within the sphere. Methods favouring lower conductivities such as harmonic averaging were found to be more effective than methods favouring higher conductivities, such as geometric averaging. Using the method of harmonic averaging, the percent residuals above the sphere can be reduced by more than a factor of two. The submitted results leverage this technique to produce a model with impedance residuals under 1% for low frequencies (up to $1\,\mathrm{Hz}$) and under 5% for the mid to high frequencies (up to $1\,\mathrm{kHz}$), all while using less than half the computation time and memory required for an equivalently performing mesh built from the standard cutoff procedure (Figure 2).

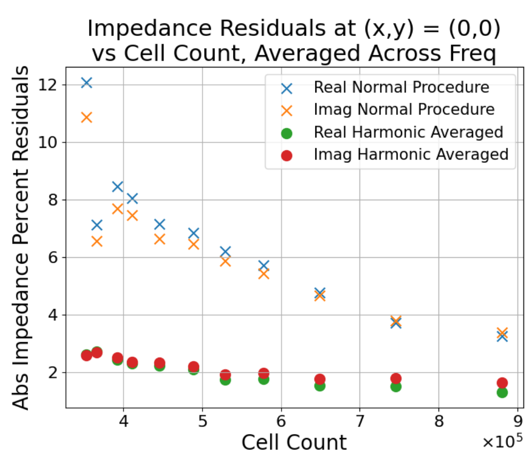

Figure 2: Harmonic averaged mesh improvements for varying cell counts.

Forward Modeling Results for the MT3DINV4 Using a Finite Volume MT Code

Atsushi Suzuki, JX Metals Resources Exploration ＆ Development Co., Ltd.

Numerical method: Finite volume method with the magnetic field as the primary variable (Suzuki, 2025)

Mesh: 114 × 114 × 96 cells, including 10 air layers; rectangular mesh

Minimum cell size: Δx = 10 m, Δy = 10 m, Δz = 40 m

Hardware: Intel Core i7-14700, 64 GB RAM

Parallelization: Only 4 CPU cores were used due to memory limitation for this calculation.

Computing time: 317 min

Reference: Suzuki (2025), doi: 10.1007/s12145-024-01666-z

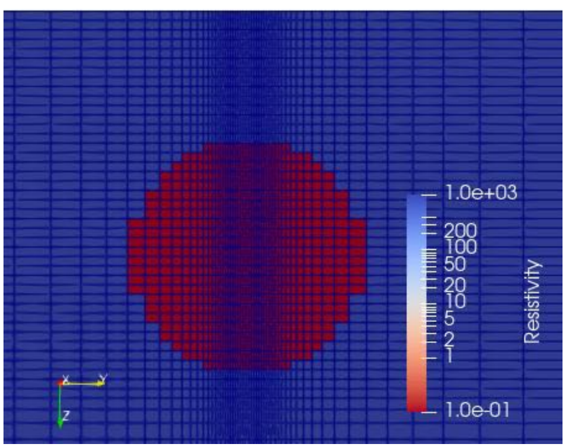

Figure 1

Mesh cross-section of the mesh near the center

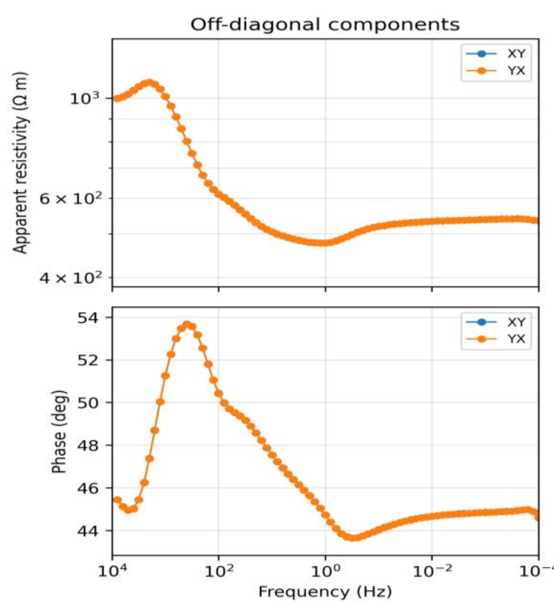

Figure 2

Calculated apparent resistivity and phase at (X, Y) = (0, 0). The phase at 10^{-4} Hz deviates slightly from the trend at adjacent frequencies. This may reflect a limitation of using the same mesh over the wide frequency range from 10 kHz to 10^{-4} Hz.

3D Magnetotelluric Forward Modeling: Benchmarking Hierarchical Finite Elements and Multi-GPU Acceleration on the Task 1 Sphere Model

Deniz Varılsüha*,[1], Özcan Özyıldırım[1]

[1] *Application and Research Center of Geothermal and Mineral Deposits, Afyon Kocatepe University, Afyonkarahisar, Türkiye.*

This study presents a 3D magnetotelluric (MT) forward modeling framework, METOD-3D, utilizing hierarchical edge-based finite element methods on unstructured tetrahedral meshes. In the context of the MT3DINV4 workshop, we utilize the "Task 1" benchmark model—a conductive spherical anomaly (0.1 Ω·m, radius 500 m) embedded in a 1,000 Ω·m half-space at a depth of 1,000 m—to validate our numerical framework against the analytical solution provided by Vallée and Moussaoui [1]. Our methodology employs Nédélec-type curl-conforming vector basis functions and a hierarchical formulation that enables flexible p-adaptivity. The system matrices are efficiently factorized using a multi-GPU sparse direct solver (cuDSS), which significantly accelerates computation times compared to standard CPU-based implementations.

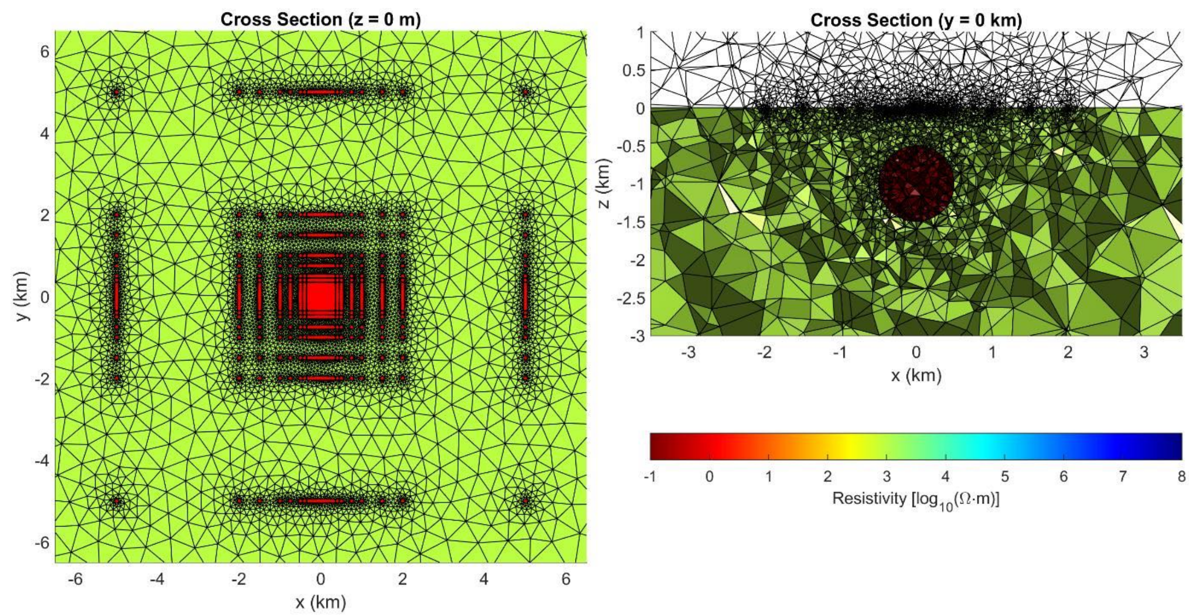

Figure 1: Overview of the unstructured tetrahedral mesh used for the Task 1 forward model. On the left, the refined mesh around the central MT sites at the surface and within the conductive spherical anomaly can be seen. On the right, the cross-section of the buried spherical anomaly is presented. The domain boundaries extend sufficiently to minimize boundary effects, which are not shown here.

Table 1: Technical Specifications for Task 1 Submission

Parameter	**Description**
Code Type;	FE (Hierarchical Finite Elements, METOD-3D)
Mesh Dimensions;	~500K quadratic elements, ~86K nodes.
Computing time:	~1 minutes to to factorize ~ 3.2M DoF matrix size
Hardware details:	24-core Intel 285K CPU, 8 x RTX 3090 Nvidia GPU
Source Code;	https://github.com/varilsuhad/METOD-3D

[1] Vallée, M., Moussaoui, M., 2023. Analytical solution for the magnetotelluric response of a sphere in a half-space, doi: 10.1080/08123985.2022.2162382.

3D MT modeling with finite element method in a hybrid domain

Shunguo Wang[1], Shikun Dai[2], Dongdong Zhao[3]

1 Geological Survey of Norway, Section of Geophysics, Trondheim, Norway

2 Central South University, School of Geosciences and Info-physics, Changsha, China

3 Guilin University of Electronic Technology, School of Electronic Engineering and Automation, Guilin, China

The method adopts a hybrid Fourier–finite element formulation. The governing three-dimensional equations are first transformed into the horizontal wavenumber domain by applying two-dimensional fast Fourier transforms (FFTs) in the x- and y-directions. This transformation diagonalizes the horizontal differential operators and decomposes the original 3D problem into a set of independent one-dimensional boundary-value problems in the vertical (z) direction, one for each horizontal wavenumber pair (k_x, k_y). Each resulting 1D equation is discretized and solved using the finite element method (FEM), which efficiently accommodates variable material properties and complex vertical stratification. After solving all wavenumber-domain problems, the physical-space solution is reconstructed by applying the inverse FFT.

For the spherical anomaly model considered in TASK1, a computational mesh of 1001 * 1001 * 251 cells was employed, with a uniform grid spacing of 10 m in the x- and y-directions, and varying grid spacing in the z-direction from 0.5 m to 82.7km. Twenty air layers were included above the surface in the negative z-direction. Simulations were performed using 50 CPU cores per frequency. Due to substantial memory requirements, computations were distributed across eight compute nodes. A total of 71 frequencies were calculated within a single job; however, memory constraints limited each node to processing at most five frequencies simultaneously. All computations were carried out on nodes equipped with AMD EPYC 9745 128-core processors.

The complete simulation required approximately 9.9 hours of wall-clock time, with a peak memory consumption of 124 GB for each frequency. The computed responses were compared with those obtained using the MTsphere program. Overall, the two solutions agree well at low frequencies, whereas clean differences emerge at high frequencies. A detailed investigation of these differences is ongoing.

In future work, the method will be extended to support irregular meshes in the horizontal directions, enabling local mesh refinement around regions of interest while maintaining a coarser discretization elsewhere without loss of accuracy.

MT3DINV4: Forward Modelling of the Magnetotelluric Response over a Buried Sphere

Andrew Williamson*, Ryan Olson, Hormoz Jahandari

Dias Geophysical Ltd.

A buried sphere of low resistivity compared to its surrounding material constitutes a simple geological model that may be roughly descriptive of many targets in mineral exploration. As such, an understanding of the magnetotelluric response of such features may provide insight towards the data recorded during MT geophysical survey activities for mineral exploration. Additionally, a general analytical solution of the MT response for a sphere exists and can be used to assess and validate the results produced by forward modelling algorithms. To this end, the forward response of a buried sphere system was produced using a forward modelling algorithm based on SimPEG. The MT impedance and tipper responses were computed for 2025 stations distributed on an irregularly spaced grid at the surface above the conductive sphere. The forward response was calculated using a tensor mesh, which created challenges in sufficiently discretizing the entire region of interest. Responses were computed at 70 logarithmically spaced frequencies in the range $10^4 – 10^{-3}$ Hz. The tensor mesh was composed of 60 cells in the horizontal x and y-directions, and 66 cells in the vertical z-direction, for a total of 237,600 cells. Cell thicknesses in the x and y-directions increased away from the model center and were chosen based on the irregular station spacing. Vertical discretization used an initial cell thickness of 50 m, with cell thickness increasing geometrically downwards by a factor of 1.15. Computed impedance responses were compared to the analytic solution of Vallée and Moussaoui (2023)[1] and were found to be within approximately 20% in apparent resistivity and 10% in phase.

1 Vallée, M. A., & Moussaoui, M. (2023). Modelling the electromagnetic response of a sphere located in a layered earth. *Exploration Geophysics*, *54*(4), 362-375.

Three-Dimensional Magnetotelluric Forward Modeling Using Vector Finite Elements on Unstructured Tetrahedral Meshes

Shuowei Zhang[1,2,3], Xushan Lu[1,2,3], and Huaifeng Sun[1,2,3]
1. State Key Laboratory for Tunnel Engineering, Shandong University
2. Institute of Geotechnical and Underground Engineering, Shandong University
3. Laboratory of Earth Electromagnetic Exploration, Shandong University

A parallel three-dimensional magnetotelluric (MT) forward modeling program based on the vector finite-element method with first-order Nédélec edge elements is used for Task 1. Built on the finite-element framework of Lu and Farquharson (2020), the code solves the electric-field curl–curl equation with the $e^{i\omega t}$ time convention and Dirichlet boundary conditions from 1D analytical electric fields. Unstructured tetrahedral meshes are generated with Gmsh, and the frequency-domain linear systems are solved with MUMPS under hybrid MPI–OpenMP parallelization.

The Task 1 sphere-in-half-space model is discretized into 1,769,138 tetrahedra with 2,062,092 edges. Both ρ_{xy} and ϕ_{xy} are calculated at 2,025 receivers and 71 logarithmically spaced frequencies from 0.001 to 10,000 Hz. Figure 1 compares our responses with those of MTSphere at 0.001, 1, and 10,000 Hz. Agreement is good at low frequencies, with mean absolute percentage errors (MAPE) of 1.09% and 2.88% for ρ_{xy} at 0.001 and 1 Hz, respectively; at 10,000 Hz the MAPE reaches 15.39%. Similar patterns occur for ϕ_{xy}, with mean absolute errors of 0.02°, 0.12°, and 3.42°. Larger high-frequency errors likely reflect skin depths smaller than the local cell size and the neglect of displacement currents in our code relative to MTSphere.

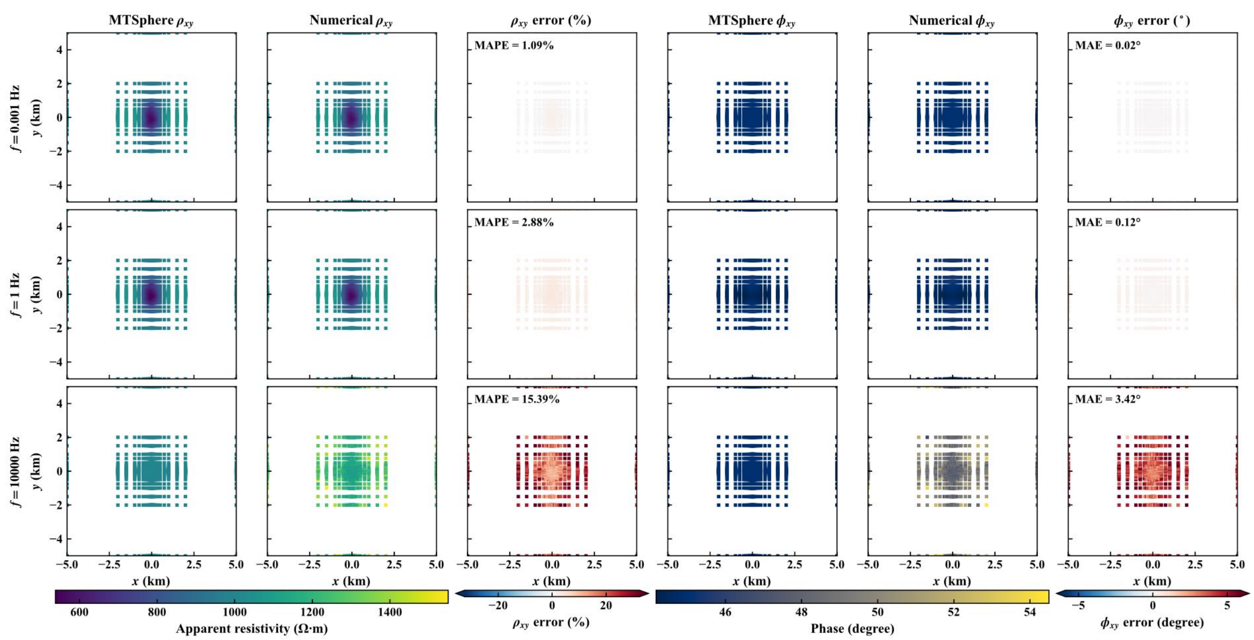

Figure 1. MTSphere and numerical ρ_{xy} and ϕ_{xy} responses at 0.001 Hz (upper row), 1 Hz (middle row), and 10,000 Hz (lower row). Columns show MTSphere, our code, and the difference for ρ_{xy}, then the same comparison for ϕ_{xy} responses (error in degrees).

References

Lu, X., and C. G. Farquharson, 2020, 3D finite-volume time-domain modeling of geophysical electromagnetic data on unstructured grids using potentials: Geophysics, 85, no. 6, E221–E240, doi: 10.1190/geo2020-0088.

MT3DINV4S – Secret Model

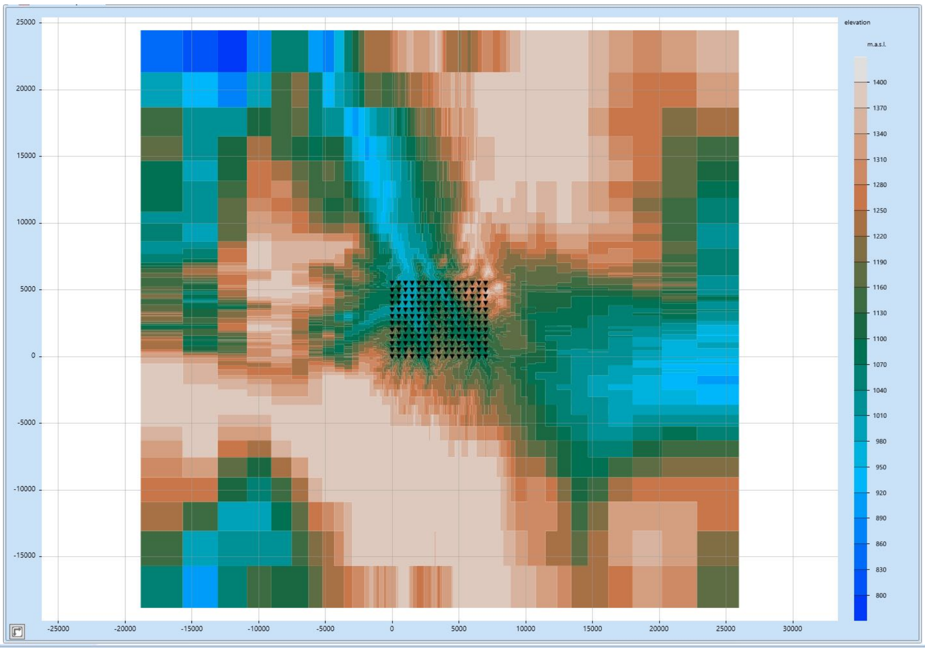

Three-dimensional MT inversion for MT3Dinv4 Workshop: Secret Model data inversion

Seyed Masoud Ansari
Geological Survey of Canada, Natural Resources Canada, Ottawa, Canada
seyedmasoud.ansari@nrcan-rncan.gc.ca

Extended summary

The work presented here considers the inversion of MT data for a secret model. Figure 1a shows a central view of the computational domain, including local mesh refinement to a depth of 2.5 km and at MT sites. Although not shown here, the lateral mesh boundaries were located 50 km from the model origin. To incorporate topographic features into the mesh, the relatively dense elevation data were downsampled at intervals of 300 m within the area of interest and 2500 m within the padding zone. Elevations were then assigned to sampled mesh points using inverse-distance weighting. The mesh skeleton was constructed in FacetModeller, and the final tetrahedral mesh was generated using TetGen. Figure 1b presents a zoommed view of the topographic Earth surface within the main area of interest.

The inversion was perfomred for the impedance data using the finite-element based inversion code of Ansari and Craven (2023). For the particular experiment presented, Gaussian noise levels of 2% and 5% were assinged to the off-diagonal and diagonal noise-free impedances, respectively. For each datum, the standard deviation was defined as the larger of the specified percentage of that datum and the corresponding percentage of $\sqrt{|Z_{xy}Z_{yx}|}$. The inversion was initialized using both the initial model and a reference model of a 25 $\Omega \cdot m$ half-space. A relatively large initial trade-off parameter (λ) was used and reduced by a cooling factor of 0.65. A minimum value of 5000 was imposed on the trade-off parameter. Figure 2 shows the progressive reduction of the data misfit (ϕ_d), and the total objective function (ϕ) with iteration. Here, a normalized RMS of 1.7 was reached after 34 iterations, after which the model was smoothed furhter in additional iterations. Figure 3 shows the inverted model for iteration 37 within a volume encompassing all MT sites. Vertical sections through the model were also shown. A prominent feature is an isolated conductivity body observed along profiles A1A2 at depths between -1000 and -500 m. Reference: Ansari, S. M., Craven, J. A., 2023. A fully finite-element based model-space algorithm for three-dimensional inversion of magnetotelluric data, Geophysical Journal International, Volume 233, Issue 2, Pages 1245–1270

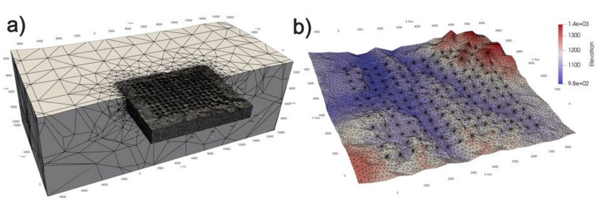

Figure 1: Views of the meshed domain used for inversin of data of the secret model: a) a central cut showing refinement in the main area of interest; b) a zoomed view of the topgraphic Earth surface at the MT sites.

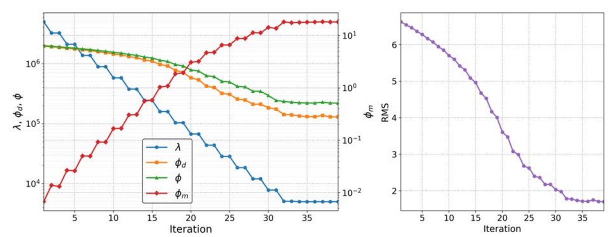

Figure 2: The behaviour of inversion parameteres including the trade-off, λ, objective functions of ϕ_d, ϕ_m, ϕ, and RMS versus iteration.

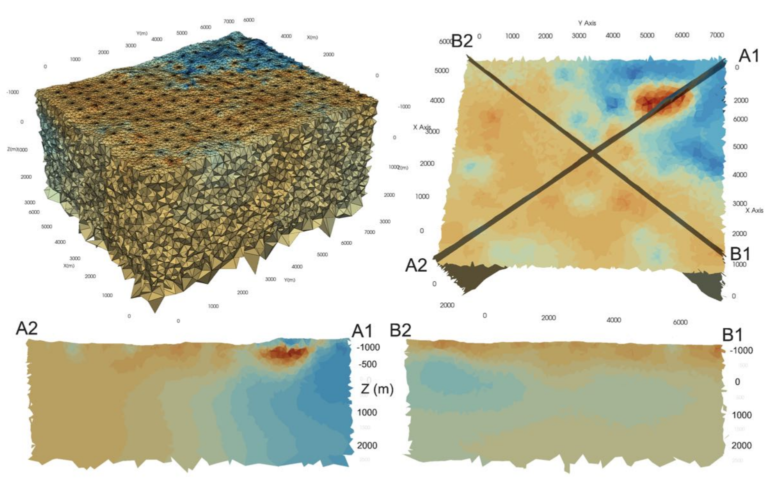

Figure 3: Inversion resistivity model after 37 iterations. Two depth sections show resistivities to a depth of 3 km.

Covariance effect on MT + tipper 3D inversion using ModEM

Thalia Aviles[1], Kate Selway[1]
[1] VOX Geophysics

This study employs forward-modeled MT and tipper data (with added noise), comprising 180 stations (12 x15 grid, 500 m spacing). Each station provides MT and tipper data across 35 frequencies (25,000 –10 Hz). Frequency-domain analysis of apparent resistivities, phase tensors, and induction arrows reveal two main resistivity zones: a conductive, 1D zone to the SW, and a more resistive zone to the NE with a deeper conductor and strong 3D effects. Inversions were performed using ModEM3D (Egbert and Kelbert, 2012; Kelbert et al., 2014) using 18 of the 35 available frequencies. The model domain was discretized into an 80x90x79 grid (N-S/E-W/depth) incorporating topography, with core cells 150 m wide. In this work, we analyzed the impact of the covariance value on data fit and on the modeled features recovered from joint inversions of MT and tipper data. Model 1 used a 30 Ohm-m homogeneous half-space as *a apriori* model, with a horizontal covariance of 0.3 (Figure 1, top). Model 2 used, as its starting model, the perturbed model obtained from the last iteration of Model 1, with a horizontal covariance of 0.1 (Figure 1, bottom). For both models, the vertical covariance was set to 0.3.

Both models reveal distinct features in the SW and NE areas. At depths less than ~500 m, the SW zone is ~30 Ohm-m and is characterized by small, disconnected conductive and resistive bodies (Figure 1) that are more exaggerated in Model 2 than Model 1. In the NE zone, C1, is a shallow feature of <3 Ohm-m and 200 to 300 m thick; and C1p is ~10 Ohm-m, ~300 m thick and extends from 300 to 500 m depth. R2 is >100 Ohm-m, reaches the surface in the NE of the model and, from 500 to 1500 m depth, appears to connect with R1 and extend across the whole model.

The reduced covariance in Model 2 increases shallow structure in the SW beyond what may be resolvable by the data. We expected that a lower covariance could better define the boundaries of the anomaly C1, but the fits of the four components (specially xy), at two stations located at the edges of C1 are markedly worse for Model 2 (Figure 1). For most other features, Model 2 improves the fit in the diagonal components relative to Model 1, while the off-diagonal fit does not change significantly. These results show that the structures R1, R2, C1p and C1 are robust enough to be recovered by both inversion approaches, while the reason for the poorer fit for station on the boundaries of the strong conductor C1 at reduced covariance remains intriguing.

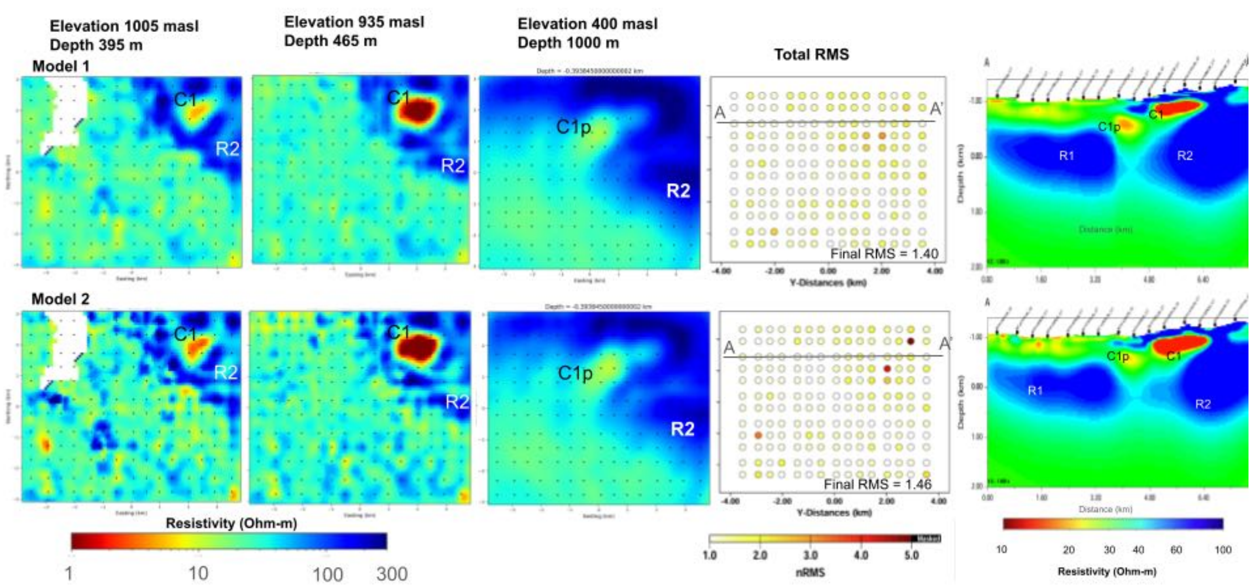

Figure 1. Horizontal slices and total RMS maps from two 3D resistivity models derived using MT and tipper data, with horizontal covariances of 0.3 (top) and 0.1 (bottom). Profile A-A' shows the main structures. The top of the model is 1400 m elevation (masl).

How to build a (reasonable) 3D EM model — Insights from the MT3DINV4 Secret Model Task

H. Dong[1,2*]
[1]China University of Geosciences, Beijing, 100083
[2]State Key Laboratory of Geological Processes and Mineral Resources, Beijing, 100083
[*]donghao@cugb.edu.cn

SUMMARY

With the rapid development of three-dimensional (3D) geophysical forward and inversion algorithms, inversion has become increasingly accessible to researchers and students. Sophisticated helper programs and GUI tools have greatly simplified the once-complicated inversion workflow — data pre-processing, mesh design, and running inversions. Those with basic knowledge of geophysics can conduct a complex 3D inversion with a few mouse clicks. However, the model structures obtained from the same observed data and inversion code can differ dramatically, with respect to both the experience of the user and the choices made during the process.

In this study, we present an experiment, in which three students (two PhDs and one Master's) were asked to independently invert a common magnetotelluric dataset generated from the MT3DINV4 secret model using the same ModEM inversion code. Each student is given a same basic inversion recipe but made independent choices during mesh design, topography integration, starting model, data error assignment, and regularization parameter selection. We compare their resulting models with each other and with one "baseline" result from the teacher. Our results show that despite identical data and algorithm, the three student models exhibit substantial differences in resistivity distribution, structural geometry, and even depth of investigation. Apparently, only by understanding how each inversion design and parameters propagates through the inversion process can one recover a model structure that meaningfully approximates the true underground structure. This experiment underscores the critical role of understanding the inversion physics — beyond mere operational proficiency, to produce geologically "reasonable" 3D models.

Keywords: Inversion, Magnetotellurics, Secret Model

Inversion of the MT3DINV4S Secret Data

Alan G. Jones[1] and Randall L. Mackie[2]

1) ManoTick GeoSolutions Ltd., alan.jones@manotick-geosolutions.com
2) Viridien, Randall.Mackie@viridiengroup.com

The noise-free data from the MT3DINV4S Secret Model were inverted using Viridien's RLM-3D code. Successive inversions across two grids, an initial relatively coarse grid with 250 m cell size in the core (total 1M cells) then a finer grid with 125 m cell size in the core (total 2.5M cells). Error floors were successively reduced with iteration runs, and four problematic sites were removed, resulting in a final model that fits the data well.

The final model fits the data at 22 frequencies from 3 kHz – 10 Hz with an nRMS=1.40 for floors of Zxx & Zyy=1.0%; Zxy & Zyx=0.5%; Tipper=0.005. Misfits are high at high frequencies for all components (impedance and tipper), inferring the top layers are not well modelled even by the 125 m grid. They are also higher at sites in the NE. Allowing distortion to take up some misfit reduces RMS somewhat without affecting the model. Misfit distribution over the array shows most misfits where resistive rocks outcrop, and also at some odd sites on sediments.

The model images two conductors of $\rho < 10\ \Omega$m in the NE of the grid. One conductor is shallower (top at 1044 m above sea level) and beneath more resistive surface rocks, whereas the other conductor is deeper (top at 670 masl) and beneath sedimentary rocks – it may bifurcate into two conductors. The two conductors are not connected at the 10 Ωm level.

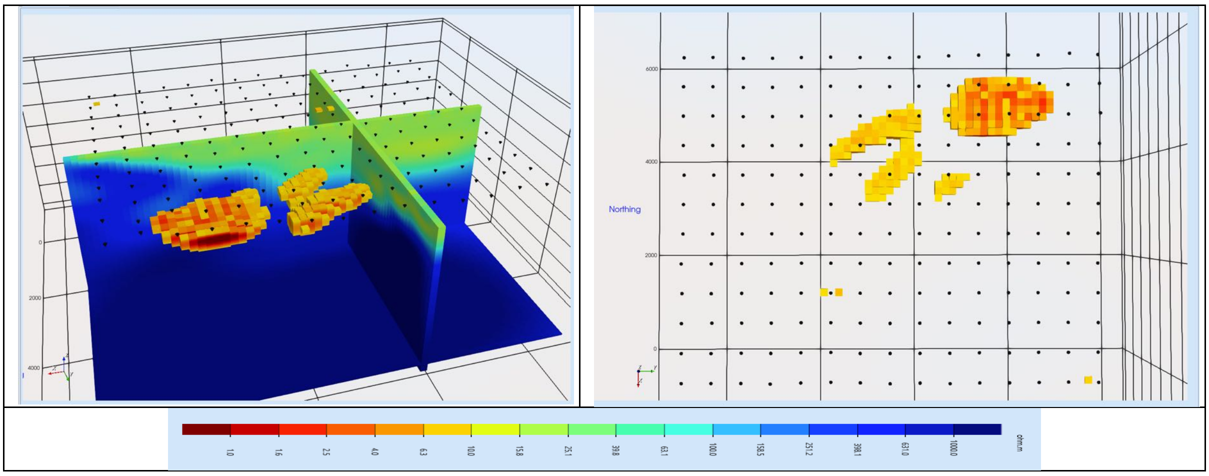

Figure 1: 3D views of the Final Model. Left: From NE; Right: From above.

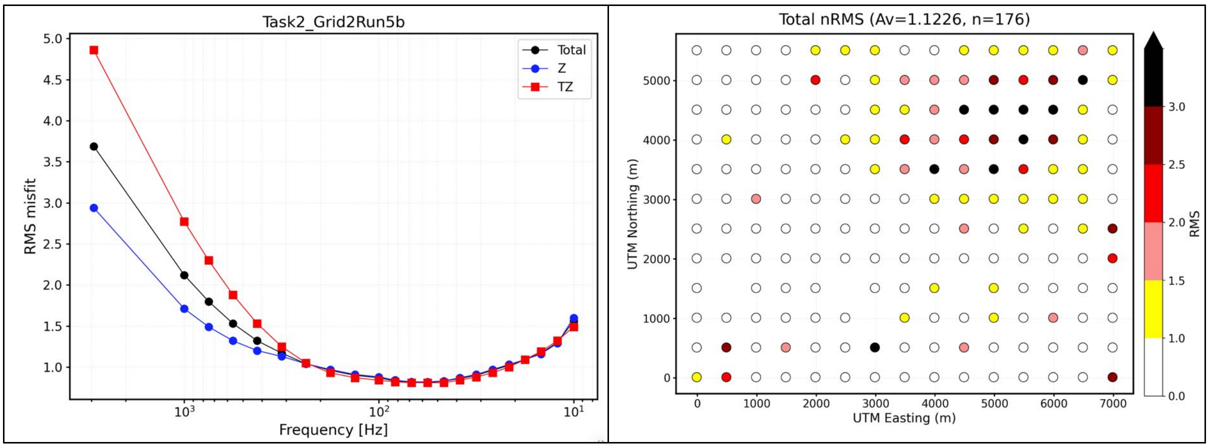

Figure 2: Misfits. Left: Averages of all sites over frequency; Right: Average over all frequencies at each site.

Acknowledgements: RLM wishes to thank Viridien for permission to present this work.

Inversion of a secret model (MT3DINV4S)

Mitra Kangazian[1], Colin Farquharson[1]
[1]Department of Earth Sciences, Memorial University of Newfoundland
St. John's, Newfoundland and Labrador, Canada

Abstract

We inverted noisy data associated with the secret model for nineteen frequencies using a 3D minimum-structure MT inversion program (Jahandari and Farquharson, 2017; Kangazian and Farquharson, 2024, 2026). The regularization term in the objective function consists of a roughness term, $\Phi_r(\mathbf{m})$, and a smallness term, $\Phi_s(\mathbf{m})$:

$$\Phi_m(\mathbf{m}) = \alpha_r \Phi_r(\mathbf{m}) + \alpha_s \Phi_s(\mathbf{m}).$$

The forward modelling response is calculated using the edge-based finite-element approach with a time-dependence of $e^{i\omega t}$. The code uses a right-handed Cartesian coordinate system in which x is positive east, y is positive north, and z is positive upward.

To invert data, a computational domain with dimensions of 71 km $\times$ 69.5 km $\times$ 71 km, with a 15 $\times$ 12 grid of 180 observation points with 500 m separation between sites, having 406,319 cells was designed. Parameterizing the computational domain using unstructured tetrahedral meshes allows us to include the topography of the study area into the mesh and place the observation points on the topography surface.

Several inversions using all components of the impedance tensor and all components of the impedance tensor together with the tipper components were performed (see Table 1). Also, two uniform conductivity values, 0.002 S/m and 0.006 S/m, as both the initial and reference models were investigated. In addition, two approaches for assigning the standard deviations of the impedance data were considered; 2% of the root-mean-square (RMS) value of the off-diagonal impedance tensor components at each frequency and a hybrid approach (e.g., Burd et al., 2013; Kangazian and Farquharson, 2026). For the tipper data, the standard deviation was assigned as 5% of the maximum tipper component magnitude at each frequency.

The models constructed using both the impedance tensor and the tipper components show more structural detail than those obtained using only the impedance tensor. Although the normalized data misfit for these scenarios – impedance data with tipper data – is still far from the optimal value, comparisons of the observed and predicted data show better agreement at some stations than in the inversion performed using only the impedance data.

The computations were performed on Rorqual cluster (Digital Research Alliance of Canada) and they are still running. We present the inversion results for the first and third scenarios in Table 1. We would be able to show the results for all scenarios during the workshop plus the other two examples that are running for a more refined mesh.

Table 1: Different inversion runs

Data	SD	σ_{ref}, σ_{ini} (S/m)	$\phi_{d,normalize}$	Computational time
Impedance	Hybrid	0.002	2.1	$\approx$ 16 days
Impedance	Hybrid	0.006	2.86	$\approx$ 8 days
Impedance & MTF	Hybrid	0.006	6.2	$\approx$ 10 days
Impedance	RMS	0.002	7.2	$\approx$ 10 days
Impedance & MTF	RMS	0.002	9.7	$\approx$ 12 days
Impedance	RMS	0.006	6.9	$\approx$ 11 days
Impedance & MTF	RMS	0.006	15.5	$\approx$ 12 days

References

Burd, A. I., J. R. Booker, R. Mackie, C. Pomposiello, and A. Favetto, 2013, Electrical conductivity of the pampean shallow subduction region of argentina near 33 s: Evidence for a slab window: Geochemistry, Geophysics, Geosystems, **14**, 3192–3209.

Jahandari, H., and C. G. Farquharson, 2017, 3-D minimum-structure inversion of magnetotelluric data using the finite-element method and tetrahedral grids: Geophysical Journal International, **211**, 1189–1205.

Kangazian, M., and C. G. Farquharson, 2024, Including geological orientation information into geophysical inversions with unstructured tetrahedral meshes: Geophysical Journal International, **238**, 827–847.

———, 2026, Constructing piecewise-constant conductivity models for 3D magnetotelluric inversions: Geophysics, **91**, E89–E109.

MT3DINV4 Task 2: 3-D finite element inversion (FEMTIC) of the MT3DINV4 secret model MT data

Yinchu Li

School of Earth and Atmospheric Sciences, Georgia Institute of Technology, Atlanta, GA, USA
yli3354@gatech.edu

In this abstract, I present the results of a blind 3-D inversion of the MT3DINV4 secret-model ground dataset with FEMTIC. The delivered noise-added ground full impedance tensor (4 complex components $Z_{xx}, Z_{xy}, Z_{yx}, Z_{yy}$) plus horizontal tipper (2 complex components T_{zx}, T_{zy}) at 180 sites and 35 frequencies (10 Hz–25.119 kHz; $180 \times 35 \times 12 = 75{,}600$ real data) were inverted jointly. Delivered $e^{+i\omega t}$ responses are conjugated exactly once on import (and once more on export); model axes are swapped to FEMTIC's X=North, Y=East without transposing the impedance or tipper tensors. Delivered EDI `VAR` gives standard deviations $\sigma = \sqrt{\mathrm{VAR}}$, then floored as $\sigma_Z = \max(\sigma,\ 0.05\sqrt{|Z_{xy}Z_{yx}|})$ and $\sigma_T = \max(\sigma,\ 0.02)$. The starting model is a homogeneous $100\,\Omega\,\mathrm{m}$ half-space beneath the true topography (air fixed at $10^{12}\,\Omega\cdot\mathrm{m}$).

A true-topography, three-dimensionally depth-graded tetrahedral mesh was built with the makeTetraMesh/TetGen workflow using repeated (4×) makeMtr volume refinement: 1,553,431 tetrahedra, 252,231 nodes, and 30,254 resistivity cells (30,253 free). Surface edges are ≈40 m and 150–300 m cells are sustained through the principal 0–3 km depth range. The inversion is model-space Gauss–Newton with the PARDISO direct solver. Roughening matrix is created using shared faces of resistivity blocks, with vertical roughness penalized half as strongly as horizontal roughness.

The initial RMS was 11.198. After 12 iterations it converged to 3.774. The recovered blind model is shown in Fig. 1. It shows a coherent conductive body in the western/south-western part of the array and a resistive block to the east/north-east. The per-frequency RMS (Fig. 2a) is ≈1 across 10–1000 Hz band and rises monotonically to ≈11 at 25 kHz; dropping only the highest frequency lowers the overall RMS to ≈3.34. This monotonic high-frequency rise is the signature of a finite-element forward-discretisation limit at the shrinking skin depth (∼17 m at 25 kHz), not of unmodelled structure. Map RMS distribution per site (Fig. 2b) are also shown here as a part of RMS statistics.

From One Inversion to Many: What Faster 3D MT Inversion Makes Possible

Jason Liu*, Junseo Shin, Paul Köttering
Vorticity Inc.
*Presenting author

Three-dimensional magnetotelluric inversion is computationally demanding because each inversion requires repeated forward and gradient calculations across many frequencies. In practice, this often limits interpretation to a small number of inversion runs, even though the recovered model can depend strongly on regularization, starting conditions, data selection, and other inversion choices.

We present a new GPU-accelerated 3D MT inversion code applied to the MT3DINV4 Task 2 Secret Model data set. The code supports multiple regularization choices, inversion parameters, starting models, and options for including or excluding different data components.

A representative full 3D inversion can be completed quickly, and multiple inversions can be run concurrently. This makes it practical to move beyond a single preferred inversion and instead explore a broader range of reasonable modelling assumptions. We use this capability to perform a parameter sweep consisting of many separate inversions, and the resulting conductivity models are compared. This is not intended to represent a complete posterior uncertainty analysis. Rather, it provides a practical assessment of feature robustness and helps distinguish persistent structure from less well-constrained features.

The primary contribution is computational rather than methodological. Faster inversion makes systematic experimentation feasible within realistic project timescales. If many 3D inversions can be completed in the time traditionally required for one, a wider range of regularization strategies, acquisition choices, data combinations, and geological hypotheses can be tested directly.

Joint Inversion of Synthetic Magnetotelluric and Airborne Tipper Data from the Secret Model Using ModEM

Leonardo A Martins[1]*
[1]Instituto de Astronomia, Geofísica e Ciências Atmosféricas, Universidade de São Paulo, Brazil, *martinsla@usp.br

Three-dimensional inversion of synthetic magnetotelluric (MT) and airborne natural-source electromagnetic tipper (AS1) data was performed for the MT3DINV4S "Secret Model" dataset using ModEM, a finite-difference forward and inverse modeling code employing the exp(+iωt) time convention. Model coordinates follow a local Cartesian frame aligned to the survey's own coordinate system via an affine transform derived from the known southwest and northeast corner locations. The MT component comprised 180 sites on a regular 500 m by 500 m station grid (15 stations E–W, 12 stations N–S) spanning 7.0 km E–W by 5.5 km N–S, with full impedance tensor and ground-based tipper responses subsampled to four frequencies per decade from the full 35-frequency, 25 kHz–10 Hz band, using noise-free data. The AS1 airborne tipper component provided an additional, independent tipper dataset, with real and imaginary Tzx/Tzy responses at six frequencies (800–25 Hz) across 15,736 locations along 56 east–west flight lines at 25 m along-line spacing and 100 m line spacing, simulating a bird height of 100 m above ground.

Two inversions were carried out. An initial inversion used the MT impedance and ground-based tipper data only, without topography, on a flat-surface mesh. A subsequent joint inversion added both surface topography and the AS1 airborne tipper dataset, using a topographic mesh with a 100 m horizontal core cell size, 12 padding cells (factor 1.30), 84 by 98 cells total, and a vertical mesh of 45 main layers (5 m start, factor 1.15) plus 19 prepended topography layers of the same growth, for 64 layers total. Topography was derived from a 5 m-resolution DEM (station elevations 1000.0–1350.0 m), with the model datum set at 1350.0 m (the highest point in the footprint) and each cell classified as air or rock against the interpolated DEM surface. Three candidate starting/prior half-spaces (10, 50, 100 Ω·m) were tested for each inversion; 10 Ω·m gave the lowest misfit in both cases and was adopted for the production runs. Impedance and ground/airborne tipper error floors were set at 5% and 4% respectively (geometric-mean scheme), with a covariance smoothing of 0.3 and initial damping (lambda) of 10; galvanic distortion was not explicitly treated in either run.

The workflow comprised: (1) construction of station and flight-line coordinate files, including the DEM affine alignment; (2) construction of the mesh, with topography layers where applicable; (3) DEM-based air/rock covariance classification for the topographic run; (4) testing of candidate half-spaces and selection by lowest misfit; (5) computation of error floors; and (6) inversion to convergence.

The MT-only, no-topography run (Figure 1) converged to a final RMS of 1.05, while the joint topography + AS1 run converged to a final RMS of 3.53. Both models showed a prominent subsurface conductive feature in the northeast of the profile.

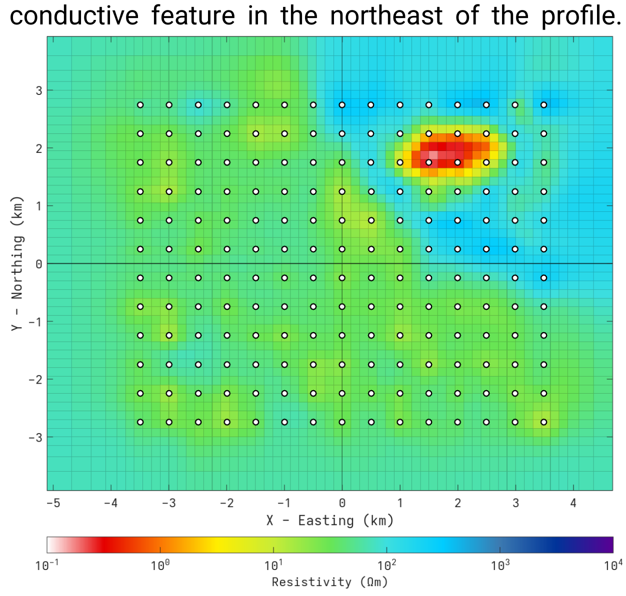

Figure 1 – Depth at 300m (No topography model)

Task 2: 3D MT Inversion of the Secret Model using jif3D

Hossam Marzouk[a]

[a]*Technische Universität Berlin, Berlin, Germany*

This contribution shows 3D inversion results for the secret model of Task 2 at the MT3DINV4 workshop, using the jif3D joint inversion framework (Moorkamp et al., 2011). The inversion uses all four components of the impedance tensor together with the tipper from 180 stations and 17 frequencies (15.85 kHz–10 Hz), covering both the noise-free and noise-added datasets. Error floors for both datasets are set to 5% of $\mathrm{sqrt}(|Z_{xy}Z_{yx}|)$ on all the impedance components and an absolute floor of 0.02 on the tipper. At a later stage, the inversion also solves for a frequency-independent 2×2 distortion matrix at each station to minimize distortion effects. The starting model is a homogeneous 100 Ω·m half-space, discretized into a mesh of 42 cells in the x-direction (northing) and 52 in the y-direction (easting), with 38 layers in the z-direction. The horizontal cell size is fixed at 150 m, while the vertical cell size starts at a constant 25 m for the top 18 layers to provide good near-surface resolution, then grows by a factor of 1.130 down to a depth of ≈1350 m. Table 1 lists the regularization and convergence for each dataset and stage. In both datasets, adding the distortion correction at a later stage and lowering λ improves the fit further, down to a final RMS of 1.3/1.8 (impedance/tipper) for the noise-free data and 1.6/2.8 for the noise-added data. Despite these differences in convergence, both inversions consistently recover the same main features with a prominent conductor in the northeast part of the model (Figure 1).

Dataset	Stage	λ	RMS (Z)	RMS (tipper)
Noise-free	Initial	100	10.6	3.1
	Converged (58 it.)	100	2.2	1.9
	With distortion (11 it.)	10	1.3	1.8
Noise-added	Initial	100	10.6	3.3
	Converged (31 it.)	100	2.4	2.9
	With distortion (6 it.)	10	1.6	2.8

Table 1: Regularization parameter λ and RMS misfit at each inversion stage.

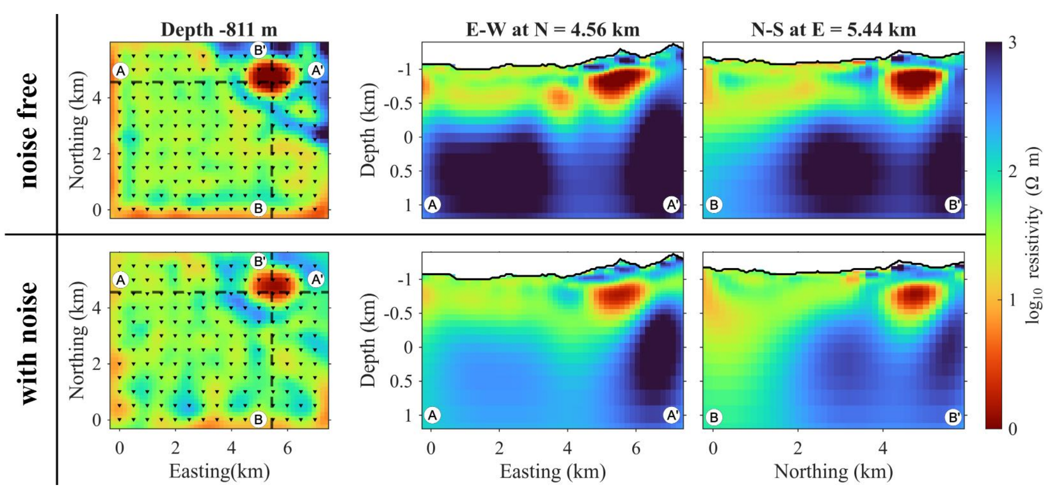

Figure 1: Depth slice at ≈ -800 m and two cross-sections for the noise-free (top panel) and noise-added (bottom panel) datasets.

References:

Moorkamp, M., et al., 2011, Geophys. J. Int., 184, 477–493.

Inverting MT3DINV synthetic data using ModEM and visualizing using pyVista

A.R.Miller[1]

[1]Georgia Institute of Technology

The synthetic data including noise was inverted using ModEM to determine a converged model. The grid is composed of 34x36x27 with cells that are 50mx50m. To compensate for the dense site spacing and the assumed shallow target the top layer is 10m and increases logarithmically to 39 km. A subset of 42 sites was used with an impedance error floor of 5% and 0.02% to the tipper data. Using an iterative workflow, a converged model was created that achieved an overall RMS of 2.15.

Two Practitioners, Two Workflows: Joint Inversion of Ground and Airborne Natural Source Electromagnetic Data with SimPEG and UBC-GIF E3DMT v2

Martin Musila*, Devin Cowan, and Lindsey Heagy
University of British Columbia, Geophysical Inversion facility

Ground MT impedance and tipper data and airborne NSEM provide complementary sensitivity and spatial sampling of 3D conductivity structure. Joint inversion can improve model constraints, but results remain sensitive to practitioner choices in software, frequency mapping, error-floor design, and inversion strategy.

In this work, two practitioners "listened" to the data by first assessing 2D data-space plots, phase tensors and induction vectors, across log-spaced frequencies between 10 Hz and 25 kHz. The diagnostics provided qualitative information on the complexity of the electrical conductivity structure in the region, which informed the two separate workflows. Both practitioners converged on a common starting/reference half-space model of 0.02 S/m. Practitioner 1, Cowan, added noise to a clean version of each dataset to emulate field observations. Ground and airborne NSEM datasets were inverted separately for the northeastern portion of the survey region using 6 logarithmically-spaced frequencies between 10 Hz and 1000 Hz, which allowed for efficient evaluation of hyperparameters for a joint inversion. Cowan then performed a data-weighted joint inversion over the full survey region using 11 ground impedance frequencies, 6 ZTEM frequencies and 6 MobileMT frequencies between 10 Hz and 1000 Hz. Practitioner 2's (Musila's) workflow was influenced by the absence of prior knowledge on the lateral and depth extent of the secret model structure. This motivated inversion of the full model domain using all available frequencies for each dataset between 10 Hz and 25 kHz with the UBC-GIF E3DMT v2 code. Musila used the datasets with noise added by a third party and designed the error-floor scheme with no assumptions on the noise distribution. In particular, the off-diagonal impedance used component-wise percentage errors, whereas diagonal impedance and both ground and airborne tipper used component–frequency floors based on a percentage from the maximum departure from a complex-median background. Outputs from independent inversions were analyzed to adjust the uncertainties assigned to each dataset before a data-weighted joint inversion of ground NSEM and airborne ZTEM data.

The final models (Fig. 1) exhibit consistent structures labelled A-D. With the same color scale used to plot both models, iso-surface values for the SimPEG model (2.5e-2 S/m and 1e-1 S/m) are higher than those for the E3DMT v2 model (1.6e-2 S/m and 5e-2 S/m). Regionally, structure A marks a subtle interface between more- and less-conductive host geology. Locally, conductor B appears within the less conductive northeastern background, with a secondary, deeper conductor C offset from it that appears larger in the E3DMT v2 model. Near-surface linear structures D show variable resolution: near-continuous in the SimPEG model, more segmented in E3DMT v2. Consistent structures (A–D, Fig. 1) across models show both workflows reliably recover the secret model, though differences in amplitude, margin, and continuity reflect each practitioner's choice of frequency range, data selection, starting model, and error-floor scheme.

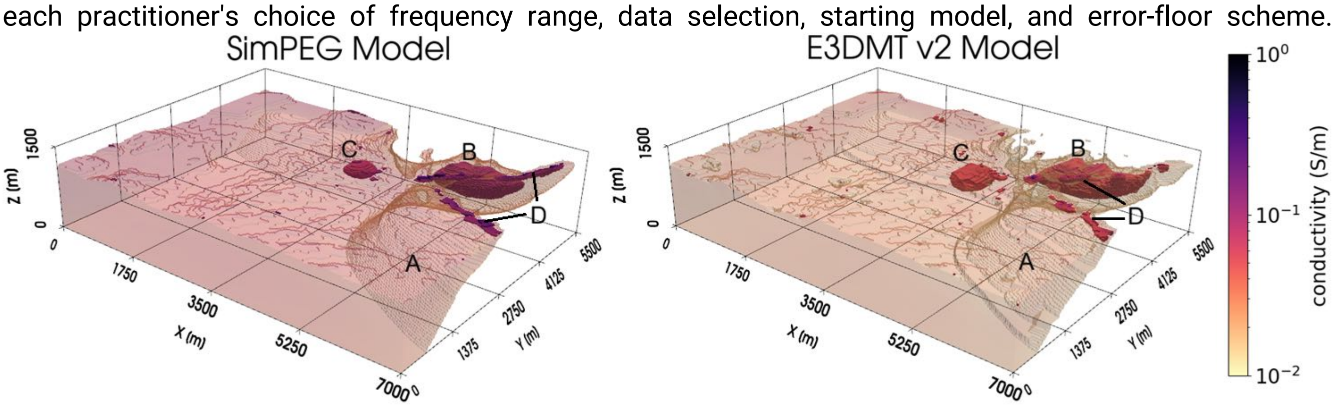

Figure 1: Isosurfaces showing conductivity structures (A-D) in the recovered models from two practitioners. (Left) SimPEG joint inversion of ground impedance and airborne ZTEM and MobileMT by Practitioner 1 (Cowan), with isosurfaces at 2.5e-2 S/m and 1e-1 S/m. (Right) E3DMT v2 joint inversion of ground impedance and tipper with airborne ZTEM by Practitioner 2 (Musila), with isosurfaces at 1.6e-2 S/m and 5e-2 S/m

3-D Inversion of the MT3DINV4 Secret-Model Ground MT and AS1 Data

Ce Qin* — Henan Polytechnic University, Jiaozuo 454000, China, ce.qin@hpu.edu.cn

We invert three MT3DINV4S data sets: noise-free ground magnetotelluric (MT), noise-added ground MT, and AS1 natural-source electromagnetic data.

For the ground MT data, the three highest frequencies (25.1, 20.0, and 15.8 kHz) are excluded because they proved difficult to fit, leaving 32 frequencies from 12.6 kHz to 10 Hz and 69,120 real-valued data. Impedance/tipper error floors are 1%/2% for the noise-free data and 1.75%/2% for the noise-added data. AS1 is decimated to 50 m along-line and 200 m cross-line spacing, leaving 3,948 flight locations. The two complex transfer functions at six frequencies provide 94,752 real-valued data. 3% relative errors and 0.002 absolute error floors are used for the AS1 data.

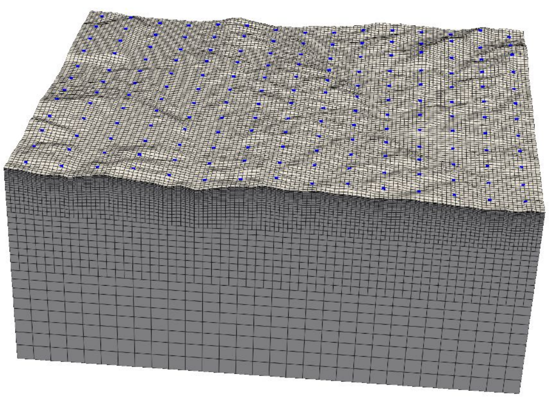

Figure 1: Topography-conforming multiscale parameter mesh.

The initial model is a 25 $\Omega\,$m half-space, and the resistivity is bounded between 0.05 and 50000 $\Omega\,$m. The multiscale parameter meshes are built by progressively refining an initially coarse, nonconforming hexahedral grid. Cells are smallest within the survey area and shallow subsurface, and grow with depth and outside the survey to limit the parameter count. The AS1 mesh is locally refined around the base station. The supplied 25 m elevation grid deforms the air–earth interface and adjacent layers (Fig. 1). For forward and Jacobian evaluations, the state mesh is additionally refined around receivers to improve response and sensitivity accuracy.

The inversion uses a Gauss–Newton method with line search to obtain a step length that guarantees a decrease in the objective function. We use MUMPS to solve the sparse linear systems arising from the forward problem. The Jacobian is assembled and stored explicitly and the normal equation is solved iteratively.

L-curves for $\lambda = 30$, 100, 300, and 1000 select $\lambda = 300$ in all cases. The selected models reduce normalized RMS from 13.43 to 1.275 after 22 iterations for noise-free MT, 5.01 to 1.576 after 10 iterations for noise-added MT, and 15.11 to 5.404 after 19 iterations for AS1 (Fig. 2(a)). Residuals are lowest in the middle of the band and increase at both ends (Fig. 2(b)).

The recovered resistivity models are omitted for space but will be presented at the workshop.

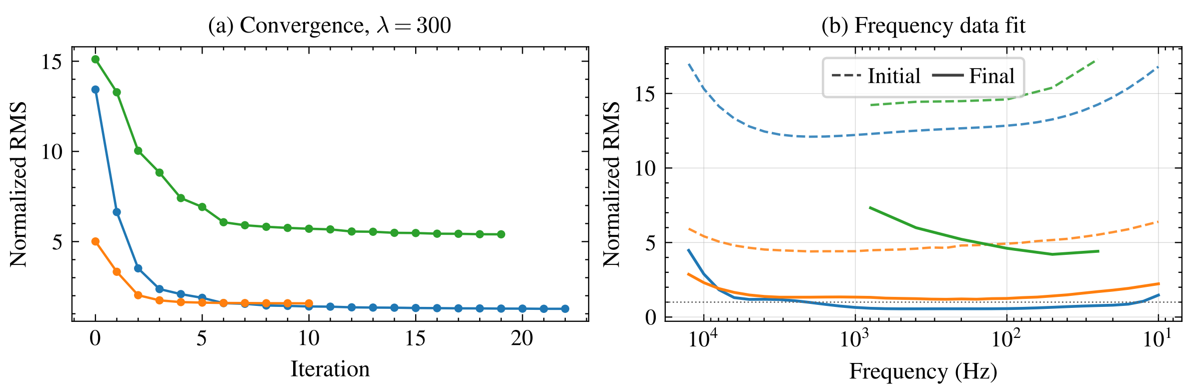

Figure 2: Inversion diagnostics: (a) normalized-RMS convergence for $\lambda = 300$; (b) initial (dashed) and final (solid) normalized RMS by frequency. Blue, orange, and green denote noise-free MT, noise-added MT, and AS1; the dotted line marks normalized RMS of one.

Inversion results for the MT3DINV4 secret model

Changkai Qiu[1*], Yunhe Liu[2], Zhejian Hui[3]

[1]Key Laboratory of Deep Petroleum Intelligent Exploration and Development, Institute of Geology and Geophysics, Chinese Academy of Sciences, Beijing 100029, China

[2]College of Geo-exploration Science and Technology, Jilin University, Changchun, Jilin 130026, China

[3]College of Geophysics, Chengdu University of Technology, Chengdu, Sichuan 610059, China

E-mail: qiuchangkai@hotmail.com;

For the inverse problem, we use a logarithmic transformation proposed by Commer and Newman (2008) to get $\mathbf{\Psi}$ which adds the upper- and lower-boundary constraints to model parameters $\mathbf{m}$. To smooth the model and impose the regularization term, we then transform $\mathbf{\Psi}$ into a new constraint domain $\widetilde{\mathbf{\Psi}}$ using the inverse distance weighting operator (Rong et al., 2023). After computing the objective function and its gradient during the n-th iteration, we use the L-BFGS method proposed by Liu and Nocedal (1989) to derive the model updates $\Delta\widetilde{\mathbf{\Psi}}$, and reconstruct the real model $\mathbf{m}$ via the inverse transformation. To achieve a faster inversion, we utilized first-order finite elements (FEs) for the forward and adjoint problem, following the specific approach described in Task 1. The time dependence is set to $e^{i\omega t}$.

Numerical computations were conducted on a dedicated cluster node equipped with an AMD EPYC 9754 128-Core Processor and 2 TB of RAM. Specifically, we allocated 128 cores for the inverse modeling. For a given frequency and a specific polarization mode (E_x or E_y), the forward modeling and adjoint modeling were performed using multi-core parallelization, whereas the execution of both polarization modes (E_x or E_y) and the outer frequency loop was sequential.

We invert the noise-added Secret Model MT data (Z_{xy} and Z_{yx}) using 31 frequencies, where the highest frequency is set to 10,000 Hz. We did not perform any custom data editing; instead, the error floors specified in the original EDI files were utilized directly. The EDI data were read and exported using the 3D Grid software provided by the 3D Consulting-GEO company. The theoretical coordinates provided on the website were used without any coordinate transformation. The topography was generated by interpolating the provided elevation data during the meshing process. The inner meshing domain is defined by the bounding box $[-1500,\ 8500] \times [-2250,\ 7750] \times [-3500,\ 6500]$ m, while the outer domain extends to 80×80×80 km. Vertically, grid refinement was performed within two depth intervals: from the Earth surface to 2,000 m, and from

Three-Dimensional Magnetotelluric Inversion Based on the Gauss–Newton Method

Shikai Shen[1,2,3*], Xushan Lu[1,2,3], Minghong Liu[1,2,3], and Huaifeng Sun[1,2,3]
1. State Key Laboratory for Tunnel Engineering, Shandong University
2. Institute of Geotechnical and Underground Engineering, Shandong University
3. Laboratory of Earth Electromagnetic Exploration, Shandong University

For MT3DINV4 Task 2, we performed three-dimensional (3D) inversions of the Secret Model using the em3d-MT code developed by Liu et al. (2024). The code minimizes a Tikhonov-regularized objective function comprising a data-misfit term and a model-roughness term. Forward responses and the Jacobian matrix were computed using a vector finite-element solver on an unstructured tetrahedral mesh. The objective function was minimized iteratively using the Gauss–Newton method. At each iteration, the model-update direction was obtained by solving the linearized least-squares system with the LSQR algorithm. The model was then updated using an optimal step length determined by a line search.

For the ground MT inversion, the model domain measured 22 km by 22 km by 14.4 km, and local topography was incorporated into the inversion mesh. Noise-free synthetic full impedance tensor data are used as inversion data at 13 frequencies spanning 10–25,118.8 Hz from 180 ground stations, and the data uncertainty of each impedance component is set to $5\%\sqrt{| Z_{xy}Z_{yx} |}$. The initial model adopts a homogeneous half-space with resistivity of 25 $\Omega\cdot$m. After 20 Gauss–Newton iterations, the root-mean-square data misfit reached 1.27. For the MobileMT inversion, topography was also incorporated. Synthetic total-field apparent conductivity at 11 frequencies spanning 25.1–12,589.19 Hz from 456 airborne stations is adopted as inversion data, and the data uncertainty is set to 1% of the data value. The initial model adopts a homogeneous half-space with resistivity of 45 $\Omega\cdot$m. After 13 Gauss–Newton iterations, the root-mean-square data misfit reached 1.04. Figure 1 compares the MT and MobileMT resistivity models along eight vertical sections oriented parallel to the x-axis at y-coordinates of 500, 1,500, 2,500, 3,500, 4,000, 4,500, 5,000, and 5,500 m. Both inversions recover a pronounced resistive anomaly in the northeastern part of the model.

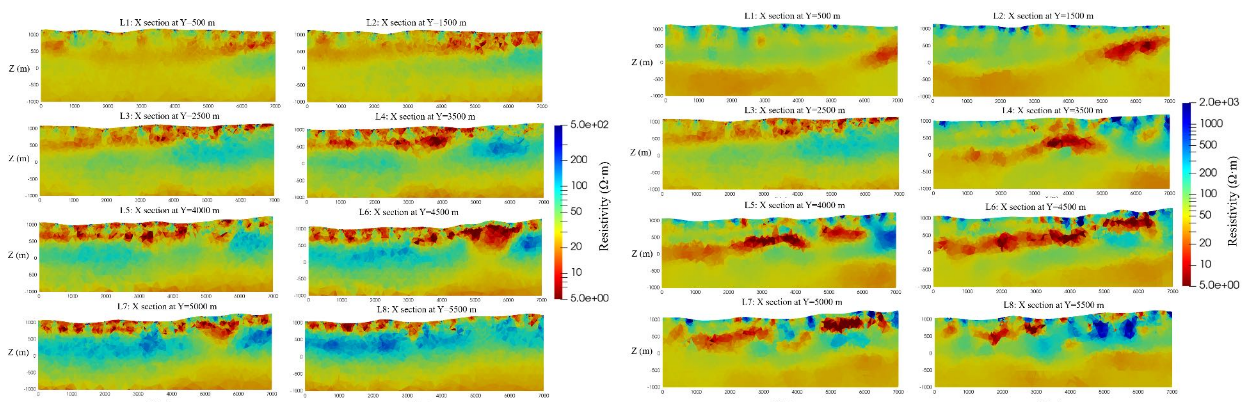

Figure 1. Vertical sections through the recovered MT (left) and MobileMT (right) resistivity models at $y = 500$, 1,500, 2,500, 3,500, 4,000, 4,500, 5,000, and 5,500 m.

3D Inversion of the synthetic data set

Arun Singh

Department of Earth Sciences, Indian Institute of Technology Roorkee, India (*arun.singh@iitr.ac.in)

Abstract

The inversion of noise free and noisy synthetic dataset was performed using *AP3DMT_RB* (Singh and Dehiya, 2025), a parallel finite-difference framework for 3D MT inversion. All impedance and tipper components were inverted jointly. For the noise-free dataset, error floors of 2% of $|Z_{xy}|$ were assigned to Z_{xx} and Z_{xy}, while 2% of $|Z_{yx}|$ were assigned to Z_{yx} and Z_{yy}. For the noisy dataset, the off-diagonal error floors were unchanged, whereas the diagonal components were assigned error floors of 5% of $|Z_{xy}|$ for Z_{xx} and 5% of $|Z_{yx}|$ for Z_{yy}.

For inversion a $91 \times 106 \times 90$ mesh (excluding 10 layers in air) was used with 100 m central cell size. Topography was incorporated by modifying the given elevation file to span 0 to 400 m while preserving the relative elevations. The topographic cells were fixed at 25 m thickness, and each 25 m air layer was split into three sublayers (1, 9, and 15 m) for accurate computation of forward responses at high frequencies. The starting model was a homogeneous 50 Ωm half-space with air resistivity as 10^{10} Ωm. For model regularization isotropic smoothing ($\alpha_x = \alpha_y = \alpha_z = 0.3$, two passes), was used and the regularization parameter reduced progressively from 100 to 10^{-6} whenever the inversion stalls. Computations were parallelized over 20 cores of a dual Intel Xeon Silver 4516Y workstation, taking approximately 24 h for the noisy dataset and 32 h for the noise-free dataset.

The inversion converged after 85 nonlinear conjugate-gradient iterations for the noise-free dataset and 67 for the noisy dataset, reducing the normalized RMS misfit from 12.18 to 1.5 and from 7.30 to 1.6, respectively. Figure 1 shows the recovered resistivity models. Both inversions recover the principal conductive and resistive structures, located in the northern and eastern parts of the model. The noise-free inversion yields sharper conductivity contrasts, more continuous conductive structures, and deeper resistive structures, whereas the model obtained from the noisy dataset shows greater fragmentation in the shallow conductive layer, though the geometry and spatial distribution of the major anomalies remain well resolved. Overall data fit is good, with the main discrepancy occurring at high frequencies ($> 10^4$ Hz), where the predicted phase exceeds the observed phase.

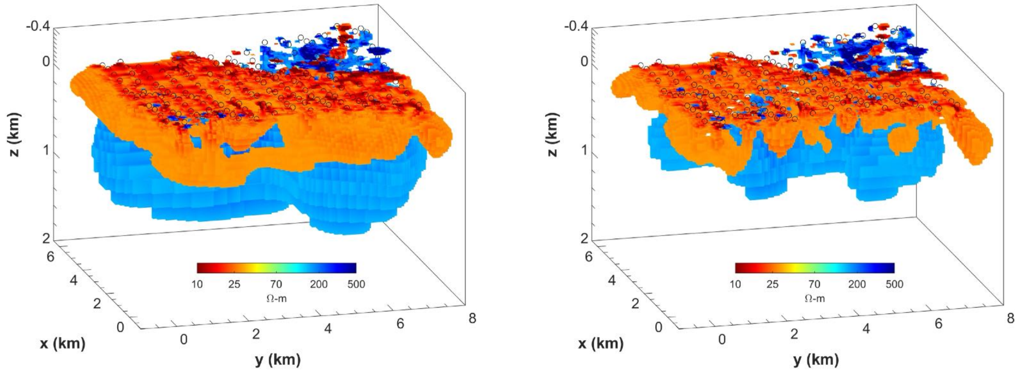

Figure 1: 3D resistivity model obtained from the inversion of (left) noise-free dataset, and (right) noisy dataset.

MT3DINV4 Task 2 secret model: custEMx

N. Skibbe[1], R. Rochlitz[1]
[1]LIAG Institute for Applied Geophysics

In the scope of the MT3DINV4 workshop we used the newly developed custEMx library to prepare the inversion task 2 for a secret model. The library is the successor of the known library custEM (Rochlitz et al., 2019). The modelling code shown in task 1 serves as forward operator for an inversion engine based on the open source library pyGIMLi (Rücker et al., 2017). The provided mathematical algorithm employed to solve the minimization task, uses a Gauss-Newton algorithm with inexact line search and general smoothness constraints in form of an L2 norm. Forward operator and inversion Jacobian calculation are fully MPI compatible and calculated in parallel.

We prepared three independent inversion runs that gave us a sufficient data misfit in the end:

a) AS1, air-borne tipper data:

We used every second station with a noise level of 3e-2 + 1% relative error. Data points with error values >100% were excluded.

b) Ground tipper data, noise-free version:

We added all data < 10kHz with an assumed noise of of 1e-2 + 2% relative error. Again, data points with error values >100% were excluded.

c) Ground impedance + tipper data: (Zxy, Zyx, Tx, Ty), noise free

Lastly the same error model was used for this case as for case b). Noisy Zxy, Zyx data would lead to the same inversion results, however noisy tipper data were not leading to sufficient inversion results.

No further data processing was applied during those inversion runs. We ran the inversion on an unstructured tetrahedral mesh with mesh dimensions of roughly 50km * 50km with a reasonable discretization for the volume of interest. We will show the different results as well as corresponding misfits of the inversion results and discuss the differences.

Rochlitz, R., N. Skibbe, and T. Günther 2019. custEM: Customizable finite-element simulation of complex controlled source electromagnetic data. Geophysics, 84(2): F17–F33.

Rücker, C., T. Günther, and F. Wagner 2017. pyGIMLi: An open-source library for modelling and inversion in geophysics. Computers & Geosciences, 109:106–123.

Secret Model inversion Task 2

M.Yu.Smirnov[1] and O.Rydman[1]
[1]Luleå University of Technology

MT data from 180 sites on a 500x500 m grid, with 15 locations along the X-axis (EW), and 12 locations along the Y-axis (NS) has been inverted. Full impedance tensor at all given 35 frequencies, 10 per decade, from 25 kHz to 10 Hz were used as input data.

The modelling domain was discretized into 120x120x58 cells mesh including 10 padding cells. Two different codes ModEm and MR3DMod were used for inversion. Both results are provided. No bathemetry or topography were used.

- Type of code: FD
- Time dependence of the code
- Co-ordinate system of the code: projected UTM coordinates
- Type of mesh: structured for the task (OcTree-multiresolution designed)
- Data inverted - components (full Z), all 180 sites at all 35 frequencies.
- Initial and Prior models: 30 Ohmm
- Error floor: 1% of main impedance compoeenents (every raw has the same absolute error)
- How has distortion been treated: Distortion has NOT been included or inverted for
- Final RMS misfit and misfits: RMS 1.

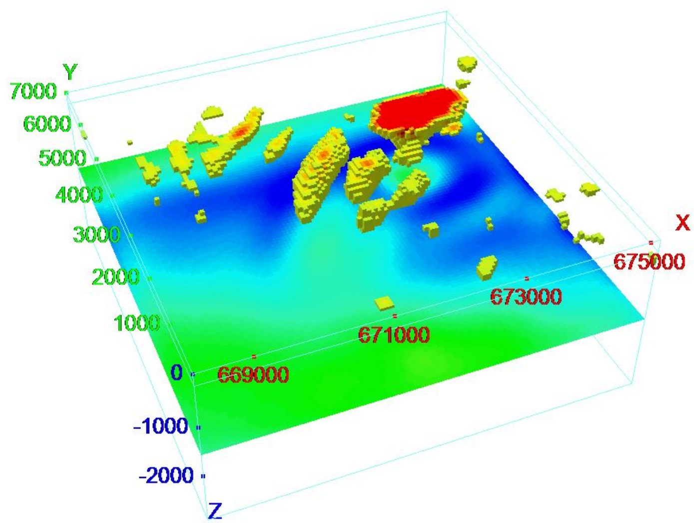

Figure 1 Resulting MR3DMod 3D model and examples of data fit.

MT3DINV4 Task 2: Secret-Model Structures Inferred from MT Data Analysis and 3-D Inversion

H. Song[1*], M. Moorkamp[1], and G. Hill[2]

[1] *Institute of Applied Geoscience, Technische Universität Berlin, Berlin, Germany*

[2] *Institute of Geophysics, Czech Academy of Sciences, Prague, Czech Republic*

We appraise the MT3DINV4 secret-model benchmark using 180 sites, 35 frequencies from 10 Hz to 25.1 kHz, the full impedance tensor, and VTFs. Clean/noisy pairs indicate approximately 3.5% component-level perturbations. Rotational invariants, phase tensors, real induction arrows, and all-frequency OCCAM1D models identify the northeast as the main area of lateral variation: a conductive southwest gives way to a resistive northeast below several hundred metres, interrupted by a localised mid-depth conductor. Using 12 frequencies (3.5 per decade), topographic 3-D inversions vary the data components (off-diagonal or full impedance, phase tensor, and VTFs), regional and locally refined meshes, OCCAM, ABIC, and L-curve inversion analysis, and galvanic-distortion estimation. Despite variable shallow textures and amplitudes, the tests support a shallow background resistivity of approximately 25–40 Ω m, a broad northeastern resistor spanning the data-resolved depth range, and a conductor at approximately 0.3–0.7 km below the local surface. The selected noisy-data model uses the same non-conforming deformed hexahedral mesh for forward modelling and inversion, grading horizontally from 25 m near the surface to 800 m below 1.6 km. A 5-m first earth layer grows vertically by 10% to 1 km depth and 20% below. Full Z plus VTFs reduce RMS from 5.4564 for a 35 Ω m half-space to 1.7727 at iteration 8. Exact boundaries, amplitudes, shallow fragmentation, and structure below 1.5–2 km vary among tests; regional trends and principal anomaly locations remain stable. Similar clean/noisy morphologies suggest residual misfit may reflect RLM-3D/FEMTIC discretisation or numerical differences rather than the added perturbation alone.

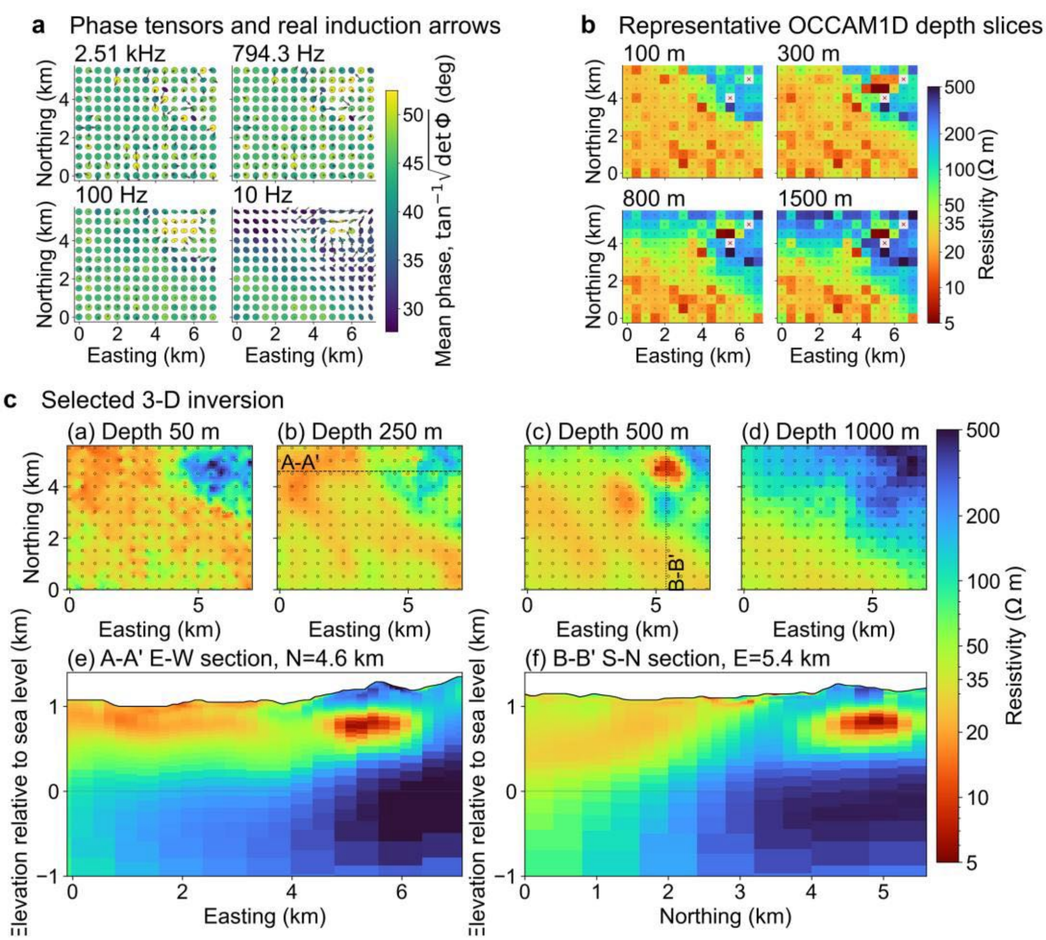

Figure 1. Integrated appraisal: (a) phase tensors and real induction arrows (stored +Re(T)); (b) station-wise SSQ OCCAM1D depth slices, with failed inversions marked by red crosses; and (c) the selected 3-D model. Map depths are below local surface; sections are relative to sea level. High resistivity is blue.

Secret Model Results for the MT3DINV4 Using a Finite Volume MT Code

Atsushi Suzuki, JX Metals Resources Exploration ＆ Development Co., Ltd.

Numerical method: Finite volume method with the magnetic field as the primary variable (Suzuki, 2025)

Computing time: 36 h

Hardware: Intel Core Ultra 9 285 K, 128 GB RAM

Mesh: 481,218 cells, topography-conforming hexahedral mesh with local refinement in the northeastern area, where the data misfit remained large in preliminary inversions without local refinement.

Minimum cell size: Δx = 62.5 m, Δy = 62.5 m, Δz = 3 m

Frequencies: 20 frequencies were used from 25 kHz to 10 Hz. The full dataset was not inverted because of computational limitations.

Error Floors: Z_{diag}=10 %, $Z_{off\text{-}diag}$=5 %, Tipper=0.05. Only MT data were used.

Initial Model: a homogeneous 100 Ωm half-space.

Regularization Term: reduced from 100 to 1 until the RMS fell below 1.0.

Final RMS: 0.76, evaluated using all 35 available frequencies.

Reference: Suzuki (2025), doi: [10.1007/s12145-024-01666-z](https://doi.org/10.1007/s12145-024-01666-z)

(a)

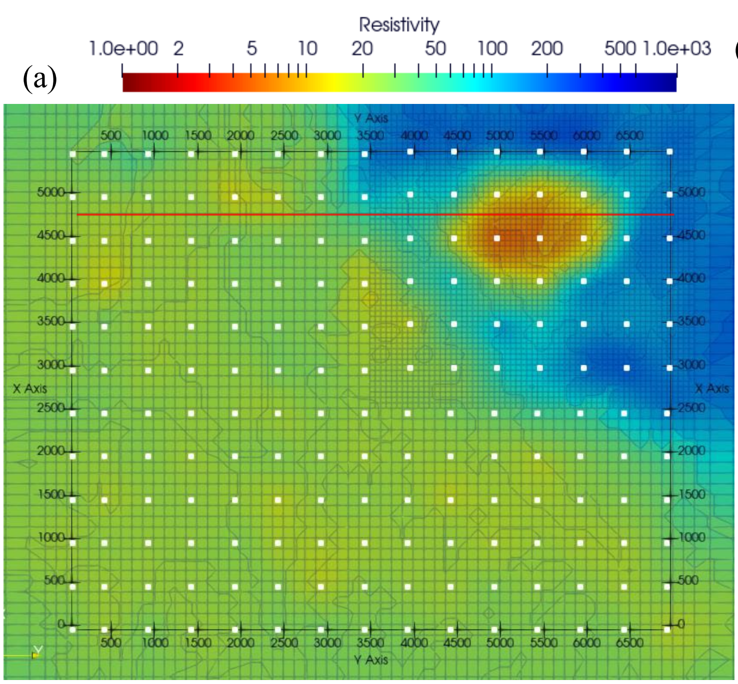

(b)

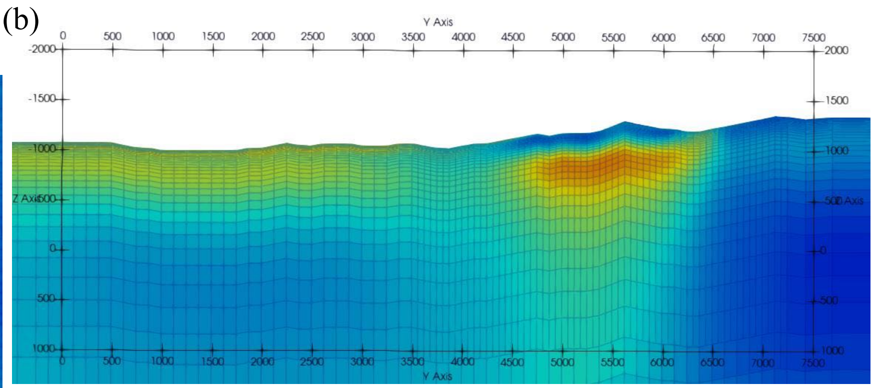

Figure 1.

Inverted resistivity model shown in (a) a horizontal slice at $Z = -800$ m and (b) a cross-section along the red line in panel (a). White dots indicate observation locations.

3D Inversion of the MT3DINV4 Secret Model: Evaluating Resolution and Noise Degradation on Ground Electromagnetic Data

Deniz Varılsüha*,[1], Özcan Özyıldırım[1]

[1]*Application and Research Center of Geothermal and Mineral Deposits, Afyon Kocatepe University, Afyonkarahisar, Türkiye.*

Our inversion strategy utilizes the Gauss-Newton (GN) inversion algorithm with unstructured tetrahedral meshes. The forward calculations within the inversion loop leverage the METOD-3D framework, utilizing unstructured tetrahedral meshes to accurately compute responses and sensitivities. We performed independent 3D inversions on both the noise-free and noisy ground datasets to establish baseline resolution limits and assess the robustness of our regularization scheme under realistic noise conditions.

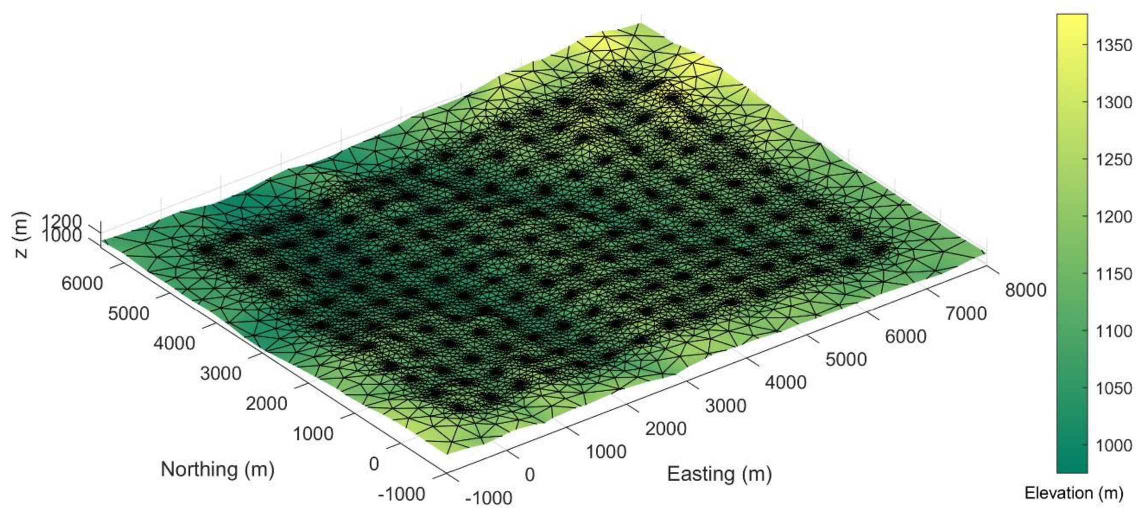

Figure 1: The surface of the unstructured tetrahedral mesh showing the elevation variation of the survey area. The receiver locations are shown as refined points.

The preliminary results demonstrate that inverting the noisy (1.75%) data and non-free data had very little impact on the shallow structures in the inverted model. This comparative analysis highlights the practical limitations and capabilities of ground-based MT inversions in complex 3D environments.

Table 1: Technical Specifications for Task 1 Submission

Parameter	Description
Inversion Algorithm	DEVA3DMT (github.com/varilsuhad/DEVA3DMT)
Data Types Inverted	Ground MT (Noisy and Noise-free)
Mesh Dimensions	~289K cells, ~165K parameters.
Error Floors Assumed	5% on impedance
Regularization Terms	L2 norm of the second spatial derivatives
Computing Time	~7 hours in total (13 inversion steps)
Hardware Details	Intel 285K CPU, 256 GB RAM, 8 x RTX 3090 GPU

MT3DINV4: 3D Inversion of Synthetic Magnetotelluric Data of a Secret Model

Andrew Williamson*, Ryan Olson, Hormoz Jahandari

Dias Geophysical Ltd.

As part of the MT3DINV4 workshop, synthetic MT and airborne data were produced for a "secret" geophysical model to be inverted by participants to compare inversion algorithms. Here, the MT data were inverted using an algorithm based on SimPEG to produce a subsurface conductivity (resistivity) model. For this model, the synthetic MT impedance and tipper data with added noise were inverted using provided frequencies from 10^4 - 10^1 Hz. The inversion was completed using a tensor mesh composed of 58 cells in the horizontal x and y-directions, and 62 cells in the vertical z-direction, for a total number of 208,568 cells. The mesh used a finely discretized core encompassing the stations and topography, and geometrically increasing padding cells away from the center. The mesh core used cells with vertical thicknesses of 25 m in regions where there was topography. Below this core, vertical cell thicknesses increased geometrically with depth by a factor of 1.15. A half-space with a resistivity of 100 Ωm and added topography was used as the starting model, based on surface resistivity values inferred by the data. The preferred inversion model was obtained after 12 iterations, with a final RMS misfit of 1.1. The most prominent feature of the inversion model was a broad, low-resistivity feature at 250 m – 450 m depth beneath the high topography on the northeast region of the model. This feature had a resistivity of ~ 1 – 10 Ωm, dimensions of ~ 1.5 km x 0.8 km, and a shallow dip towards the west. The model showed noticeably higher surface resistivity values of 100 – 1000 Ωm along the high topography in the northeast corner of the model, and lower surface resistivity values of 10 – 100 Ωm elsewhere.

MT3DINV4R – Real Data

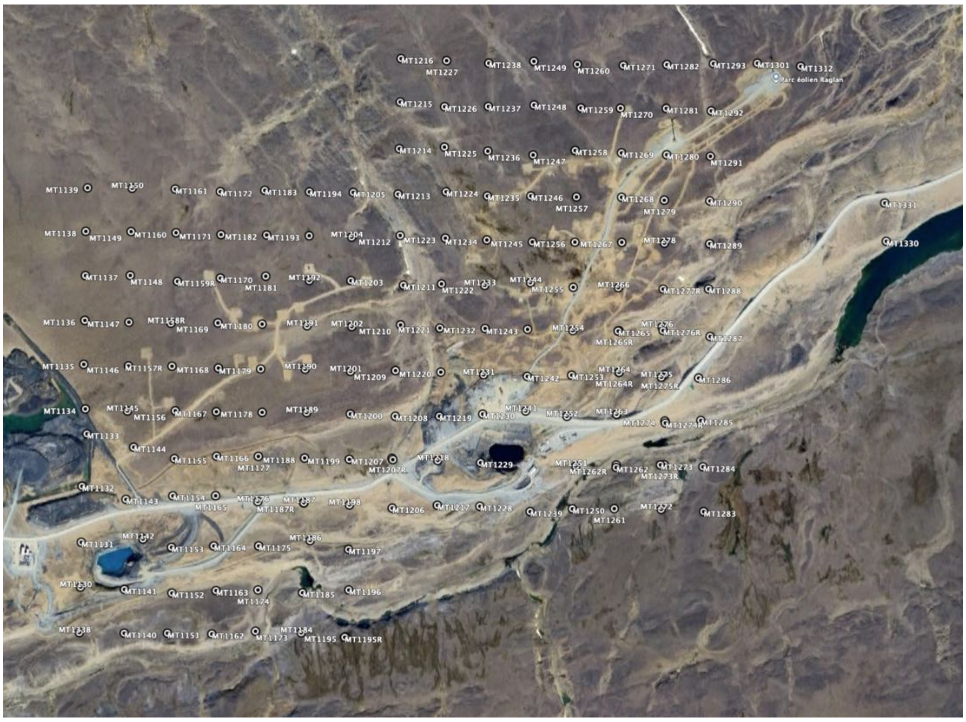

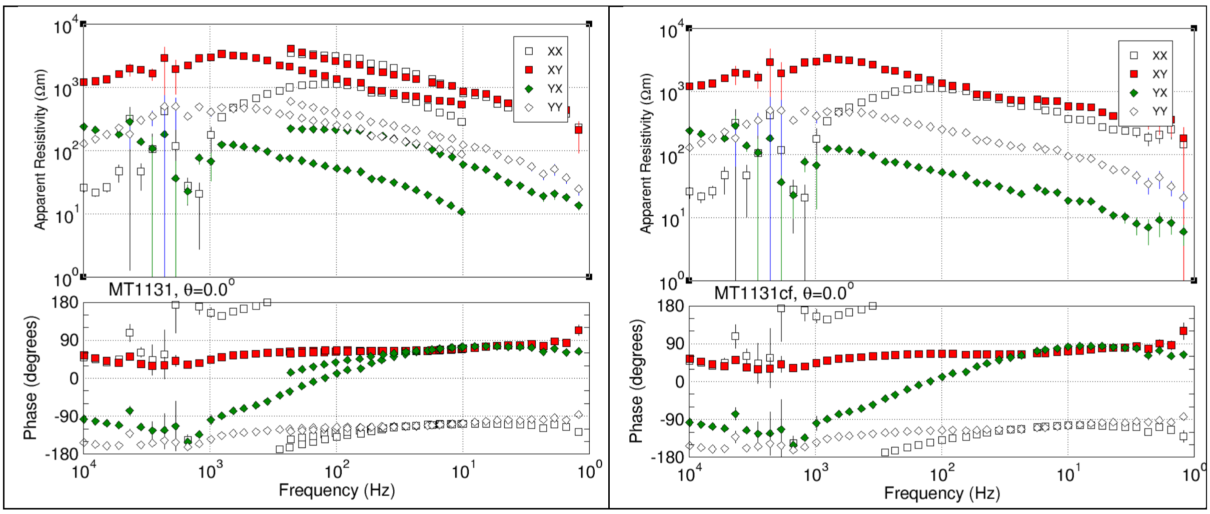

Figure 1: Site MT1131 original data (left) and corrected data (right).

3D inversion of MT data from Raglan Mine in northern Quebec, Canada, using a hybrid mesh

Erik Gallardo-Romero[1]*

GGI Gallardo Geophysical Imaging[1]*

Email: egallardo@ggi-geophysics.com

The corrected MT3DINV4 real data from the Raglan Mine provided by Prof. Alan Jones were inverted using a newly developed Finite Element inversion code for a three-dimensional hybrid-discretized mesh based on the nonlinear conjugate gradient method. The converted XY-YX apparent resistivity and phase curves, as well as the corrected XX and YY impedances were all considered in the inversion. In preparation for inversion, only unrealistic anomalous data points were carefully identified and discarded. Following the bad data quality in the low frequency range and the depth focus of the study, only frequencies greater than 0.1 Hz were considered for inversion. Out of the 178 available EDI files, 166 files that correspond to distinct site locations within a 3.6 km × 3 km study region were used for inversion. The subsurface is represented by a 500 km × 500 km × 250 km domain discretized into 27 layers of triangular prisms in the first 1.3 km followed by 229,159 tetrahedral elements distributed below the prismatic elements. A total of 591,445 model cells were used in the inversion. Topography was incorporated and propagated at depth by the nodes in each layer of prisms. The thickness of the prismatic elements closest to the surface is set to 4 m, and increased at depth by factor of 1.4 up to a maximum thickness of 60 m. Within evaluation points, the lateral edge length of the prismatic elements is set to 60 m. A maximum lateral edge length of 100 m is set to all prismatic elements within the study region.

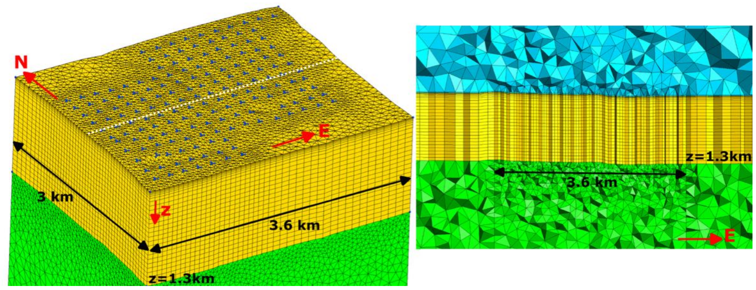

Figure 1. Left: 3D view of the hybrid mesh below the study region. MT stations are shown as blue points. Right: Vertical slice of the mesh along the white dotted line.

34 frequency values from 0.15 Hz to 10.13kHz were considered for inversion. As the data are clearly affected by galvanic distortion, the elements of the simple distortion matrix $\boldsymbol{C} = \begin{pmatrix} Cxx & 0 \\ 0 & Cyy \end{pmatrix}$ are included in the inversion. Errors floors for apparent resistivity, phase and impedance data were 7%, 3° and 15% the value of $\sqrt{Z_{xy}Z_{yx}}$, respectively. A homogeneous 1000 $\Omega.m$ half-space was used as starting model. A simple smoothing regularization term considering the sum of the squared model difference between adjacent cells was employed in the inversion. To avoid unwanted shallow heterogeneities, an anisotropic smoothing factor favoring layered models was applied in the first iterations and then gradually reduced.

After 1025 iterations, a global RMS value of 2.15 was achieved. One horizontal and two vertical sections of the resulting model are shown in Figure 2. The overall shape of the resulting conductive structure is also shown in Figure 2 as a three-dimensional view of the 50 Ω. m isosurface.

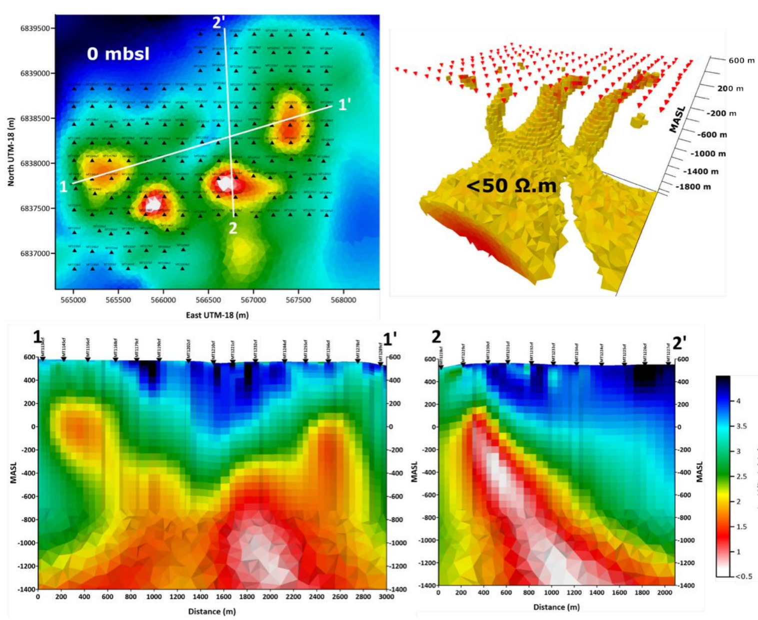

Figure 2. Top left: Horizontal section of the inverse model at 0 mbsl. Top right: 3D visualization of the conductive body. Bottom left and right: Vertical sections of the inverse model along the white lines shown in the horizontal section.

Comparative Analysis of 3D Magnetotelluric Inversion: The Effect of Site Clustering and Initial Models on Convergence and Computational Cost

C.Giménez-Berenguer[1], J.Ledo[1], P.Piña-Varas[2] and P.Queralt[2]
[1]Dept. of Physics of the Earth and Astrophysics, Faculty of Physics, Universidad Complutense de Madrid, Madrid, Spain
[2]Dept. Dinàmica de la Terra y l'Oceà, Universitat de Barcelona, Barcelona, Spain

SUMMARY

Three-dimensional magnetotelluric (MT) inversion constitutes one of the primary computational challenges in large-scale mineral exploration projects. The increasing density of acquired data raises both processing times and the difficulty of conducting consistent quality control and selection through visual inspection. In this work, we present a methodology based on unsupervised learning to optimize data preparation and the construction of starting models for 3D MT inversions.

The methodology was applied to the Raglan mining district (Quebec, Canada), using the phase of the impedance tensor determinant to minimize galvanic distortion effects. From 168 MT sites, an analysis was implemented using Self-Organizing Maps (SOM), employing as input variables the determinant phase, its first and second-order derivatives, and the Dynamic Time Warping (DTW) distance. This procedure allowed for the identification of a representative subset of 25 sites. The final selection further incorporated a spatial criterion based on site distance, ensuring that the representative sites of each cluster maintained a homogeneous distribution throughout the study area, thus guaranteeing both geophysical representativeness and the spatial coverage of the original data set.

The selected subset was used to perform an initial inversion on a low-resolution mesh. The resulting model was subsequently refined, generating a high-resolution starting model for the final inversion of the full data set. The results show that this hierarchical approach significantly reduces the number of iterations required to reach convergence compared to a conventional 100 Ωm homogeneous model and a three-layer 1D starting model, notably decreasing total computation time.

As shown in *Figure 1*, this proposed strategy demonstrates that the integration of unsupervised learning techniques into the MT inversion workflow allows for optimized data selection, reduces the dependence on subjective decisions during pre-analysis, and improves computational efficiency without compromising the geological coherence of the resulting models.

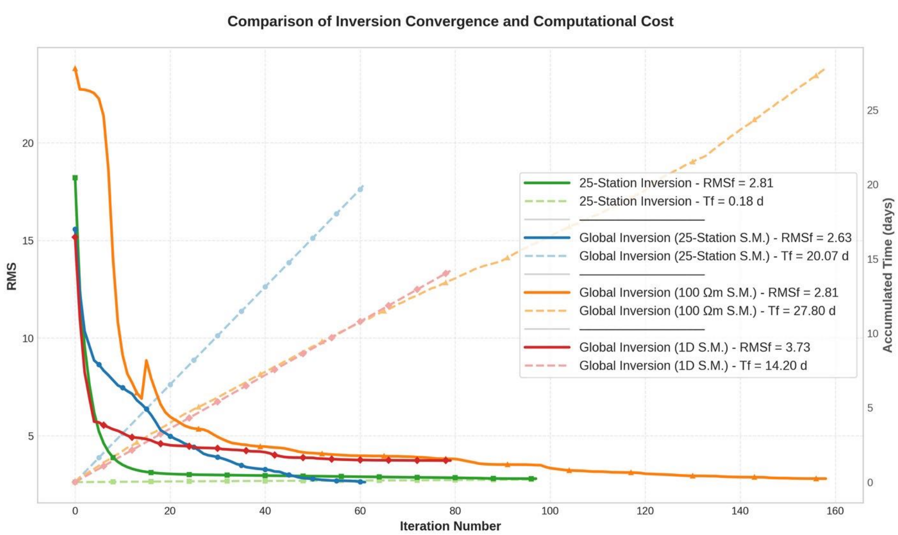

Figure 1. *Comparison of inversion convergence using different starting models (S.M.). The left y-axis shows the RMS evolution, while the right y-axis shows the accumulated computational time per iteration. RMSf and Tf indicate the final values obtained at the end of each inversion for each starting model.*

Inversion of the Raglan Zones 2-3 data

Alan G. Jones, ManoTick GeoSolutions Ltd.

alan.jones@manotick-geosolutions.com

AMT/BBMT data from 164 sites at Raglan Zones 2–3, acquired by Quantec in 2017, were corrected for the serious mismatch – in phase as well as in amplitude (Figure 1, left) – between the high frequency (HF) data, acquired using Geometrics G100K coils, and the low frequency (LF) data, acquired using Phoenix MTC-50 coils. Its cause was not discovered, and a heuristic correction method was adopted (Figure 1, right).

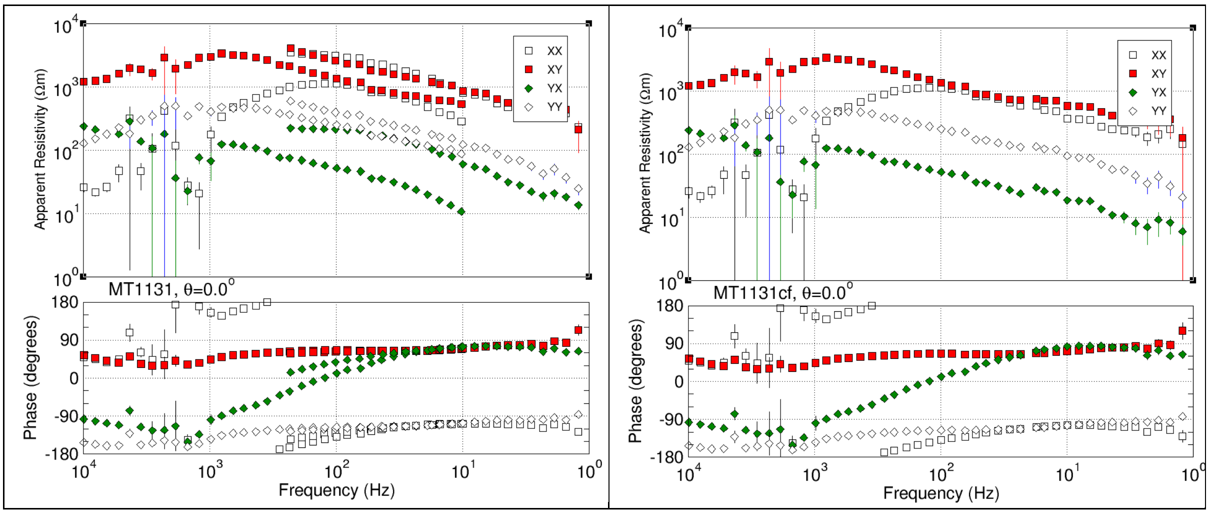

Figure 1: Site MT1131 original data (left) and corrected data (right).

Inversion used Viridien's RLM-3D code, solving simultaneously for full galvanic distortion tensors. Successive inversions across three grids, with progressive data editing, converged on a preferred model (nRMS = 1.31) containing three discrete north-dipping conductors (ρ < 1 Ωm) between sea level and ~600 m depth (Figure 2). These conductors are robust: all four final models, derived from different grids, data subsets, and inversion parameters, recover essentially identical bodies. The 400–4 Hz band, spanning the conductors' depth range, is best fit (RMS < 1.25) and thus best resolved, while shallower and deeper structures are less constrained. Distortion is strong to very strong at most sites (mean 0.83), particularly to the SW.

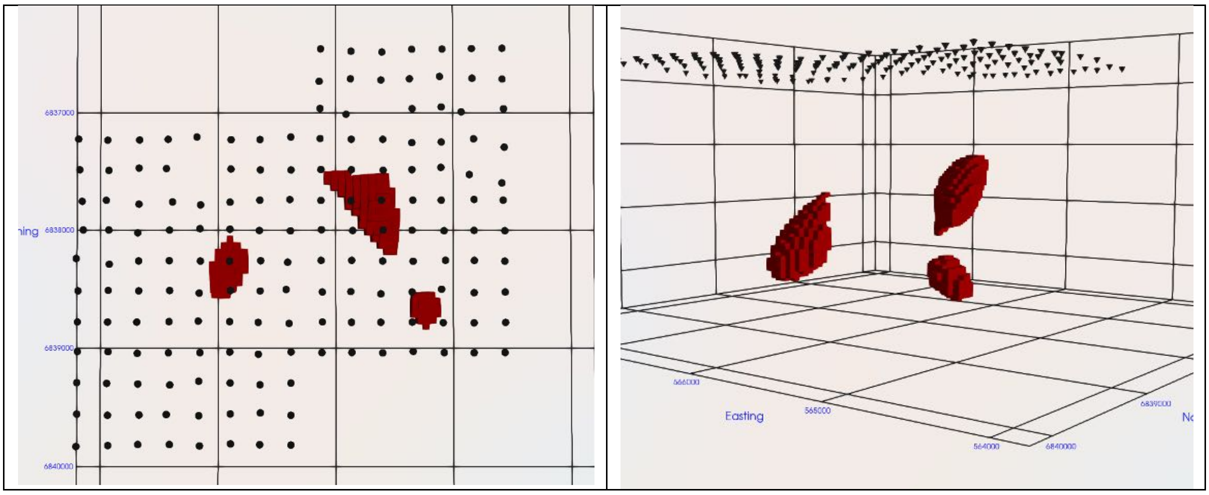

Figure 2: 3D views of the conducting bodies with ρ < 1 Ωm. Left: View from top. Right: View from SouthEast

Acknowledgements: The author wishes to very gratefully thank Raglan Mine, Glencore for allowing this work to be presented.

MT 3D Modelling and Inversions using a finite element method with unstructured tetrahedral meshes

Jianbo Long [1*] and Peter Lelievre [2]
1. Department of Earth Sciences, Memorial University of Newfoundland
2. Department of Computer Science and Mathematics, Mount Allison University

Task3 – Inversion of Real Data Set

The data for this inversion are the “corrected” version (by MTGS) over the Z3-Z2 grid only (excluding the edge stations MT1301, MT1312, MT1330, and MT1331) in the Raglan mine region. Only data with frequencies > 10 Hz were used due to the “band shift” issue observed during the original data processing from raw time series data. A total of 10 frequencies that are logarithmically spaced from 10k Hz to 10 Hz were used for the inversion. Data are interpolated in the frequency domain when necessary. All four components of the impedance are used for the inversion. No other “manual editing” was applied to the data due to time constraint.

The topography surface was smoothed to generate an unstructured tetrahedral mesh which has an active depth of region for inversion of 10 km. The forward modelling was using a vector finite element method that solves the E-field equation in which the linear system of equations is solved by the MUMPS direct solver. The mesh has ~ 0.5 million cells in total.

A standard minimum-structure Gauss-Newton algorithm was used in which an L2-norm model regularization and a reference model (e.g., 1000 Ohm-m) were applied without additional constraints. The normal equation in the Gauss-Newton minimization was solved with a conjugate gradient iterative method. The sensitivity computation was done with the so-called “pseudo-forward method” for the advantage of no need of explicitly storing the sensitivity matrix.

Three-Dimensional Magnetotelluric Inversion Based on the Gauss–Newton Method

Xushan Lu[1,2,3*], Minghong Liu[1,2,3], Shikai Shen[1,2,3], and Huaifeng Sun[1,2,3]
1. State Key Laboratory for Tunnel Engineering, Shandong University
2. Institute of Geotechnical and Underground Engineering, Shandong University
3. Laboratory of Earth Electromagnetic Exploration, Shandong University

For Task 3, we performed a three-dimensional (3D) inversion of ground-based magnetotelluric (MT) data acquired over Zones 2 and 3 of the Raglan mining district in northern Quebec using the em3d-MT code developed by Liu et al. (2024). The code minimizes a Tikhonov-regularized objective function comprising a data-misfit term and a model-roughness term. Forward responses were computed with a vector finite-element solver on an unstructured tetrahedral mesh, and the objective was minimized iteratively with the Gauss–Newton method. At each iteration the model-update direction was obtained with LSQR, and an optimal step length was determined by a line search.

The inversion domain measured 46 km $\times$ 46 km $\times$ 28 km. Local topography was used to build a mesh of 569,604 tetrahedra, of which 372,969 subsurface elements were active. Full impedance tensor data are utilized for inversion at 16 frequencies spanning 0.97–8063.8 Hz from 168 ground stations, and the data uncertainty for each impedance component is set to $5\%\sqrt{|\ Z_{xy}Z_{yx}\ |}$. The initial model adopts a homogeneous half-space with resistivity of 100 Ω·m. After 20 Gauss–Newton iterations the root-mean-square data misfit was 7.97. Figure 1 shows the recovered resistivity model along six vertical sections parallel to the Y-axis at $X = -1442$, −847, −243, 156, 765, and 1356 m.

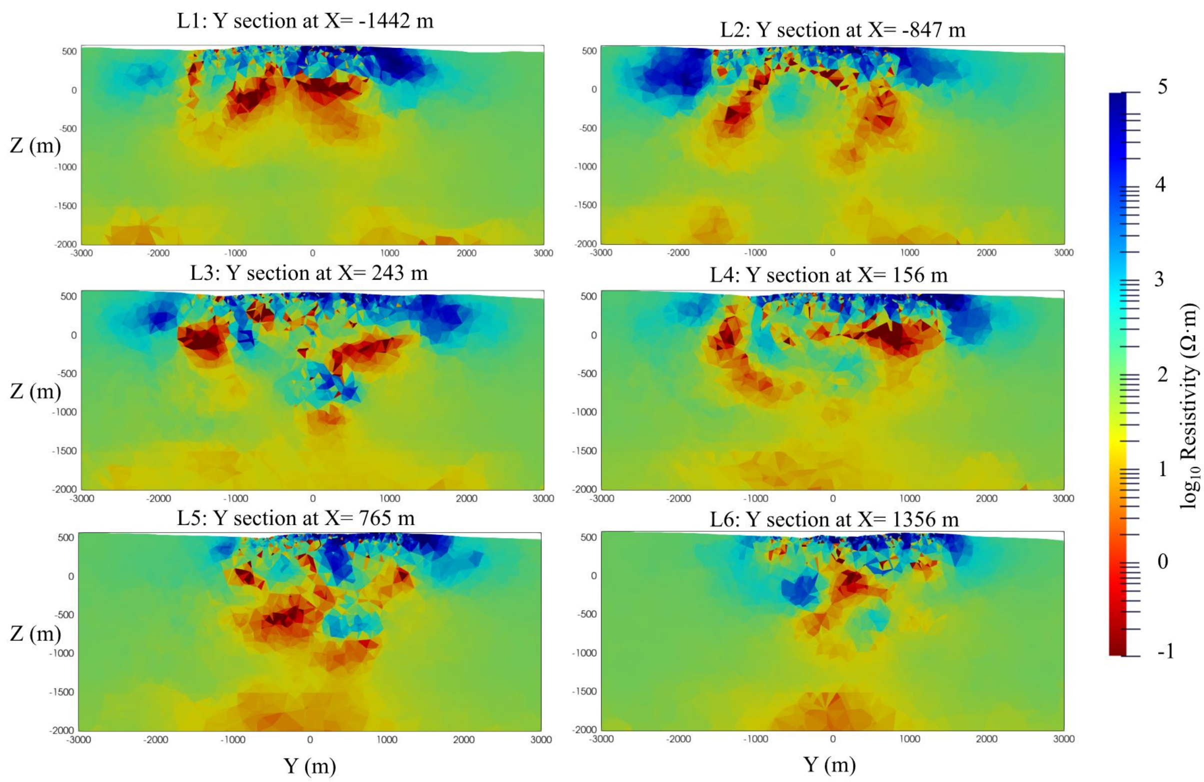

Figure 1. Vertical sections L1–L6 through the recovered three-dimensional resistivity model, oriented parallel to the Y-axis at $X = -1442$, −847, −243, 156, 765, and 1356 m, respectively.

Three Dimensional Inversion of Magnetotelluric Data from Zones 2 and 3 of the Raglan Mine District Using ModEM

Leonardo A Martins[1*]
[1]Instituto de Astronomia, Geofísica e Ciências Atmosféricas, Universidade de São Paulo, Brazil, *martinsla@usp.br

Three-dimensional inversion of magnetotelluric data from the Raglan Mine district (Zones 2 and 3), northern Québec, was performed using ModEM, a finite-difference forward and inverse modeling code employing the exp(+iωt) time convention. Model coordinates follow a local Cartesian frame referenced to UTM Zone 18N (NAD83/WGS84). The dataset comprised 164 distinct sites from 178 original files, with the higher-quality response retained at each of 14 repeat-occupied locations. Full impedance tensor components were inverted; tipper data were excluded, as vertical magnetic field measurements were not acquired in the field survey.

Two inversions were carried out. An initial inversion, without topography, used a frequency range of 10,000 Hz to 0.1 Hz, subsampled to 4 frequencies per decade, on a flat-surface mesh. A subsequent inversion incorporated surface topography and restricted the frequency range to 10,000 Hz to 1 Hz, removing the lowest-frequency band retained in the first run, using a topographic mesh with a 50 m horizontal core cell size, 16 padding cells (factor 1.30), 90 by 94 cells total, and a vertical mesh of 34 main layers (20 m start, factor 1.15) plus 5 prepended topography layers of the same growth, for 39 layers total. Topography was derived from a 30 m ArcticDEM tile (station elevations 506.3–585.0 m, 78.7 m of local relief), with the model datum set at 585.0 m (the highest point in the footprint) and each cell classified as air or rock against the interpolated DEM surface. Three candidate starting/prior half-spaces (10, 50, 100 Ω·m) were tested with topography included; the 50 Ω·m half-space gave the lowest misfit and was adopted for the production run.

Impedance error floors were assigned using a geometric-mean scheme with a 5% error value, applied uniformly across all four tensor components in both inversions. Both inversions used a covariance smoothing parameter of 0.3 and an initial damping parameter (lambda) of 10. Galvanic distortion was not explicitly parameterized or corrected for in either run.

The workflow comprised: (1) construction of the station coordinate file and mesh, with topography layers where applicable; (2) for the topographic run, ArcticDEM-based air/rock covariance classification referenced to the highest-elevation datum; (3) testing of candidate starting half-spaces (10, 50, 100 Ω·m) and selection by lowest misfit; (4) computation of impedance error floors; and (5) inversion to convergence.

The no-topography inversion (Figure 1), using the 10,000 Hz to 0.1 Hz frequency range, converged to a final RMS of 3.45. The topography-included inversion, using the restricted 10,000 Hz to 1 Hz frequency range, converged to a final RMS of 5.1.

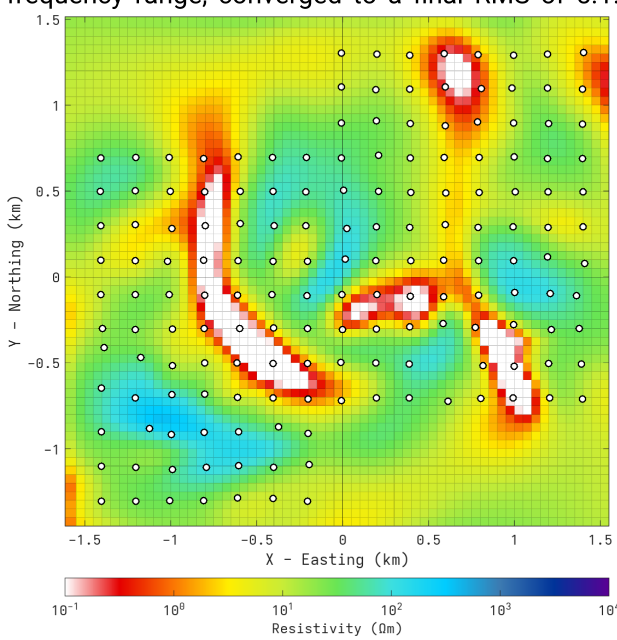

Figure 1 – Depth slice at 500m (No topography model)

Three-dimensional inversion of the Raglan Zones 2–3 magnetotelluric data

Pankaj K Mishra | *Geological Survey of Finland, email*: pankaj.mishra@gtk.fi

We inverted the Raglan Zones 2–3 data set with a GPU variant of ModEM, using 1 CPU and 4 NVIDIA GH200 GPUs on Roihu, Finland's national supercomputer. From the 'corrected' release we selected 161 sites and masked noisy parts of the transfer functions. The final data set used 27 frequencies between 1.22 Hz and 9.94 kHz, with no interpolation of the transfer functions. Error floors were set component-wise: each off-diagonal element at 7 % of its own magnitude, and each diagonal element at 10 % of the geometric average of the two off-diagonal magnitudes. The model grid is 66 × 70 × 58, about 268,000 cells, with 60 m horizontal cells across the survey footprint and topography carried as air cells, computed (DEM-interpolated) from the GeoTIFF and written back into the data file. We built the vertical discretisation finer than the data strictly require: a 10 m first layer growing geometrically at 1.1, which places eleven layers within the upper 200 m. Galvanic distortion was not parameterised as per-site tensors; instead, the near-surface refinement was intended to let small shallow bodies enter the model as resolved structure. Both inversions started from a 500 Ω·m half-space, which also served as the prior. We ran two inversions that differ in one respect: mesh, data, error floors and damping schedule were identical, and only the number of applications of the covariance smoothing operator changed, once and then twice. The first reached RMS 1.671 in 232 iterations. The second reached RMS 2.424 after 92. We submit the first one as our preferred model.

Type of code: FD (ModEM-GPU) • Analysis & visualisation: MTGeophysics.jl • Coordinate system: X=N, Y=E, Z=down • Mesh Type: structured • 161 sites, 27 frequencies • Start & prior: 500 Ω·m half-space, both • Regularisation: 0.3 in x/y/z, λ: initial 10, final 1e-4 • Time dependence: exp(+iωt) • Data inverted: full impedance tensor

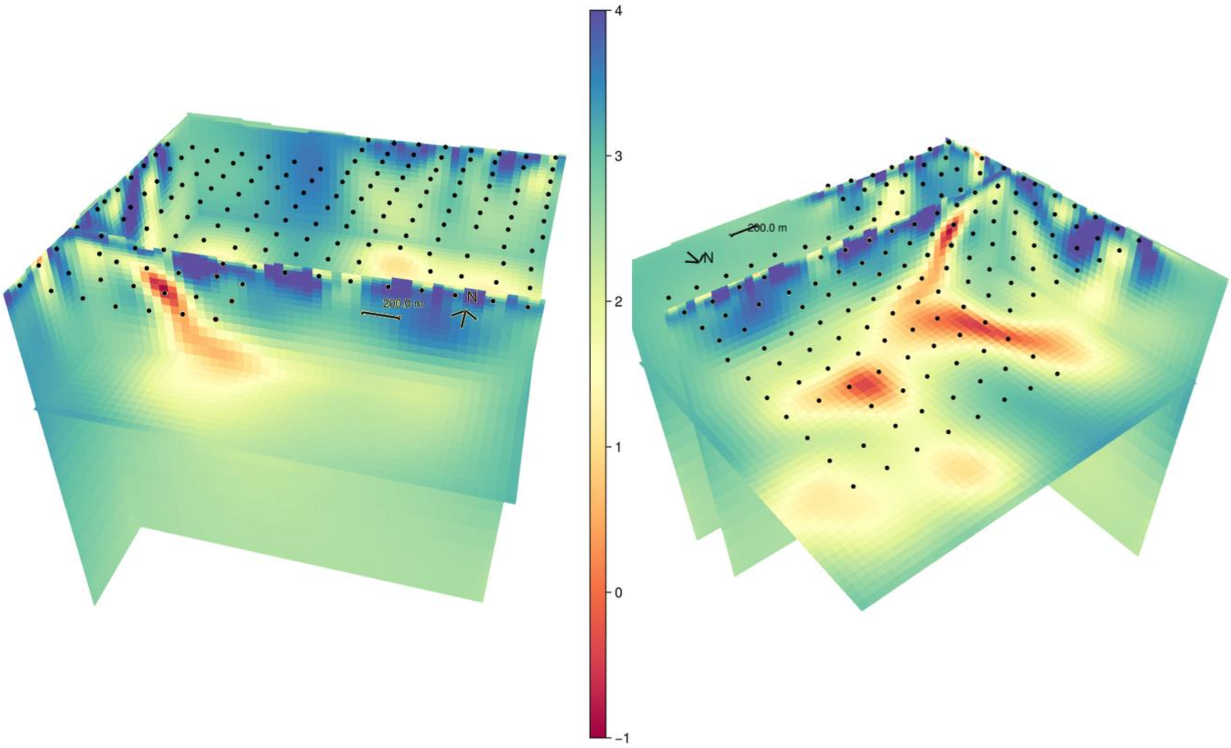

This work was supported by the Research Council of Finland (project 359261). We acknowledge CSC - IT Center for Science, Finland, for computational resources and Prof. Jochen Kamm and Dr. Cedric Patzer for insightful discussions about magnetotelluric geophysics.

Inversion of real MT data from the Raglan mining district in northern Quebec with ModEM

Aideliz M. Montiel Alvarez; Geological Survey of Norway (NGU), aideliz.alvarez@ngu.no

Magnetotelluric data acquired at 164 MT sites in the Reglan mining district in Quebec, Canada, are inverted in three dimensions using ModEM (Kelbert et al., 2014), a finite difference (FD) inversion code widely used in academic research that has demonstrated successful application to varied datasets and geological environments.

The real data are inverted using ModEM3DMT and following proposed guidelines for 3D MT inversion (e.g., Miensopust et al., 2013; Montiel-Álvarez et al., 2025; Robertson, 2021; Tietze and Ritter, 2013;). Considerations to build the prior model include the total dimensions, cell size, and initial resistivity values. The prior model extends approximately six times the survey area. In that area, the horizontal cell size is 32 m, and padding cells increase in size outward by a factor of 1.2. The initial resistivity value is 200 Ohm-m across the model. Topography is incorporated using 10 m thick vertical layers within the upper 200 m.

The available period range varies between sites depending on whether data were recorded during the day or at night. Overall, the dataset spans periods from $1x10^{-4}$ to $1.2x10^{3}$ s across 90 frequencies. For the inversion, the dataset was reduced to 40 frequencies by selecting every other frequency and removing noisy short- and long periods, as well as frequencies within dead-bands.

The inversion was performed in two stages. First, only the off-diagonal elements of the impedance tensor were inverted using a relatively high regularization value (100) and covariance (0.4). The resulting model was then used as the starting model for the inversion of the full impedance tensor using a regularization value of 1 and covariance of 0.2.

The resulting model shows a thin, top resistive layer. At about 100 m above sea level, two elongated conductors oriented almost N-S are imaged along the western side of the survey area, together with a smaller one in the northeast, and additional smaller conductors in the central part of the model. These conductive features gradually fade out at below 300 m below sea level.

References

Kelbert, et al., (2014). ModEM: A modular system for inversion of electromagnetic geophysical data. *Computers & Geosciences*, *66*, 40-53.

Miensopust, et a., (2013). Magnetotelluric 3-D inversion—A review of two successful workshops on forward and inversion code testing and comparison. *Geophysical Journal International*, *193*(3), 1216-1238.

Montiel-Álvarez, et a., (2025). The first three-dimensional electrical resistivity model of the lithosphere beneath Britain. *Journal of Geophysical Research: Solid Earth*, *130*(10), e2025JB031813.

Robertson, et a., (2020). Quality over quantity: on workflow and model space exploration of 3D inversion of MT data. *Earth, Planets and Space*, *72*(1), 2.

Tietze, K., & Ritter, O. (2013). Three-dimensional magnetotelluric inversion in practice—the electrical conductivity structure of the San Andreas Fault in Central California. *GJI*, *195*(1), 130-147.

3-D Inversion of the MT3DINV4 Raglan Field MT Data

Ce Qin* — Henan Polytechnic University, Jiaozuo 454000, China, ce.qin@hpu.edu.cn

We present a three-dimensional magnetotelluric (MT) inversion of the MT3DINV4 Raglan Zones 2 and 3 field data incorporating topography.

We use the corrected EDI data provided by Alan Jones at 164 distinct sites. Frequencies below 0.1 Hz are discarded, site-specific AMT dead-band intervals are masked, and impedance elements whose apparent-resistivity uncertainties exceed 100% of the corresponding apparent resistivity are rejected. The retained samples are assigned to a common set of 55 frequencies from 9.94 kHz to 0.122 Hz; no interpolation is applied across missing or masked samples. All four complex impedance-tensor elements are inverted, yielding 56,032 scalar data values. A 3.5% relative impedance error floor is used in data weighting.

The resistivity model is parameterized on a locally refined, nonconforming hexahedral mesh constructed from a coarse graded grid. Three nested horizontal refinements reduce the 300 m base-cell width to 37.5 m in the shallow survey volume, and approximately 10 m vertical cells resolve the air–earth interface. The mesh contains 277,812 cells, including 230,924 subsurface inversion cells and 46,888 fixed air cells. Topography is incorporated by deforming the mesh near the air–earth interface. For each frequency, the first-order Nédélec finite-element forward mesh is further refined around the MT sites, improving the accuracy of responses and derivatives without globally increasing the number of inversion cells.

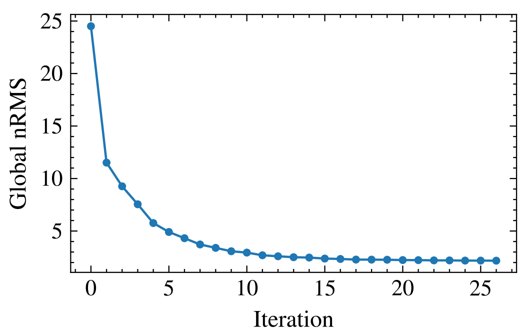

Figure 1: Convergence of the preferred full-impedance-tensor inversion ($\lambda = 100$).

The same inversion methods and regularization are used as in the inversion of the MT3DINV4S data sets. Seven trial values of the trade-off parameter from $\lambda = 1$ to 1000 were tested, and $\lambda = 100$ was selected from the L-curve. The preferred inversion reduces the normalized root-mean-square (nRMS) data misfit from 24.51 to 2.177 in 26 iterations (Fig. 1). Smaller values of λ give lower data misfits but produce rougher models. The final frequency-dependent nRMS is approximately 1.3–2.4 over most of the band, with larger residuals at the highest AMT frequencies and below approximately 0.3 Hz (Fig. 2(a)). Site nRMS is below 4 at 161 of the 164 sites (Fig. 2(b)).

The recovered resistivity model is omitted here due to space limitations but will be presented at the workshop.

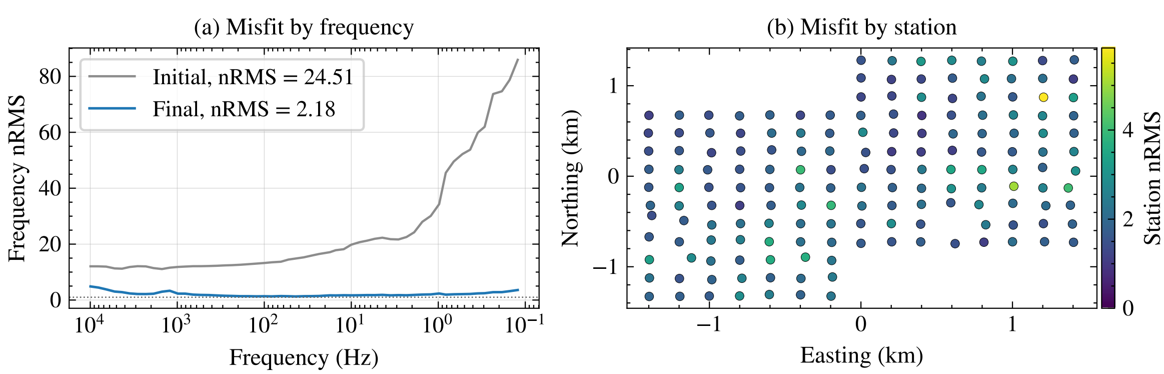

Figure 2: Frequency-dependent nRMS and final site nRMS for the preferred full-impedance-tensor inversion ($\lambda = 100$).

3D Inversion of Magnetotelluric Data over Raglan Using AP3DMT_RB

Arun Singh

Department of Earth Sciences, Indian Institute of Technology Roorkee, India (*arun.singh@es.iitr.ac.in)

Abstract

The Raglan MT dataset was inverted using the *AP3DMT_RB* code (Singh and Dehiya, 2025). A total of 166 MT stations were included in the inversion. The data were first subjected to quality control, and unreliable measurements were removed. The final dataset comprised the full impedance tensor at 33 frequencies spanning 1000 Hz to 1 Hz, resulting in a total of 16,072 complex data points. Error floors were assigned following a component-dependent strategy: 5% of $|Z_{xy}|$ for the Z_{xy}, 10% of $|Z_{xy}|$ for Z_{xx}, and similarly 5% of $|Z_{yx}|$ and 10% of $|Z_{yx}|$ for Z_{yx} and Z_{yy}, respectively.

The inversion employed a computational mesh consisting of $80\times80\times52$ active cells, excluding ten air layers, with a central cell size of $100\ \mathrm{m}$. Topography was not incorporated in the inversion. The first subsurface layer was assigned a thickness of $2\ \mathrm{m}$, while the thickness of successive layers increased geometrically by a factor of 1.15. A homogeneous half-space of $50\ \Omega, \mathrm{m}$ was used as the starting model. The inversion simultaneously estimated both the subsurface resistivity distribution and the galvanic distortion parameters. After 94 nonlinear conjugate-gradient (NLCG) iterations, the normalized root-mean-square (nRMS) misfit decreased from an initial value of approximately 15 to 4.7.

The recovered resistivity model is shown in Figure 1. The model reveals a prominent folded conductive structure that extends to the surface in the southern part of the survey area. This conductor is overlain by a relatively resistive layer, whose thickness increases progressively towards the north. The overall geometry of the conductive and resistive units is consistent with the major geological structures reported in the Raglan region.

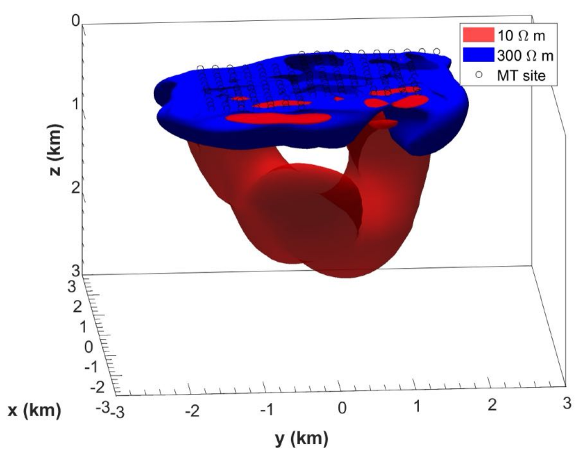

Figure 1: 3D resistivity model obtained from the inversion of field data. Isosurface corresponding to 10 and $1000\ \Omega - m$ are shown.

References

Singh, A. and Dehiya, R. (2025) *Geophysical Journal International*, Volume 243, Issue 3.

Real data inversion Task 3

M.Yu.Smirnov[1] and O.Rydman[1]
[1]Luleå University of Technology, Sweden

The data were acquired by Quantec Geoscience of Toronto in 2017, and comprise data at 164 distinct locations. Fourteen sites were repeated (denoted then an "R" in the filename) and best estimate was chosen at 14 locations. After data QC total 142 sites at 19 frequencies in the range 1-1000 Hz were selected for inversion. No trails were attempted to include higher frequencies due to rather large scatter in the AMT deadband. Similar surveys inversion showed no significant improvement after inclusion of high frequencies.

The modelling domain was discretized into 100x100x46 cells including 10 padding cells. Two different codes ModEM and MR3DMod were used for inversion. Both results are provided. No bathymetry or topography were used.

- Type of code: FD
- Time dependence of the code
- Co-ordinate system of the code: projected UTM coordinates
- Type of mesh: structured for the task (OcTree-multiresolution possible)
- Data inverted - components (full Z), 142 sites at 19 frequencies in the range 1-1000 Hz
- Initial and Prior models: 1000 Ohmm
- Error floor: 1% (5%) of main impedance components
- How has distortion been treated: Distortion has NOT been included or inverted for in ModEM, but was added to MR3DMod inversion
- Final RMS misfit: Final ModEM RMS 2.7 was reached after robust IRLS iterations with starting RMS of 219.

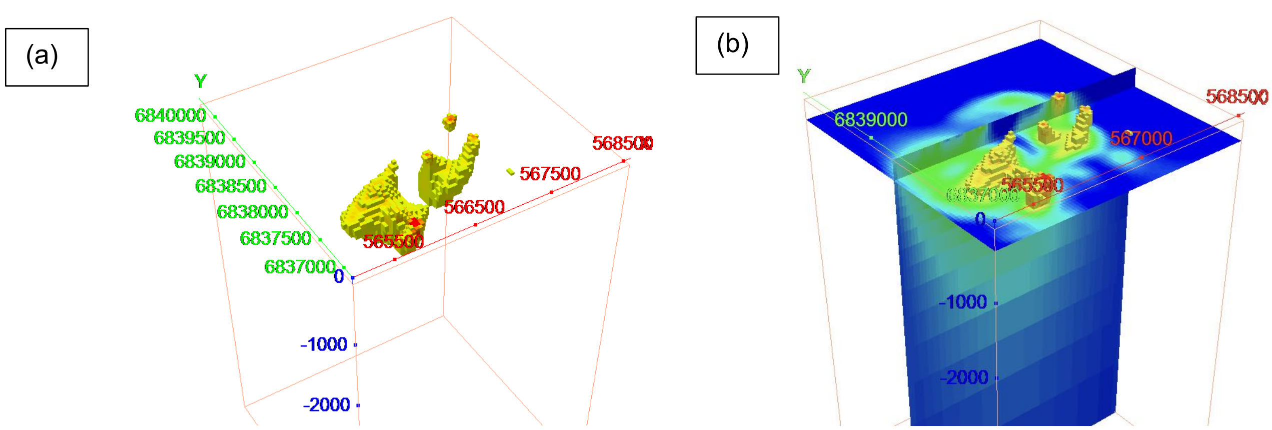

Figure 1 Recovered 3D model after (a) ModEM and (b) MR3DMod inversions

MT3DINV4 Task 3: Electrical Structure beneath Raglan Inferred from 3-D MT Inversions

H. Song[1*], M. Moorkamp[1], and G. Hill[2]

[1]*Institute of Applied Geoscience, Technische Universität Berlin, Berlin, Germany*
[2]*Institute of Geophysics, Czech Academy of Sciences, Prague, Czech Republic*

We analyse and invert the 164-site MT3DINV4 Raglan data set through a workflow combining rotationally invariant response analysis, phase-tensor diagnostics, 1-D Occam inversion, and 3-D inversion. Regional SSQ and determinant responses indicate a resistive-over-conductive tendency, whereas their station-to-station spread and spatially variable phase tensors support explicit 3-D treatment. The inversions use the full impedance tensor at 12 frequencies from 1.2207 to 984.41 Hz and a topography-conforming deformed-hexahedral mesh with a 20.6 m first earth layer. Smooth 1-D Occam models provide the initial model but do not reproduce the initial full-tensor 3-D response. We compare a fixed-alpha FEMTIC model selected by L-curve analysis with a FEMTIC-DABIC model selected using the ABIC criterion. Starting from the same Occam-derived 1-D layered model with an initial RMS of 9.859, both recover a broad shallow resistor beneath the central and northern array, lower resistivities to the south and at depth, and a deeper conductive system. The ABIC model localizes this system more strongly and reaches an RMS of 1.545, compared with 2.778 for the fixed-alpha model. Historical Zone 2, Zone 3, and Zone 2-3 drill collars lie near lower-resistivity features along the southern margin of the resistor, but the detailed conductor geometry and amplitudes remain regularization dependent and require comparison with downhole and petrophysical constraints.

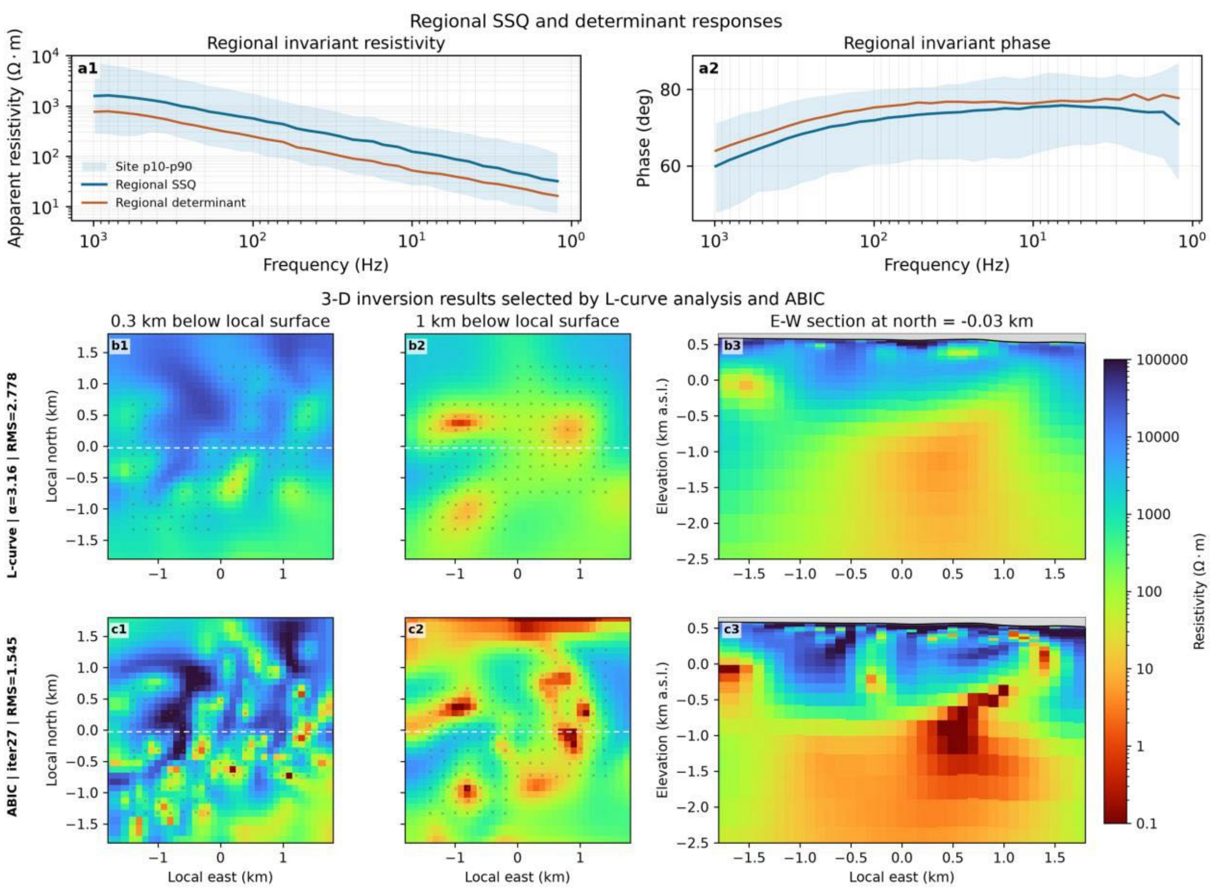

Figure 1. Regional SSQ/determinant responses and station p10-p90 range (a1-a2); L-curve FEMTIC (b1-b3; alpha=3.16, iteration 14) and ABIC FEMTIC-DABIC (c1-c3; iteration 27) models at 0.3 and 1 km depth and on an absolute-elevation section. Crosses mark MT sites and the black line marks the surface. The white dashed line marks the E-W section trace. All model panels use the same unsmoothed 0.1-100,000 ohm m scale.

3D Inversion of Magnetotelluric Data over Raglan Using SimPEG

Rylan Stutters* Johnathan Kuttai Lindsey Heagy

Geophysical Inversion Facility, Department of Earth, Ocean and Atmospheric Sciences, University of British Columbia

*Presenting author

Three-dimensional inversion of magnetotelluric (MT) data is computationally demanding, and practical workflows for real field datasets often rely on proprietary software, limiting accessibility and reproducibility. We demonstrate that the open-source SimPEG framework, combined with octree mesh discretization and parallelized forward/sensitivity computations, can effectively invert noisy, real-world MT data on modest hardware without sacrificing resolution where it matters most.

A total of 164 stations (Quantec Geoscience, 2017) were available, with frequency coverage varying by station. Data quality was assessed through frequency coverage maps, temporal consistency checks, and impedance tensor diagnostics (phase, skew, and geoelectric strike), which were used to identify and remove unstable sites and frequencies. The XY and YX impedance components at eight frequencies between 8 Hz and 800 Hz were retained as the most consistent subset, yielding 5272 data points.

Inversions were carried out using SimPEG's finite volume natural source electromagnetics module. We initially performed 2D inversions along individual North–South lines, followed by a 3D inversion on an octree mesh refined near stations and topography to balance resolution against computational cost. The data misfit was measured with an L2 norm, with uncertainties of 5% and an error floor of 0.1 assigned to the data. A smoothness-based regularization and a uniform half-space of 1500 Ω-m starting model were used. Forward and sensitivity (Jacobian) calculations were distributed across frequencies using SimPEG's `Multiprocessing MetaSimulation` on a cluster, reducing runtime from days to hours. The inversion converged after 12 β-iterations, reaching a target misfit of $\chi = 0.88$, and the normalized Root-Mean Squared (RMS) measure for each station is generally under the value of 1 as shown in Figure 1a.

The inversion model reveals a large, folded conductive structure, delineated in Figure 1b by the thresholded voxels, or alternatively, two orthogonal faults offsetting the formational conductor. This structure reaches the surface in the south, while a highly resistive unit dominates to the north, with the contact between the two dipping northward to place the resistive unit above the conductor. A 1D or 2D approach would likely smear or miss this fold geometry and its dipping contact; resolving it in 3D underscores the interpretive value of the octree-based inversion.

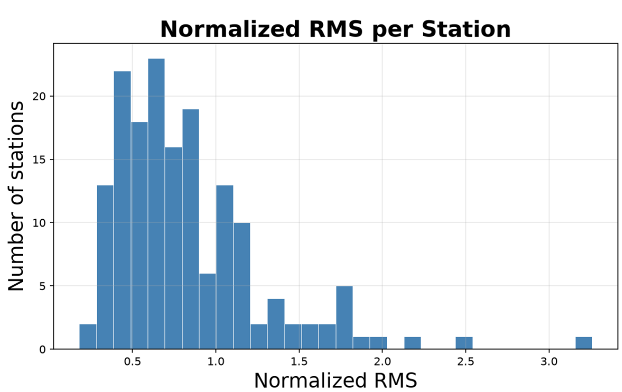

(a) Histogram of normalized RMS misfit by station for the final inversion model.

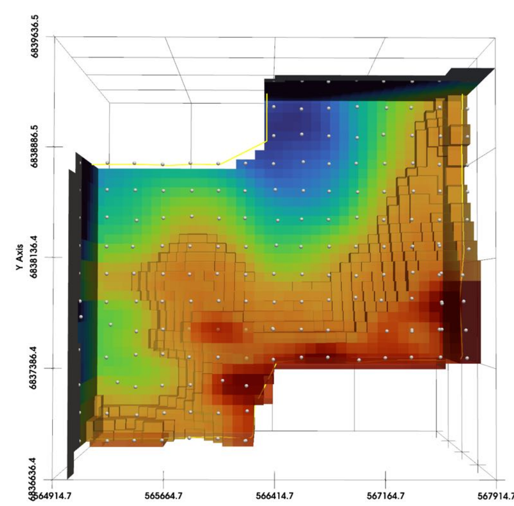

(b) 3D Voxel resistivity model with 500 Ω-m cell cuttoff and -313m elevation plan view. Red is conductive and blue is resistive.